Università Ca' Foscari

Doctoral School in Global Change Science and Policy

Ph.D Programme in Science and Management of Climate Change

A.A. 2011-2012

XXV° Ciclo

Atmospheric Blocking and Winter Mid-Latitude Climate Variability

Settore scientifico-disciplinare di afferenza: FIS/06

Tesi di Dottorato di Paolo Davini, matricola 955704

Direttore della scuola di dottorato:
Prof. Carlo Barbante

Tutore del dottorando:
Dr. Chiara Cagnazzo

"You don't need a weatherman
to know which way the wind blows"

B. Dylan - *Subterranean homesick blues*

January 18, 2013

Abstract

Atmospheric blocking is a mid-latitude weather pattern that describes a quasi-stationary, long-lasting, high-pressure system that modifies the westerly flow, blocking (or at least diverting) the eastward movement of the migratory cyclones. Blocking events can have major impacts on the mid-latitude weather, sometimes leading to extreme events as cold spells in winter or heat waves in summer. In this thesis, Northern Hemisphere winter blocking and its impacts on mid-latitude climate are analyzed through the introduction of a set of new bidimensional diagnostics based on the geopotential height that provide information about the occurrence, the duration, the intensity and the wave breaking associated with the blocking. We are able to distinguish among three main categories of blocking: one placed at low latitudes over the Pacific and Atlantic oceans, unable to block or divert the flow. A second one is detected at high latitude occurring over Greenland and North Pacific, north of the jet stream and dominated by cyclonic wave breaking. Finally a third category is defined as the traditional mid-latitude blocking, and it appears as being only localized over Europe and driven by anticyclonic wave breaking.

We address the relationship between the North Atlantic Oscillation (NAO) and the blocking occurrence, showing that blocking over Greenland (Greenland Blocking, GB) is not only a key element to describe the NAO index, but it is essential also to modulate its pattern. Consistent with this, we link the eastward displacement of the NAO pattern observed in the recent years to the decreasing frequency of Greenland Blocking. On the other side, we notice that blocking events over Europe (European Blocking) are not correlated with the NAO. We also analyze the relationship between the Atlantic eddy driven jet stream displacements and blocking occurrence. We find that Greenland Blocking is linked with the equatorward displacements of the jet stream, while European Blocking is associated with poleward displacements of the jet (and only in some case it leads to a split flow).

In order to quantify the potential impacts of blocking changes in the future, global long-term climate projections from the Climate Model Intercomparison Project - Phase 5 (CMIP5) are analyzed. This is performed in order to understand the reasons behind the biases of the models and to evaluate the predicted change in blocking frequency and its pattern of variability in the next century. The majority of the state-of-the art models still exhibit large biases especially over Europe. In future climate scenario, the blocking frequency is predicted to decrease in association with an intensification and a reduction of variability of the Atlantic and Pacific jet streams.

Contents

Chapter 1

Introduction

1.1 Motivation and aim of the thesis

Mankind has always been concerned about "the weather that will occur tomorrow". From the farmer up to the sailor, knowing the winds or the rainfall of the following days has always had a striking importance for all human activities. For this reason, strong weather anomalies associated with droughts, floods or large snowfalls (called *extreme events*) have always deserved special attention. Prediction of these events has both social and economical implications, and has become a challenging theme for scientists in the 20^{th} century.

In the recent years the relevance of climate and meteorological sciences is further increased, and these topics are receiving broader space in newspapers, press and broadcasts. The interest of the public opinion is still increasing for at least two reasons. On the one hand, the large availability of information provided by television and internet makes possible reporting extraordinary weather phenomena from everywhere in the world. On the other, the attention has been moved from the everyday weather to the possibility that the Earth's climate is changing. The increasing warning concerning the anthropogenic component of the climate change has paved the way to several political and ethical implications.

Especially this latter point has moved the scientific community to develop new techniques that go beyond the classical interpretation of synoptic charts and historical timeseries: in the last 50 years mathematical models of increasing complexity able to simulate the Earth's climate and weather have been developed. These modeling systems, based on fundamental physical and chemical equations, can provide simulations of the atmosphere, the ocean, the

biosphere and the cryosphere of the Earth. Originally mostly used for everyday weather forecasting, nowadays they are used also to investigate the properties of the present and the future climate. This latter category of models defines the Earth System Models (ESMs) or climate models.

Making use of both observations and climate models outputs, many scientists are thus trying to deepen our knowledge of the main elements of climate variability of the Earth. This is done in order to try to unveil their dynamics, to improve the ability of reproducing the natural variability by climate models and to try to provide predictions of the Earth's climate for the next century.

The comprehension and the evaluation of the natural variability of the Earth is still one of the most challenging problems for the state-of-the-art climate science. This is especially a big issue for the mid-latitude regions in the Northern Hemisphere.

The European continent is an extraordinary example of this variability, due to its peculiar position in the Earth's geography. Climate over Europe is characterized not only by strong natural variability but also by very low skills by climate and weather models. This has forced the scientific community to put a special effort to understand the weather phenomena occurring in the mid-latitudes.

Indeed, *atmospheric blocking* is one of these weather phenomena: it is one of the most important weather pattern recurring in the mid-latitudes, typical occurring over Europe and the Eastern Pacific. Atmospheric blocking can affect the weather over large portions of those regions, influencing both temperature and precipitation patterns. Long-term changes in the frequency or the patterns of atmospheric blocking can imply important changes in the average temperature or precipitation and in the frequencies of extreme events.

The words *"atmospheric blocking"* suggest the existence of some kind of phenomenon that is able to block or stop the atmospheric flow. In the common view of such concept, the first thing that may arise to someone's mind is a sort of wall, or mountain or even dam, but we know that, due to the characteristics of fluids, such block will be easily bypassed by the atmospheric flow.

Therefore, to introduce the weather description of atmospheric blocking, we need to visualize the mid-latitude flow, that is characterized by strong westerly winds called *jet streams*. Due to land-sea contrasts, such winds are strongest over the Atlantic and the Pacific ocean. Sometimes, especially during wintertime, these winds break up, leading to the

formation of long-lasting, quasi-stationary, equivalent barotropic[1], high pressure anomalies that have been defined as *atmospheric blocking*.

This definition comes from blocking main properties: after its onset, blocking is able to block the westerly flow coming from the jet streams, diverting it northward or southward. Synoptic disturbances (i.e. storms or extratropical cyclones) are deflected around the blocking high-pressure, bringing precipitation over unusual regions. Moreover, the stationarity and the persistence of blocking can lead to temperature anomalies under the blocking centre of several degrees.

The history of atmospheric blocking goes far back in time, since the first synoptic meteorology descriptions are dated back to the end of 19^{th} century. From then on, blocking dynamics have been widely studied throughout the 20^{th} century. Nowadays we know that blocking is a large scale event, of the order of 1500 km, characterized by a positive pressure anomaly and by an anticyclonic circulation[2]. It may lead to extreme events, as droughts in summer and cold spells in winter. Blocking occurs throughout the year, but higher frequencies are recorded in winter and spring. It also occurs in the Southern Hemisphere, even if with smaller frequencies. Moreover, blocking inter-annual variability is very large, to the extent that two consecutive winters can present a number of "blocked days" different by one order of magnitude.

Anyhow, even though hundreds of scientists have worked on this topic for several decades, there are still many unsolved issues concerning atmospheric blocking. We try to summarize them here below:

- It is hard to define what is blocking, and what is not.
- Climate models underestimate the frequency of atmospheric blocking.
- No unique theory has been proposed to describe blocking onset and persistence.

[1] A barotropic fluid is one in which the pressure depends only on its density, and not on temperature (as in the *baroclinic* case). In this context, it means that the vertical structure of the pressure anomaly associated with atmospheric blocking is not tilted with height.

[2] In the Northern Hemisphere, an anticyclonic circulation is characterized by air moving clockwise around a high pressure anomaly. In a first order approximation, winds are blowing according to the *geostophic wind* relation. They are parallel to isobars, due to the balance between the pressure gradient force and the Coriolis force.

- Inter-annual variability of atmospheric blocking is large and it is not straightforward identify what modulates it.

- Atmospheric blocking relationship with other elements of the climate system still have to be explored.

Obviously, due to the large literature and the complexity of the topic, it is impossible to face all these points in a single work. The motivation behind this thesis is to try to improve the atmospheric blocking knowledge, entering into the complex and wide literature of blocking. Our attention will be anchored to the winter season, due to the larger blocking impacts and the higher frequency typical of this season. More in detail, we aim at developing a new method for blocking identification and providing a new climatology that can be used to address the spatial and temporal variability of blocking. In addition to this, we will investigate the linkage among blocking and other main elements of the mid-latitude climate system. Finally, we will provide a new evaluation of the state-of-the-art climate model ability in simulating atmospheric blocking, and we will assess the predicted change of blocking frequencies in future climate scenarios.

1.1.1 Methodology and thesis outline

Due to the large amount of literature, analyzing atmospheric blocking without a brief introduction would be impossible. For this reason, Chapter 2 is devoted to a short review of what atmospheric blocking has been in the last century literature and what are the main open issues regarding its dynamics.

After that, in order to evaluate blocking, a new method for the detection of atmospheric blocking has been developed. Chapter 3 introduces this new method, that tries to "learn" from the many different methodologies adopted in literature. Together with this new method, we develop a series of diagnostics that aim at providing further details on blocking events, as their intensity, duration and impacts on the flow. An important assessment of the blocking index is then carried out: this precedes a detailed analysis of blocking and its characteristics in the Northern Hemisphere making using of different meteorological reanalysis dataset[3].

[3]Meteorological reanalysis are extensive dataset of many meteorological fields that are obtained forcing a climate model with observational data through a fixed data assimilation system. The most known are the ERA-40 Reanalysis (Uppala et al., 2005) and the NCEP/NCAR Reanalysis (Kalnay et al., 1996).

Hence, Chapter 4 is devoted to the analysis of blocking dynamics and variability over the Euro-Atlantic sector. A first part involves the relationships between blocking and the Atlantic jet stream, while a second one is more focused on the inter-connection between the North Atlantic Oscillation and blocking. A special attention will be reserved to the spatial variability of the North Atlantic Oscillation and its relationship with blocking occurring over Greenland.

Finally, in Chapter 5 an assessment of the Centro Euro-Mediterraneo sui Cambiamenti Climatici (CMCC) climate model is carried out. Making use of two different runs, we will investigate the role of Sea Surface Temperatures (SSTs) in modulating blocking activity over the North Atlantic. Hence, a more comprehensive analysis of a set of models involved in the Coupled Model Intercomparison Project - Phase 5 (CMIP5)[4] will be carried out, providing results concerning the model biases and the changes in blocking frequency for the 21^{th} century. Conclusions and possible further topics of research are finally discussed in Chapter 6.

Conversely, the remaining sections of this chapter, aim to provide a brief and simple outline of the main elements of the climate system in order to facilitate the reader's comprehension of the following chapters.

1.2 General mid-latitude variability and circulation

This section goes in the direction to provide a brief introduction to the main elements of the climate system that will be tackled in the course of this thesis. The atmospheric mid-latitude mean state, the properties of the jet streams, the characteristics of Rossby Waves, the concept of the North Atlantic Oscillation and a brief overview about Earth System Models will be briefly presented in the following pages.

1.2.1 Mid-latitude mean state

In order to evaluate the observed Earth's climate, scientists have often recurred to the concept of *mean state* of the atmosphere or of the ocean. Unfortunately, such concept may be

[4]The CMIP5 project is an extensive modeling effort, involving more than 20 climate modeling groups, that aims at evaluating the last generation of coupled models through the comparison of predefined experiments. Such experiments involves simulations of both the past and future climate, decadal predictions, etc. Further details may be find in Chapter 5.

somehow misleading, because actually the time mean state of a meteorological field never occur in real world. For instance, the wind mean state at a certain altitude is computed as the temporal average of different measures, but represents a bidimensional pattern that is irreproducible (or very unlikely to be reproduced) by the every day weather.

Even though this caveat has some theoretical implications, the adoption of the concept of mean state to study the atmosphere it is extremely helpful to face the general circulation. However, a further distinction must be introduced, trying to distinguish between the zonal mean (i.e. the average along latitudinal bands) and its departure, the so-called *eddies* or *stationary waves*. These are large wave-like oscillations of the mid-latitude circulation at planetary scale, often associated with Rossby Waves (see Section 1.2.3). A last feature that is used to describe the global circulation are the *transient eddies*, that indicate temporal deviations from the mean. Practically, they are represented by synoptic scale phenomena like cyclones with timescales of few days.

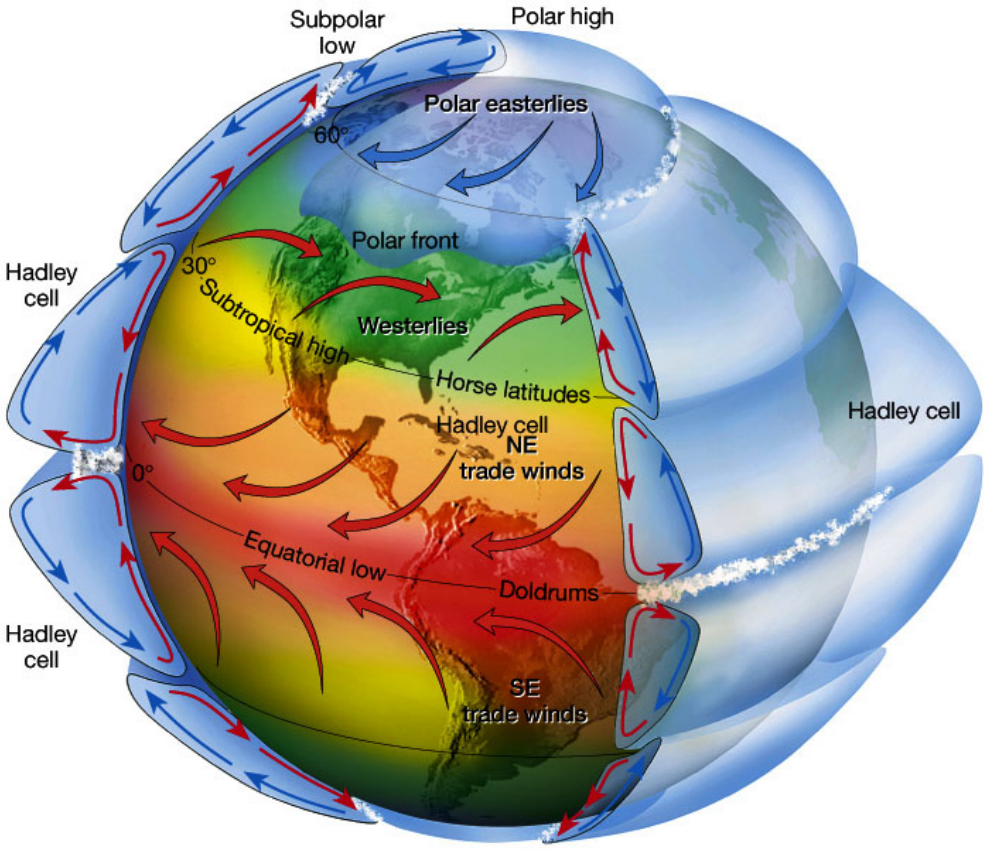

Figure 1.1: *A schematic overview of the general circulation of the atmosphere. From Lutgens and Tarbuck (2001)*

The zonal mean tropospheric circulation is dominated by the meridional circulation, that can be distinguished into the Hadley, Ferrel and Polar cells. Figure 1.1 provides a simplified sketch of the general circulation of the atmosphere. The Hadley cell is maintained by convection, where warm air rises close to the equator and sinks in the subtropics, warming adiabatically and forming the subtropical high pressure systems (Held and Hou, 1980). Conversely, the Ferrel and Polar cells are consequences of the heat and momentum transport by extratropical eddies (Peixoto and Oort, 1992).

As results of this circulation, forced by the thermal difference between the equator and the poles and by the angular momentum conservation, the main features of the wind field emerge: the easterlies winds in the tropics, also knows as *trade winds*, the subtropical westerly belt around 30-40°N and weak easterlies around the pole. Mid-latitude extratropical westerly winds are characterized by increasing speed values with altitude and they are called *jet streams*.

However, this schematic view of the general circulation is strongly reductive since, as stated above, we are considering only the zonal mean. The non-uniform landmass distribution of the Earth creates several land-sea contrasts, especially in the mid-latitudes of the Northern Hemisphere, that significantly alters this zonal perspective. Figure 1.2, showing the upper tropospheric zonal winds, depicts how the wind field varies with longitude.

For such reasons, a more detailed description of the jet streams (Section 1.2.2) and the introduction of the concept of Rossby Waves (Section 1.2.3) will be presented in the following sections.

1.2.2 The jet streams

Jet streams are typically defined as the intensification of the westerly winds occurring in the troposphere. Even though they are not always discernible, they can be classified in two groups: the *mid-latitude eddy-driven jet stream* and the *subtropical thermally-driven jet stream*.

Subtropical jet streams are found about at 30°N, close to the descending branch of the Hadley cell. Their existence relies on mainly two reasons: firstly, *thermal wind*[5] provides

[5]Thermal wind is the vertical shear of geostrophic wind caused by the presence of a horizontal temperature gradient. This is typical of *baroclinic* atmosphere, that is an atmosphere where the density of the air column depends on both temperature and pressure. In the case of subtropical jets, the meridional gradient of

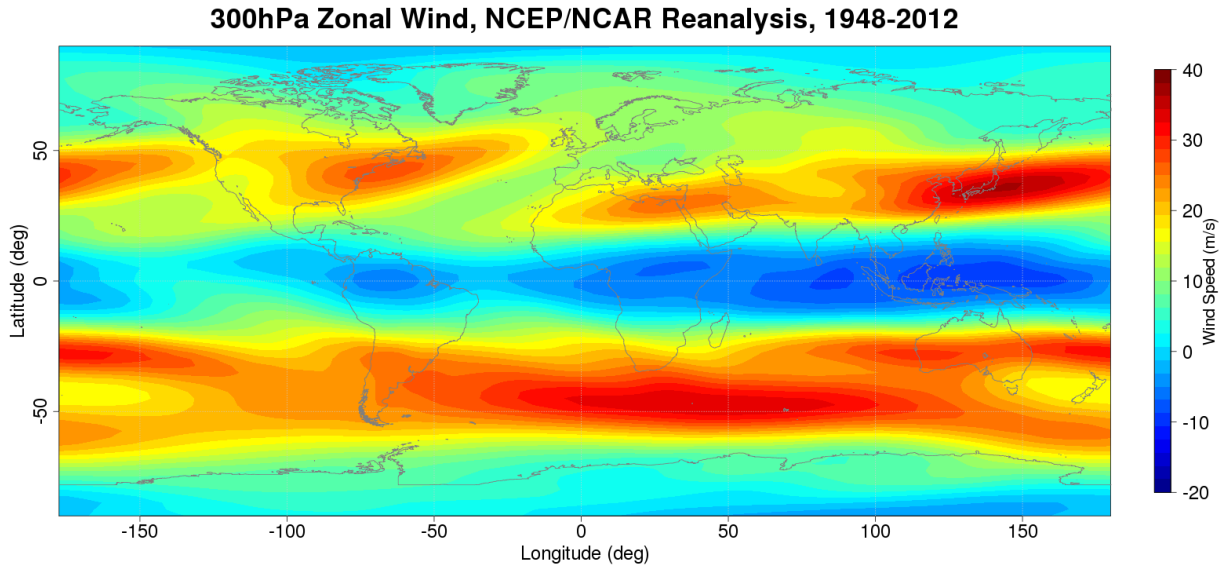

Figure 1.2: *Annual mean climatology of NCEP/NCAR Reanalysis 300-hPa zonal winds from 1948 up to 2012.*

an explanation of their increasing strength with altitude (subtropical jets are baroclinic). Secondly, the angular momentum conservation in the Hadley cell provides an explanation for their sharpness. Indeed, the Hadley cell drives a source and sink of westerly momentum from the equator up to the subtropics, that contributes to the sharpening of the jet in the proximity of the descending branch of the Hadley cell (Schneider, 2006).

On the other side, eddy-driven jets, sometimes defined also as *sub polar jets*, are connected with frontogenesis (i.e. baroclinic eddies) occurring in the mid-latitudes. In contrast with subtropical jets, their maximum speed is observed in low-middle troposphere and they are substantially barotropic. They are often associated with the *storm track*[6]. The reasons behind the formation of such jets must be searched in land-sea contrasts and in momentum convergence driven by eddies disturbances.

The eddy-driven jet develops in areas of high baroclinicity (i.e. regions of marked temperature gradient), that favor the formation of baroclinic (transient) eddies. The growth of these waves, that propagate both poleward and equatorward, is responsible for the westward

temperature, parallel to the westerly winds, causes the increase of their intensity with height.

[6]Storm tracks are the areas where the most of the extratropical cyclones travel. Two main storm tracks exist in the Northern Hemisphere, placed in correspondence of the Atlantic and Pacific jet streams.

meridional convergence of momentum. This leads to the acceleration of the westerly mean flow and to the jet formation (Hoskins et al., 1983).

Baroclinic zones are present over the Western Atlantic and Pacific ocean, thus the eddy-driven jets are more evident in these areas. Furthermore, continental landmasses are characterized by strong surface drag, especially over orographic reliefs as the Tibetan plateau or the Rocky Mountains, but they present few meridional heat transport, leading to the formation of sharp surface thermal gradient. These features of the continents lead to the weakening of the winds over the Western side of the landmasses and favor the formation of baroclinic zones over the Eastern side (e.g. Brayshaw et al., 2009). These stronger winds encounter less friction while they move over the ocean, where they may be further enhanced by the baroclinicity over the Sea Surface Temperature (SST) fronts associated with the Gulf Stream and the Kuroshio Current (Sampe et al., 2010) and by the large availability of moisture that favors the maintenance of the baroclinic zone (Hoskins and Valdes, 1990).

As can be seen in Figure 1.2, the Northern Hemisphere zonal wind is not so easy to categorize. This occurs because in areas where the subtropical jet is strong, baroclinic eddies are trapped in the westerly flow, leading to the formation of a single jet stream. Conversely, when subtropical jet is weaker, the eddy-driven jet is able to develop poleward of it (Eichelberger and Hartmann, 2007).

In Figure 1.2, it is possible to identify clearly two jets. The first one around 40°N over the Western Atlantic, the second one from Eurasia up to the Central Pacific, a few degrees southward.

While the Atlantic one is merely an eddy-driven jet, its Pacific counterpart is a mixture of both the thermally-driven component (that is visible over Asia and Eastern Africa at about 25°N) and the eddy-driven component over the Western Pacific (Li and Wettstein, 2011). In wintertime jets are stronger due to the increased meridional thermal gradient and to the increased land-sea thermal contrasts (Peixoto and Oort, 1992).

On other side, in the Southern Hemisphere the two jets are coincident in the austral winter, while they tend to split during the summer season (Held, 2000). A partial view of this behavior can be seen over the South Pacific in Figure 1.2. The uniformity of the topography (i.e. the absence of landmass) provides an absence of drag that allows the jet to blow stronger (in the well-known 40°-50°S band, the *Roaring Forties* and *Furious Fifties*)

There is also a third category of jet stream, but it is typical of the stratosphere. The

polar night jet (i.e. the meridional "boundary" of the stratospheric polar vortex) is a strong westerly wind blowing in the wintertime stratosphere around 60°N.

Obviously, the jet streams as seen in Figure 1.2 are just the result of a climatological average. The intensity and position of the jets, especially for the Atlantic jet stream, are changing with timescales of the order of few days. Sometimes the eddy-driven jet stream oscillates forming large meanders in the westerly circulation. These oscillations are strictly connected to Rossby Waves dynamics and will be analyzed in the following section.

1.2.3 Rossby waves

As mentioned in Section 1.2.1, the Earth's general circulation cannot be treated only in terms of zonal mean. Land-sea contrasts, orography and seasonality lead to considerable zonal asymmetries that maintain a characteristic wave-like pattern, especially in the Northern Hemisphere. Such eddy pattern may be seen in Figure 1.3, that shows the strong differences between the tropical region and the mid-latitudes. In the Northern Hemisphere, a stationary wave-2 pattern emerges. Indeed, atmospheric blocking is recurring in the areas where stationary ridges are present (i.e. the Alaskan ridge, over Eastern Pacific, and the Atlantic ridge, over Europe).

Atmospheric Rossby Waves can be viewed as major modulation of the westerly mid-latitude winds. They were firstly introduced by Rossby et al. (1939), and they have extensively treated in the last century (e.g Holton, 2004).

A single free propagating Rossby wave may be forced by tropical convection or by other sources of vorticity, even though the classical stationary wave pattern is caused by the orographic barriers and land-sea contrasts. They can be considered the main component of the Ferrel cell, transporting momentum and heat from the equator up to the poles.

Their physical original is connected to the conservation of the potential vorticity. In a second order, they are due to the changes of the Coriolis force with latitude, the so-called β effect, and/or to the change of the height of the air column (i.e. due to orography).

Rossby Waves present several interesting characteristics that makes them a robust paradigm for studying the mid-latitude variability. They are linear, dispersive (i.e. their frequency is not a linear function of the wavenumber) and they have strictly westward phase speed. Longer waves have also westward group speed (i.e. energy propagates westward), while smaller waves have eastward group speeds (Holton, 2004). Some of them, generated by tropical convection,

can propagate from the tropics up to the extra tropics (Hoskins and Karoly, 1981). Others, generated in areas of high baroclinicity close to the jet streams, propagate poleward and equatorward. In this way they are responsible for the momentum convergence and for the eddy-driven acceleration of the jet streams (Vallis, 2006).

Conversely, larger Rossby waves may have easterly phase speed large enough to counter-balance the westerly advection by the zonal flow, shaping into a stationary wave pattern, the so-called *topographic Rossby waves*. They are typical of the Northern Hemisphere winter and they are mainly forced by the squashing of the air column over the Himalaya and the Rockies (Holton, 2004).

Sometimes, when their amplitude become too large, they can break just like a surface sea wave, in a phenomena called Rossby Wave Breaking (RWB, McIntyre and Palmer, 1983) . RWB is defined as a rapid (few days) and irreversible mixing of material contours of some meteorological field, as for instance potential vorticity (Holton, 2004). These events are typical occurring on the poleward and equatorward flanks of the jet streams (e.g. Strong and Magnusdottir, 2008). RWB can be classified into cyclonic and anticyclonic according to the tilt and the direction of rotation of the trough-ridge pair (Thorncroft et al., 1993; Peters and

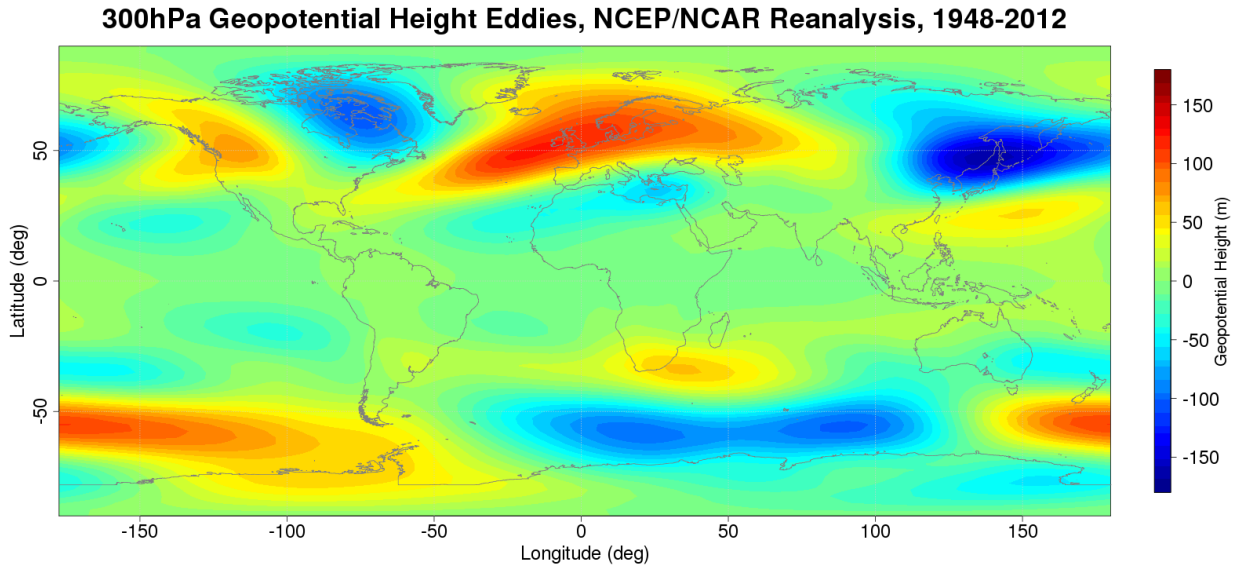

Figure 1.3: *Annual mean climatology of NCEP/NCAR Reanalysis 300-hPa geopotential height eddies from 1948 up to 2012. Eddies are computed as the difference between the climatological 300-hPa field and its zonal mean.*

Waugh, 1996).

More importantly, RWB provide a new interesting framework for the interpretation of many of the dynamics of the mid-latitude variability. Indeed, jet stream displacements (Woollings et al., 2010b), atmospheric blocking (Pelly and Hoskins, 2003) and the North Atlantic Oscillation (Benedict et al., 2004; Franzke et al., 2004; Woollings et al., 2008) are linked to RWB dynamics.

1.2.4 The North Atlantic Oscillation

The North Atlantic Oscillation (NAO) is one of the most prominent pattern of variability of the Northern Hemisphere (Barnston and Livezey, 1987; Hurrell et al., 2003). It affects the climate of the whole North Atlantic sector, with significant impacts on precipitation and temperature patterns not only over Europe and Greenland, but also over Russia, North Africa and Eastern North America. The NAO affects also the sea-ice distribution (e.g. Hilmer and Jung, 2000), while its variability is linked with other elements of the climate system, as the stratospheric polar vortex (Baldwin and Dunkerton, 2001; Scaife et al., 2005) or the oceanic circulation (e.g. Rodwell et al., 1999). It has major impacts during the winter, and in a lesser extent during spring. However, it can be identified also during summer and autumn.

The NAO is defined as the North Atlantic dipolar seesaw in sea level pressure between the subtropical high-pressure system and the mid-latitude low-pressure system (Hurrell et al., 2003). The existence of this pattern of variability is known far back in time: for instance, the Danish missionary Hans Egee Saabye in 1745 reported of contrasting weather between Greenland and Denmark (Stephenson et al., 2003), a weather pattern typically associated with the NAO.

The first definition of the North Atlantic Oscillation is due to Sir Gilbert Walker (Walker, 1924), who during a comprehensive study of correlation between sea level pressure time series all over the world noted the existence of such seesaw over the North Atlantic. From then on, the NAO polarity has been measured through the NAO index, the normalized pressure difference between Azores (or even Portugal) and Iceland (Walker and Bliss, 1932). The advantage of the NAO index is its ability of condensing the NAO variability in only one timeseries.

The alternation between the positive and negative phases can be briefly summarized by the shift in the position of the eddy-driven Atlantic jet stream. This characteristic is

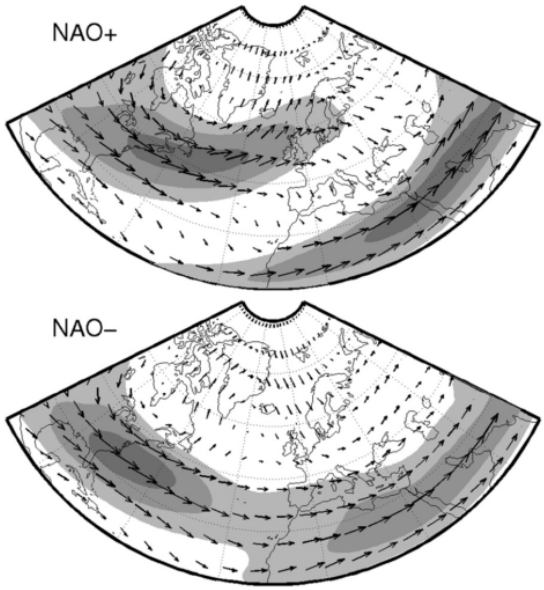

Figure 1.4: *The wintertime (DJF) positive and negative phase of the NAO as seen from the 300-hPa wind field. Positive and negative phases are defined using a one standard deviation threshold. Shading represents the 20, 30 and 40 m/s isotachs. Reproduced from Woollings et al. (2010c)*

summarized by Figure 1.4. During the positive phase the eddy-driven and the subtropical jet streams are well-separated: the storm track shifts polewards and strong winds blow over the North Atlantic up to the British Isles. The advection of moist and warm air brings precipitation and warmer temperatures over Scandinavia and Northern Europe, while colder periods even associated with droughts may occur over the Mediterranean area. Furthermore, the influence of the NAO is not confined to the Euro-Atlantic sector: positive phase leads to warmer Eastern United Stases and colder Eastern Canada and Greenland.

Conversely, during the negative phase of the NAO the Atlantic jet shifts equatorward and merges with the subtropical jet. The storm track moves equatorward, bringing precipitation over Western Europe and leaving a colder climate over Northern Europe, sometimes leading to strong cold spells and snowfalls. Temperature and precipitation anomalies are almost symmetric with respect to its positive phase, with warmer Greenland and colder Eastern United States.

The detection of these above-mentioned spatial patterns can be obtained with several techniques, that provide further information with respect to the canonical definition based

on Sea Level Pressure (SLP) difference between Iceland and Azores.

The teleconnectivity approach can be used to identify the pattern of the NAO, as done by (Wallace and Gutzler, 1981): in order to detect the centers of action of a teleconnection pattern [7], one point correlation maps are used in order to search pairs of grid points that exhibit the highest negative correlation. Nowadays, the most used technique makes use of the Empirical Orthogonal Functions (EOFs)[8] over the Euro-Atlantic sector (e.g Ambaum et al., 2001). The associated Principal Component is used to define the NAO index. In addition to this two methods, the NAO patterns can be detected exploiting weather regime analysis (Legras et al., 1987), even though some asymmetries between the positive and negative phase are in this case evident (Cassou et al., 2007)

Often NAO is analyzed together with its non-regional hemispheric counterpart, the Arctic Oscillation (AO). Defined as the first EOF of the Northern Hemisphere SLP field, the Arctic Oscillation has been introduced more recently by Thompson and Wallace (1998) and is characterized by a hemispheric latitudinal shift of the mid-latitude jet streams. The similarities between the NAO and the AO are also reflected by the high correlation between their indices (Ambaum et al., 2001). However, the physical significance of the Arctic Oscillation has been questioned (e.g. Ambaum et al., 2001).

The NAO exhibits considerable variability on both inter-seasonal and inter-annual scale: long-lasting periods of negative or positive phase are common. The variability is not confined to its polarity, but changes in the position of its pattern have been observed. For example, seasonal variability has been showed for both its center of actions (Hurrell et al., 2003).

On longer timescales, no specific periodicity of the NAO signal emerges. The NAO power spectrum presents a red noise shape (Feldstein, 2000; Hurrell et al., 2003). However, in the 80s and 90s an increasing trend of the NAO index (Hurrell, 1995) and an eastward displacement of the positive and negative centers of actions (Hilmer and Jung, 2000) was recorded. Anyway, the negative decade observed during the new millennium, with extremely low values of the

[7] A teleconnection pattern refers to a recurring, persistent, large-scale pattern of circulation anomalies extended over wide geographical areas. They owe their name to the fact that two distant points (i.e. thousands of kilometers) on the Earth observe correlated or anti-correlated timeseries of some meteorological field (e.g. SLP).

[8] Empirical Orthogonal Functions, also known as Principal Component Analysis, are defined as the eigenvectors of the spatial cross-covariance fields. It is a method widely used in climate science to extract patterns of variability from a meteorological field. For details, see North et al. (1982).

NAO index in the winter 2009/2010[9], questioned the reliability of the positive trend.

Moreover, the origin of the NAO remains a widely debated question. The NAO has been described as an intrinsic natural mode of variability of the northern hemisphere climate with a typical timescale around 10 days (Stephenson et al., 2000; Feldstein, 2000). However, there is a wide evidence that the NAO can react to external forcing such as volcanic aerosol, solar activity, oceanic anomalies and tropical disturbances. Simulations with climate models suggest that a positive trend may arise with a greenhouse gases concentration increase (Gillett et al., 2003).

Recent studies have reconnected the NAO dynamics to Rossby Wave Breaking (RWB) events, that have been introduced in Section 1.2.3. Indeed, many authors found evidence of a relationship between the NAO and Rossby Wave Breaking (Benedict et al., 2004; Franzke et al., 2004; Riviere and Orlanski, 2007; Kunz et al., 2009a). These works suggest that the cyclonic RWB is tightly associated with the negative phase of the NAO, while anticyclonic RWB depicts a positive phase. According to those works, RWB acts as a driver to the NAO, and contributes significantly to determine its phase. However, Strong and Magnusdottir (2008) proposed that in addition to the direction of rotation of the RWB the latitude where the event is occurring is important as well.

A group of recent papers (Croci-Maspoli et al., 2007a; Woollings et al., 2008, 2010c) showed that the phase of the North Atlantic Oscillation is strongly linked with the presence or absence of atmospheric blocking over Greenland. This interpretation of the NAO as a dualism between a "blocked and a "non-blocked" state fits notably well, both statistically and physically, with observational data (Woollings et al., 2008). The negative phase of the NAO is largely correlated with the presence of blocking over Greenland (Greenland Blocking), and with an associated southward shift of the eddy driven jet stream, which merges with the subtropical jet. These features will be analyzed in Chapter 4.

1.3 General Circulation Models

The most important problem of atmospheric and oceanic sciences has always been the impossibility of reproducing meteorological events in a "Earth-like" laboratory. The huge di-

[9]For the complete NAO time series, refer to the NOAA Climate Prediction Center website, `ftp:/ftp.cpc.ncep.noaa.gov/wd52dg/data/indices/nao_index.tim`

mensions of the climate system allowed only the realization of small-scale experiments, that even if extremely helpful, cannot face planetary-scale problems such as the North Atlantic Oscillation or the El Niño Southern Oscillation.

Moreover, Earth's climate presents two other fundamental characteristics: it is a non-linear chaotic system, and it performs only a "single realization". Such conditions make it difficult to evaluate and examine the role of the natural variability of the climate system. Therefore, it appears as extremely evident why the creation of numerical models able to simulate the Earth's climate can be helpful. It would be possible to reproduce the climate of the Earth several times in order to analyze different features and different problems.

Despite the evident benefit that numerical models can provide to climate science, the original boost towards the creation of those models was given by the tentatives to predict the weather of the upcoming days.

The first step aimed at this goal, even if unsuccessful, has been carried out by Lewis Fry Richardson (1922). He foresaw that the fundamental equations governing the atmospheric motions can be written as an approximated set of algebraic differences at a fixed number of points in space. For every point, extrapolating the equations applying a small increment in time, it would be possible to forecast the value of every variable for the following "time step". After the computation is performed for all the variables, the method can be applied again in order to obtain the variables values for the following time step, and so on.

Unfortunately, the computation performed by Richardson forecasted an atmospheric pressure change that was wrong by one order of magnitude. The failure of the Richardson's experiment was due mainly to the large source of error related to atmospheric noise[10] and in a second measure to the poorness of the initial data. Moreover, Richardson estimated that to perform the same computation at planetary scale, about 64,000 people would be needed.

Those caveats explain while the following steps towards the development of Numerical Weather Prediction Models must be awaited up to the 1950s. In these years two different events helped the creation of the first models. On the one hand, the World War II caused a large effort for the implementation of a meteorological observation network, and on the other the introduction of the first digital computers made it possible to perform complex

[10]Richardson did not include in his computation any filtering of gravity and sound waves, therefore producing spurious solutions that can easily increment their amplitude and affect the whole meteorological field. For further details on this filtering, see Holton (2004).

computations, going beyond the manual effort carried out by Richardson. In 1950, a first equivalent barotropic model based on the conservation of potential vorticity achieved the first successful numerical forecast.

From this point on, numerical models of increasing complexity have been developed, involving more vertical layers and increasing horizontal resolution. The discretization to a fixed number of grid points is carried out through the *finite difference method* or with the *spectral method*. Due to the spherical shape of the Earth, nowadays many models use *spherical harmonics*, truncated at a certain wavenumber (that defines their horizontal resolution). Many models make use of *Gaussian grids*, others use regular longitude-latitude grids or even icosahedrical grids. Vertical grid spacing is usually defined on *hybrid levels*, that follow the terrain at the lower levels and that flatten progressively with height. Vertical levels can also be defined on pressure levels or on *sigma levels* (i.e. terrain following levels).

Nowadays, models are constructed around a dynamical core based on the primitive equations of motion. This nucleus is made by the fundamental equations of the atmosphere: momentum balance equations (which often include the hydrostatic approximation), conservation of mass, heat balance equation and conservation of water. It computes the main variables, such as vorticity, divergences, temperature, water content, etc.

The core of the model is surrounded by a wide set of parametrized physical processes that force the atmospheric flow. Such processes include radiative heat transfer, boundary layer dynamics, convection, precipitation, vertical and horizontal diffusion, etc. The most recent generation of these models can include the parametrization of the main chemical processes, as the ozone chemical reactions.

Generally speaking, the same models can be used for both climate and weather prediction, even though the different temporal window permits the adoption of high resolution only for weather forecast models. Very high resolution at global scale leads to extremely costing computational time, that makes running centennial simulations impossible. Moreover, models aimed at short-range forecasting can include more complex parametrizations and neglect the hydrostatic approximation.

Both Regional and General Circulation Models (GCMs) have been developed. Nowadays, they are clustered into Atmospheric GCMs (AGCMs) or Oceanic GCMs (OGCMs) if they simulate the atmosphere or the ocean. The possibility of joining together the two main elements of the Earth's climate leads to the creation of the Coupled Atmosphere-Ocean

GCMs (AOGCMs).

AOGCMs sometimes provide the simulation not only of the atmosphere or the ocean, but also of the cryosphere and the biosphere, and of the interactions among these different components (e.g. they may include the carbon cycle). For these reasons, they are usually called Earth System Models (ESMs). ESMs can be validated comparing them to the climate of the last century (making use of Reanalysis or observations), and they can be used to analyze certain defined feedback or process.

In recent years, due to the growing concern about human emissions of Greenhouse Gases (GHG), an increasing demand is forcing to make use of AOGCMs or ESMs to perform climate projections for the next century. However, even if the degree of reliability of such projections is increasing, they still must be treated with caution, at least for four reasons:

- The chaotic nature of the climate system and its natural variability may hide the climate change signal, producing simulations with large uncertainty.

- The significant bias that many climate models present in some defined atmospheric and oceanic process suggests that the representation of those climatic elements may be misinterpreted by the models. Hence, their projections may be not completely reliable.

- The role played by long-term processes (e.g. century-scale oscillations), that may be neglected by climate models. Our knowledge of the Earth's climate is mainly based on direct observations, which fully cover the globe since late 70s. Therefore unknown century-scale processes (not yet identified in observations) may not be represented and may offset the results of climate projections.

- The "tuning" of some parametrizations and the role of determined feedbacks that may be valid in the present day climate, but not in a future scenario.

However, those above mentioned issues should not discourage the interpretation of the results of climate models. Especially for the present time, they can be used as a powerful tool to validate a specific theory (e.g. a feedback, a teleconnection, a dynamical theory, etc.). Moreover, future projections with a high degree of significance can be obtained if the field analyzed presents small atmospheric noise. For example, a century-time projection on global-scale temperature is highly reliable, while a local scale precipitation is not (Deser et al., 2012).

Atmospheric blocking is unfortunately one of the phenomena which representation in ESMs still present large bias. Many climate models of the previous generation (D'Andrea et al., 1998; Scaife et al., 2010) showed underestimated blocking, especially over Europe. In any case, as we will see in Chapter 5, interesting results can be obtained analyzing the simulation of blocking by the last generation of climate models.

Chapter 2

A brief review of atmospheric blocking

This chapter provides a brief introduction to atmospheric blocking and its main features and properties. Section 2.1 will introduce the fundamental literature on atmospheric blocking, analyzing blocking from both a meteorological and climatic point of view. Then, Section 2.2 will provide an overview of the different indices adopted to detect this weather phenomenon. Finally, Section 2.3 will try to shed light on the controversial issue of the dynamics underlying the onset and maintenance of atmospheric blocking. This is done presenting an overview of the several theories proposed in the last 50 years.

2.1 Atmospheric blocking

Mid-latitude climate is characterized by strong westerly winds. They are called *jet streams*, they blow around 30-40° N, and they have been widely described in Section 1.2.2. Conversely to what can be imagined, such jets are not stationary at all. Especially during wintertime, planetary waves can break this "equilibrium", leading to the formation of circulation anomalies characterized by a strong meridional component. Atmospheric blocking is an event associated with this perturbation: a high pressure system characterized by an anticyclonic circulation that 'blocks" the westerly jet, which may last for several days.

The occurrence of these anomalous events has been well known back in time in synoptic meteorology (e.g Garriot, 1904), and it has always pushed the scientific community to the investigation of these persistent weather anomalies, originally defined as "blocking" or "blocking action".

The first steps towards the classification of this phenomenon are due to the works per-

formed in the late 40s. Namias (1947) described blocking as a weather pattern associated with a reduction of the zonal flow on a limited sector of the Northern Hemisphere. This pattern was almost stationary, it lasted for several days (sometimes even weeks) and it tended to retrogress westwards. A few years after, analyzing a blocking pattern which occurred in February 1944, Elliott and Smith (1949) noted a strong meridional circulation associated with the "blocking action" and the "obstruction of the normal eastward progress of migratory cyclones". The same year Berggren et al. (1949), making use of upper-air observations, were able to depict the development and evolution of the planetary waves during the blocking action, highlighting the "splitting" of the jet stream.

Later on, Rex (1950a,b) provided a more rigid definition of the phenomenon. He defined blocking as a quasi-stationary, long-lasting, barotropic weather system that modifies the westerly flow, blocking (or at least diverting) the eastward movement of the migratory cyclones. Blocking onsets rapidly and it can last for several days, shifting the atmospheric state from a "high energy state" (i.e. strong zonal flow) to a "low energy state", characterized by a strong meridional component and by a "a train of cyclonic and anticyclonic vortices". He also pointed out the main feature of this weather pattern, i.e. the presence of "a quasi-stationary warm ridge or anticyclone just downstream from the point of the breakdown" of the westerly flow. This surface anticyclone has been commonly defined in synoptic meteorology as a *blocking high*, and it usually occurs when a mass of low vorticity subtropical air is advected poleward, here developing an anticyclonic circulation. The original blocking definition required a 10-day persistent anomaly with a zonal extension of at least 45° (Rex, 1950a). He also provided a first climatological analysis of these events, reporting blocking events from 1932 to 1950 (Rex, 1950b) with a description of the temperature and precipitation anomalies associated with blocking. He showed the prevalence of blocking occurrence over the Eastern side of the Atlantic and Pacific basins (i.e. over Europe and Western North America).

2.1.1 Blocking as a weather pattern

After the first definition by Rex (1950a), atmospheric blocking has received increasing attention in meteorology. A few years after, Sumner (1954) was able to distinguish between two main categories of blocking. The first one, originally called *diffluent block*, is now usually defined as a *Rex block*. This group of events owes its name to the fact that collects

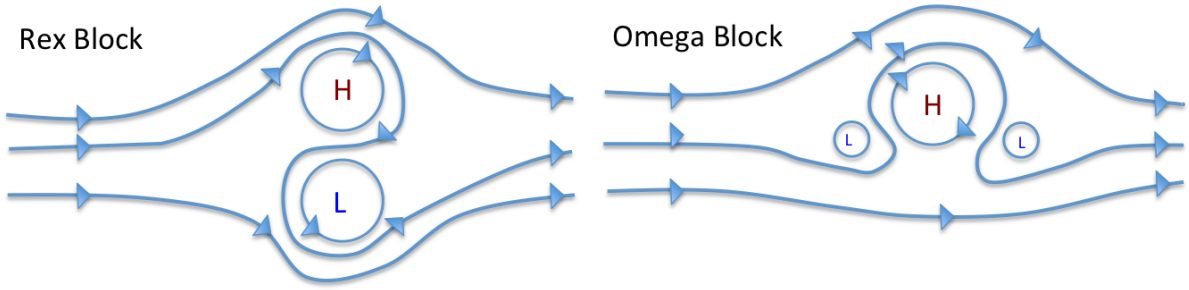

Figure 2.1: *A schematic representation of the mid-troposphere flow (i.e 500 hPa) during a Rex dipole block (left) and an Ω-block (right).*

the phenomena analyzed by the homonymous author few years before (Rex, 1950b). It is characterized by a meridionally oriented dipole of high pressure and low pressure with the former poleward, and it is typical of the Euro-Atlantic area. The second categories, classified as *meridional blocking* according to Sumner (1954) it is nowadays defined as Ω-*block*: it owes its name to the shape of the pressure pattern that is reminiscent of the capital Greek letter, with two low pressure systems lying upstream and downstream of a large high pressure system. This occurs more often over the Eastern Pacific. A simplified representation of this distinction is shown in Figure 2.1.

Obviously, this strict classification in two simple categories is largely reductive. Blocking can occur with different weather patterns, with mixture between the Rex and the Ω-block or with specific cut-off high and low. Anyhow, this distinction between Rex-block and Ω-block is still accepted in synoptic meteorology.

From that first assessments, blocking have been widely investigated and its phenomenological characteristics has been studied by several authors, that provided studies on climatologies (Dole and Gordon, 1983; Tibaldi and Molteni, 1990; Tyrlis and Hoskins, 2008a) and case studies (Green, 1977; Hoskins and Sardeshmukh, 1987).

Nowadays we know that blocking occurs throughout the year, even if it is more frequent during winter and spring. In general, to define a blocking event the anomalies must persist for about 4-5 days and extend for at least 12-15°of longitude (e.g. Tibaldi and Molteni, 1990; Pelly and Hoskins, 2003; Barriopedro et al., 2006). It can also be defined as a persistent anomaly of geopotential height or potential vorticity (Dole and Gordon, 1983; Schwierz et al.,

2004; Scherrer et al., 2006). It occurs also in the Southern Hemisphere, even though with lower frequency due to the weaker land-sea contrast (Wiedenmann et al., 2002; Berrisford et al., 2007). In the Northern Hemisphere, it typically develops at the exit of the Pacific and Atlantic jet streams, and it affects significantly the weather of the underlying regions. The subsidence in the blocking anticyclone leads to clear-sky condition that can lead to droughts and heat waves in summer, while the temperature inversion in winter can bring very low temperature in winter. Moreover, on the southern and eastern flanks (i.e. downstream) of the block the anticyclonic circulation bring arctic air from higher latitudes, possibly causing severe snowstorms. For such reasons, the link between blocking and extreme events has been widely investigated in literature (Green, 1977; Trigo et al., 2004; Buehler et al., 2011; Sillmann et al., 2011).

A striking example of atmospheric blocking pattern of the most typical kind occurred in early February 2012. The snapshot of the atmospheric circulation on the 31st of January 2012, showing the significant geopotential height anomaly associated with the blocking high over the Northern Europe, is reported in Figure 2.2. A high-pressure system developed over Western Russia and joined together with a new anticyclone developing over the British Isles, causing an anomalous circulation over Central and Eastern Europe. The final weather pattern resulting from this is a large Rex block extended for more than 100° of longitude. The retrieval of Arctic air from inner Russia and Western Siberia leads to a cold spell over

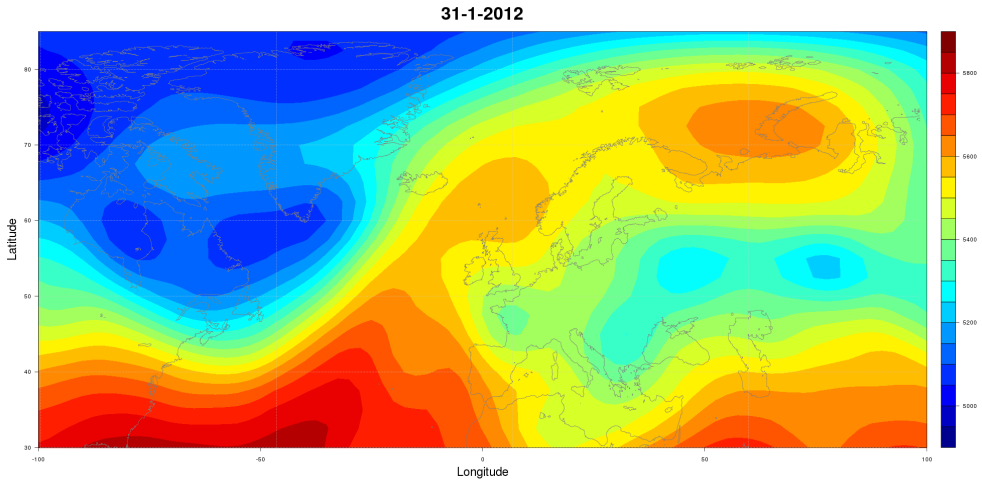

Figure 2.2: *NCEP/NCAR Reanalysis (31 January 2012) for geopotential height at 500-hPa. The Rex Block dipole of high/low pressure is evident over the Barents Sea/Western Russia*

Southern and Eastern Europe that lasted several days, associated with a series of massive snowfall events.

2.1.2 Blocking as a component of climate

The recurrence of blocking with significant frequency (i.e. on average, around 15-20% of winter days over Euro-Atlantic can be classified as "blocked days") has suggested the possibility to face the atmospheric blocking phenomenon not only from a meteorological point of view, but also under a long-term climatic perspective.

Due the large impact that blocking has on the large-scale circulation, a small change in blocking pattern and intensity may have a large impact on the underlying regions. Moreover, as pointed out in Section 2.1.1, strong blocking episodes are associated with extreme events (e.g. Trigo et al., 2004), therefore long-term changes in persistence and intensity of blocking can modify the distribution and the frequency of extreme events.

For the aforementioned reasons, in recent years climatic analysis of blocking has gained space and importance. In this sense, atmospheric blocking may be viewed as a *weather regime*. The concept of weather regime comes from practical observations. It is evident that some large-scale "atmospheric configuration" tends to occur more often than the others and that is possible to recognize this pattern. It would be thus possible to detect a few of these preferred atmospheric states that can explain the majority of the low-frequency variability of a meteorological field.

A weather regime must be recurrent, persistent and quasi-stationary (Michelangeli et al., 1995), three features that are typical characteristics of blocking. For these reasons, in the late 80s the identification of blocking as one of the most important regional or hemispheric weather patterns has been rapidly developing. Many methods have been introduced to detect atmospheric blocking through the so-called "weather regime analysis" (see Section 2.2).

Anyhow, the weather regime approach to blocking has been partially questioned by Stan and Straus (2007). Considering blocking events over Eastern Pacific and the related Alaskan Ridge regime, they showed that the number of blocking episodes occurring during the Alaskan Ridge regime is far less than expected if blocking and the weather regime were coupled. They concluded suggesting that this may be due to the low-dimensional phase space used for regime identification that is not optimal to detect local anomalies.

Even though such considerations may reduce the importance of the weather regime

paradigm, the importance of the analysis of the blocking variability and trends is undoubted. Many works suggested a reduction of wintertime blocking activity in the last 50 years over Greenland and Europe (Barriopedro et al., 2006; Croci-Maspoli et al., 2007b). Moreover, future climate projections suggest that this reduction will continue in the next century (e.g. Matsueda et al., 2009).

Conversely, the very high blocking inter-annual variability is hard to be reconciled with external or internal forcing of the climate system. In this sense, modulation of blocking by the solar cycle has been investigated (Barriopedro et al., 2008), arguing that with low solar variability Euro-Atlantic blocking events last longer, even if their overall frequency is unaltered. A potential role of snow cover influencing blocking inter-annual variability has been also explored (García-Herrera and Barriopedro, 2006).

Influence by the major element of the internal variability of the climate system, the El Niño Southern Oscillation (ENSO), has been confirmed, with a special regard to changes of blocking frequency over Western Pacific (Renwick and Wallace, 1996; Barriopedro et al., 2006). In this area, positive and neutral ENSO phases do not significantly impact the blocking frequency and duration. On the other hand, longer and more frequent blocking are observed during negative ENSO phase (i.e. La Niña events).

On the other hand, there is wide evidence of influence of atmospheric blocking on *Sudden Stratospheric Warmings* (SSWs)[1]. Blocking events in specified areas of the Northern Hemisphere have been shown to be a source of upward-propagating wave activity that acts destabilizing the polar vortex (e.g. Martius et al., 2009; Woollings et al., 2011), suggesting that blocking may be a necessary but not sufficient condition to produce the onset of SSWs.

As already pointed out in section 1.2.4, a large number of studies have linked blocking with the North Atlantic Oscillation and the other regional teleconnection patterns over the Euro-Atlantic sector. Shabbar et al. (2001) proposed that the phase of the NAO may influence the frequency of blocking over Europe. Conversely other works suggested an opposed relation, where blocking frequency may impact the phases of the NAO (Croci-Maspoli et al., 2007a). Woollings et al. (2008) pointed out a very clear relationship between the NAO and blocking over Greenland. They suggested that short-term variability associated with blocking is influencing the NAO, and NAO can be seen as a see-saw between the negative "blocked"

[1]Sudden Stratospheric Warmings are abrupt warmings of the winter stratosphere, associated with the breaking up of the stratospheric polar vortex and the brief onset of easterly winds

phase and the positive "non-blocked" phase. In any case, the role of short-term scales (as blocking or Rossby Wave Breaking) in modulating the NAO is still debated (Rennert and Wallace, 2009; Athanasiadis and Ambaum, 2009). These works suggest that the NAO phase is modulated on longer timescales, of the order of one month.

However, the importance of short-term variability associated with blocking is gathering new evidence. In this direction and even beyond goes the work on blocking effect on oceanic currents by Häkkinen et al. (2011). They argue that the long-term variability over the North Atlantic (Atlantic Multidecadal Variability) may be influenced by the blocking action. This may occur through the modulation of the oceanic gyres of the Atlantic circulation by surface winds, shifted during the occurrence of atmospheric blocking.

2.1.3 Blocking in climate models

An interesting and still unsolved issue is the representation and the prediction of blocking by climate and weather models. Indeed, many models still present an underestimation of blocking even in the most modern ESMs, with a marked bias over Europe (D'Andrea et al., 1998; Scaife et al., 2010; Vial and Osborn, 2012). Few but interesting improvements have been obtained with a huge effort in increasing in the horizontal and vertical resolution of these models (Matsueda et al., 2009; Jung et al., 2011; Woollings et al., 2010a). On the other hand, the predictability of these events (characterized by an abrupt onset) that once was very low (e.g. Tibaldi et al., 1994) is improving especially over the Pacific basin (Matsueda, 2009).

The issues associated with the weak model skills will be presented in Chapter 5, where also an assessment of the state-of-the-art ESMs will be given. In the next section we will analyze other two main open issues of blocking: first, the large amount of different indices that have been used to objectively identify blocking. Secondly, the controversial problem concerning the dynamical mechanism underlying the onset, development and maintenance of atmospheric blocking.

2.2 Blocking indices

In order to detect atmospheric blocking, an important problem that must be faced is the presence of a multitude of different objective methods for blocking definition. Several papers

have investigated the differences among some of them (Doblas-Reyes et al., 2002; Barriopedro et al., 2010; Barnes et al., 2011). Following this methodology, in the next paragraphs we will try to provide a brief overview of this wide range of methods that have been used in literature.

A first distinction must be drawn between methods that adopt an automated routine to detect blocking, i.e. objective method (e.g. Tibaldi and Molteni, 1990), and methods that need a visual inspection by an operator in order to recognize blocking, i.e. a subjective method (e.g. Rex, 1950a). There exists also methods that developed a combined approach between the two, as done by (e.g. Lupo and Smith, 1995).

Important differences arise from the physical field considered for the analysis, that can range from sea level pressure, up to potential vorticity, passing through potential temperature and geopotential height and zonal and meridional wind. Additional differences emerge whether the field is considered as regional or local departure from a climatological mean or as absolute values.

However, blocking indices may be classified in four main categories, listed here below:

1. Indices based on persistent reversal of the meridional gradient of a meteorological field.

2. Indices based on persistent local anomalies of a meteorological field.

3. Indices based on persistent eddy or regional anomalies of a meteorological field.

4. Indices based on the detection of atmospheric blocking as a weather regime.

The first category mainly includes indices based on the reversal of the meridional gradient of the geopotential height, usually measured at 500 hPa: several authors adopted different versions of this indicator, from the original Lejenäs and Okland (1983) up to the improved Tibaldi and Molteni (1990). The same methodology, making use of the geostrophic approximation, has been sometimes applied to the 500 hPa zonal wind field (e.g. Scaife et al., 2010).

Recently, "the reversal of the meridional gradient method" has been computed making use of the potential temperature measured at the tropopause level (i.e. the 2-PVU surface), as done by Pelly and Hoskins (2003). Some adjustments must be applied to avoid issues arising from the noisiness of the potential temperature field, but very interesting results have been obtained.

An issue commonly arising in the past from this family of indices was related to their "reference latitude". Indeed, all these authors started from the assumption that blocking may occur only at a defined latitude, i.e. close to the jet stream. Therefore these above-presented blocking indices were all 1-dimensional. A difference among them often relies in which latitude consider when looking for the blocking pattern. Historically, a fixed latitude placed at 60 ° N was used (Lejenäs and Okland, 1983). A little variability around the fixed latitude was introduced by Tibaldi and Molteni (1990), that considered 60°N ± 4°. Pelly and Hoskins (2003) proposed to use a non-fixed latitude, with the aim of following the storm track location in order to properly detect events where the gradient reversal leads to a blocked flow. Therefore they chose to follow the latitude where the maximum of the annual mean high-pass transient eddy kinetic energy (EKE) is placed.

More recently, this controversy has been overtaken opting for a bidimensional approach. These new blocking indices, even though they produce bidimensional climatology and can detect blocking events at uncommon latitudes, solve the problem related to the choice of a reference latitude. They have been developed for both the geopotential height (Scherrer et al., 2006) and the potential temperature (Berrisford et al., 2007).

Conversely, the bidimensional approach has always been fundamental in the second category of indices, the one based on the detection of anomalies from a climatological mean. Among them, the most known is the one developed by Dole and Gordon (1983) that looked for geopotential height anomalies. More recently Schwierz et al. (2004) exploited the vertically-averaged potential vorticity in order to to detect blocking events.

Obviously, there exist many other methods for blocking detection that do not perfectly fit in these above-mentioned categories. For example, methods based on the combination of both anomalies and absolute fields (Barriopedro et al., 2010).

A second problem related to blocking detection is the introduction of spatial and temporal markers to ensure that the required persistence is attained. While concerning the temporal constraints a general agreement has been reached in literature defining a blocking event an anomaly that lasts at least 4 or 5 consecutive days, the situation is more complex when the spatial constraints are analyzed. Some indices requires a minimum number of continuous degrees of longitude without conceding any displacement of the event in time (Tibaldi and Molteni, 1990). Other requires that a minimum distance is satisfied and allow for a small longitudinal movement (Pelly and Hoskins, 2003). Others finally go in the direction of trying

to produce a real "tracking" of the blocking event (Schwierz et al., 2004; Croci-Maspoli et al., 2007a), following day-by-day the evolution of the weather anomaly.

A completely different approach is the one that identifies blocking through the anomalies of the eddy field. For instance, methods that consider anomalies from the zonal mean over a regional Atlantic and Pacific sector (Hartmann and Ghan, 1980) have been developed. Making use of the 500-hPa geopotential height eddy field surrounded by a meridional anomalous wind, other authors were able define blocking through the eddy field (Kaas and Branstator, 1993; Cash and Lee, 2000).

A final and different approach is the one related to weather regimes. The main methodology adopted for weather regime detection is based on cluster analysis, firstly introduced by Legras et al. (1987). Classified in into non-hierarchical (Michelangeli et al., 1995) or hierarchical (Cheng and Wallace, 1993), it is able to identify blocking as a recurring pattern. Similar results have been obtained with non-linear equilibrium methods (Vautard, 1990) and with methods that looks for maxima in the probability density distribution (PDF) of the phase space of the atmosphere (Kimoto and Ghil, 1993b,a).

The presence of many different indices for blocking detection present both drawbacks than benefits. On the one side, different indices provide different approaches to the problem and therefore are able to produce a more comprehensive and accurate series of study of the blocking phenomenology. On the other side, this maze of different indices and diagnostics implies large difficulties in the comparison of the results among different works. However, in several cases the analysis leads to similar conclusions, as pointed out by Barnes et al. (2011) comparing geopotential-height-based indices, potential-temperature-based indices and zonal-wind-based indices.

In this complex framework, we decided to choose an approach to identify blocking able to preserve some fundamental characteristics such as the bidimensionality, the quasi-stationarity and the persistence. In the same, we tried to keep the algorithm as simple as possible. In Chapter 3 a new blocking detection scheme, that will be adopted throughout the thesis, will be presented together with the related climatology.

The next Section will introduce the different dynamical theories hypothesized to explain blocking onset and persistence.

2.3 Blocking theories

Before the creation and development of powerful computer tool to perform mathematical simulation of the climate system, different theories have been hypothesized regarding atmospheric blocking. The first steps towards the idea of a dynamical interpretation was performed by Rossby (1950) and by Rex (1950a). They proposed that blocking was activated and sustained in a way similar to the hydraulic jump, where the jet stream acts as a channel that drives the breakdown from an upstream high kinetic energy state to a downstream low kinetic energy state. However, this mechanism has been questioned due to the absence of a turbulent flow, typical of the hydraulic jump, during the blocking mature stage (Egger, 1978).

In the 60s and the 70s a few advancements have been performed. The introduction of the first quasi-geostrophic models introduced the possibility of simulating the climate system, finally permitting the validation or confutation of many dynamical theories about the climate system. The next sections will address some of these theories concerning blocking: the role of the planetary waves, the modon and soliton theories, the role of barotropic and baroclinic instabilities and the interaction of the eddies with the mean flow.

2.3.1 The role of stationary waves

Many authors tried to reconcile planetary-scale waves with atmospheric blocking: this idea comes from the evident geographical overlap between the position of such waves and the regions where higher blocking frequency is observed. From this consideration it emerges as possible that blocking may arise from an amplification of the stationary Atlantic and Pacific warm ridges.

The stationary ridges are originated by zonal asymmetries, i.e. land-sea contrasts and mountain orography over the Asian and North America continent (Valdes and Hoskins, 1989; Held et al., 2002). Therefore blocking may be connected with the thermal contrasts (Austin, 1980) or by continental elevation (Grose and Hoskins, 1979).

Other authors addressed the role of the interference between free traveling Rossby waves and the stationary planetary waves. Both the linear resonance (Tung and Lindzen, 1979) and the non-linear interaction (Egger, 1978) have been proposed as possible mechanism for blocking development.

The possibility that only specific wavenumbers may affect blocking has also been investigated. For instance, Austin (1980) found that Euro-Atlantic blocking occur with reinforcement of both wavenumber-1 and 2. More recently, Lejenäs and Madden (1992) showed that almost 40% of the blocks occur in presence of a planetary-scale wavenumber-1 ridge, while Hansen and Sutera (1993) noted that the majority of the blocking events occur in association with a regime with amplified planetary waves.

In more recent years, many works analyzed the interaction between stationary waves and transient eddies. Details about this are given in Section 2.3.6.

2.3.2 Tropical forcing theories

The influence of tropical anomalies on the mid-latitude climate was formerly pointed out by the well-known work by Hoskins and Karoly (1981). Making use of a spherical linearized baroclinic model they showed that a significant response in the mid-latitudes can be obtained applying a thermal forcing at low latitudes. They showed that with a subtropical thermal forcing the upper-level response of the model can be interpreted as a Rossby wavetrain, with longer waves propagating polewards and with shorter waves being trapped south of the mid-latitude jet stream. The out of phase signal resulting between the two wavetrains may be responsible for blocking-like anomalies. The role of the subtropics was further addressed, with a special focus on tropical SSTs anomalies, in both case studies (Hoskins and Sardeshmukh, 1987) and specific GCM simulations (Ferranti et al., 1994). They both found an important impact caused by SSTs anomalies over Indonesia and the Caribbean Sea on Euro-Atlantic blocking variability.

More recently, Cassou (2008) proposed that the Madden-Julian Oscillation phases excite series of wavetrains that may influence the weather over the North Atlantic. Both the positive and negative phases of the North Atlantic Oscillation, which have been shown to be connected with blocking (Woollings et al., 2008), are associated with Rossby wavetrains propagating in the Northern Hemisphere that finally break over the North Atlantic.

2.3.3 Multiple flow equilibria

One of the most fascinating theories proposed to explain atmospheric blocking dynamics is surely the one that deals with the idea of the multiple flow equilibria. Historically, it always

has been noted that the whole atmosphere oscillates between period of strong wave activity and period of strong zonal flow. The idea of this large-scale climate regime moved Charney and DeVore (1979) to investigate the possibility of the existence of global quasi-stable states of the atmospheric circulation. They used a highly-truncated one-layer barotropic channel model in a β-plane perturbed by a sinusoidal topography. The non-linear interaction among the topography, the externally forced zonal flow and wave perturbations leads to more than one equilibrium state. The number and the stability of the equilibrium states depended on the characteristics of the forcing. One of the stable ones, characterized by a large wave component, resembled significantly the blocking pattern.

Other authors were able to reproduce these findings improving the experimental setup: these improvements ranged from models that include baroclinicity (Charney and Straus, 1980; Reinhold and Pierrehumbert, 1982) to models with a more realistic topography (Charney et al., 1981) passing through models with a smaller truncation (Legras and Ghil, 1985). In the same period, other authors, introducing wave perturbations in the zonal flow, explored the possibility that the non-linear resonance found by Charney and DeVore (1979) was not only due to the topographic forcing but may be dependent on the zonal flow itself (Malguzzi and Speranza, 1981; Benzi et al., 1986).

On the other hand, Malguzzi and Speranza (1981) and Pierrehumbert and Malguzzi (1984) proposed a multiple equilibria flow theory in which the solution is not arising from a global scale resonance of planetary waves, but is due to local blocking events independent from the global scale circulation. They found multiple equilibria similar to the Charney and DeVore (1979) occurring simultaneously in different sectors of the globe.

In the following years, many authors tried to reconcile the Charney and DeVore (1979) findings with the real atmosphere. Hansen and Sutera (1986), looking at the amplitude of the observed planetary waves, found a bimodality that can be interpreted as a part of the multiple equilibria flow theory in a 15-year dataset from 1965 to 1980. However, Tung and Rosenthal (1985) noted that the choice of parameters introduced by Charney and DeVore (1979) was too far from the conditions of the real atmosphere. The existence of multiple equilibria in less severely truncated models has been hence questioned in both barotropic and baroclinic idealized models (Tung and Rosenthal, 1985; Cehelsky and Tung, 1987)

In more recent years, other authors were not able to confirm the multiple flow equilibria theory looking to observations (Nitsche et al., 1994; Stephenson et al., 2004; Ambaum, 2008).

They did not find a statistically significant multimodal character of the Northern Hemisphere flow and therefore supported the idea of a large scale atmospheric circulation that fluctuates around a single equilibrium. Ambaum (2008), analyzing the 500-hpa geopotential height field covering 40 years, pointed out that the results obtained by Hansen and Sutera (1986) were likely altered by a sampling error since an apparent bimodal behavior is emerging in the 1960-1970 decade.

Therefore, even though extremely interesting and widely proved in simplified and highly truncated model, the idea of the existence of multiple flow equilibria in the real atmosphere, or even in less idealized models, is still questionable.

2.3.4 The role of instabilities

Other authors investigated the role of natural instabilities, in a similar way of what occur during the cyclogenesis in which the cyclone grows on both baroclinic and barotropic energy (e.g. Frederiksen, 1983, 1997). He analyzed results from a quasi-geostrophic two-layer model, showing that the fastest growing mode in a low-unstable flow was a dipole at the end of the Atlantic and Pacific storm track. He argued that this blocking dipole is the most important mode of instability in a condition with low baroclinic instability. However, these modes of instability were not actually the fastest ones during the blocking onset, and they become important only during the blocking mature stage.

Adopting a barotropic model, Simmons et al. (1983) investigated recurrent patterns similar to the the Pacific/North American pattern and the East Atlantic pattern (which are related to blocking activity). They argued that the fastest growing modes responsible for these patterns derive their energy from the basic state through barotropic instabilities. Such instabilities may be responsible for a significant portion of the low frequency variability of the geopotential height field during wintertime.

More recently, Swanson (2001) proposed that blocking may arise simply from the local instability of a zonally varying flow. The planetary-scale instability could produce a block without the contributions of the transient eddies (see Section 2.3.6).

2.3.5 Modons and solitons

Another theory formulated to explain blocking formation and persistence regards a specific class of solutions of the quasi-geostrophic potential vorticity equations. Two main branches have been explored: the strongly non-linear "modon theory" and the weakly non-linear "soliton theory".

The first one was originally proposed by McWilliams (1980). In this framework, blocking is seen as an exact solution of the quasi-geostrophic PV equation, characterized by a couple of steady positive and negative PV anomalies into a westerly zonal flow, resembling the shape of a Rex blocking event. McWilliams (1980) was able to show that there exist "certain consistent features" between a modon solution of the inviscid equivalent barotropic equation and a strong blocking occurred over Europe on the January of 1963.

Even though other works emphasized that the modon solutions are robust to external perturbations (McWilliams et al., 1981) and they exist also in spherical geometry (Tribbia, 1984), many caveats of the modon theory remained unsolved (as already pointed out by McWilliams 1980). The main restriction is the requirement that the westerly flow speed exceeds a certain defined threshold (McWilliams, 1980), that is not easily found in the real atmosphere (Malguzzi and Malanotte-Rizzoli, 1984). Moreover, this high speed condition would forbid the existence of Rossby waves, because their wavenumber would be unrealistically large. Secondly, modon theory cannot describe properly the onset of blocking. Finally, the baroclinicity and the strong horizontal shear of the real atmosphere would affect the robustness of the modon solutions.

The weakly non-linear counterpart of the modon theory, named soliton theory, has been also proposed (Malguzzi and Malanotte-Rizzoli, 1984; Malguzzi and Malanotte Rizzoli, 1985). The fundamental ingredient behind this theory is the Korteweg-de Vries solitary wave equation, where the advection term balances the damping due to Rossby waves dispersion. However, Haines et al. (1993) were unable to find a clear evidence of this theory, making use of a dataset of 15 winters from Reanalysis data.

Unfortunately, even though they are highly suggestive and challenging, neither the modon nor the soliton theories have been completely accepted by the scientific community due to the impossibility of finding in observations the same features typical of these theoretical solutions.

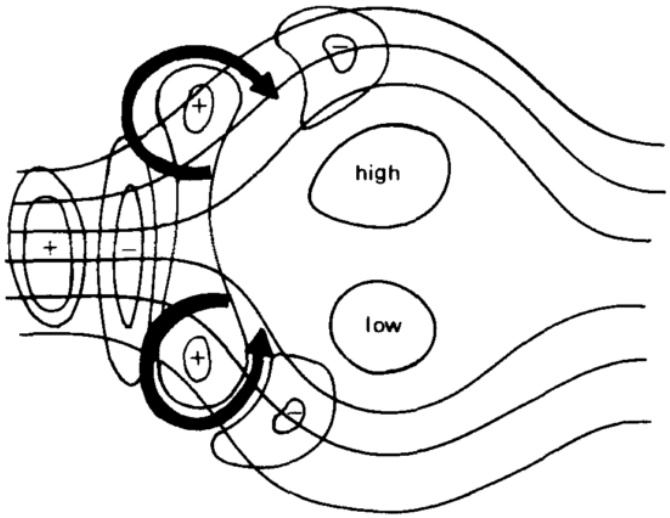

Figure 2.3: *A schematic representation of the eddy straining mechanism. As long as the transient eddies approach the split jet (i.e. the blocking anticyclone), they are subject to a meridional elongation. Finally, they transfer vorticity to the large scale anomaly, as indicated by the black arrows. Reproduced from Shutts (1983)*

2.3.6 Transient eddies and their interaction with large scale flow

One of the most investigated topics concerning blocking regards the role played by synoptic eddies during the onset and the maintenance of the block. First hypotheses in this direction were formulated by Berggren et al. (1949): they noted that small synoptic disturbances (i.e. cyclones) approaching to a pronounced ridge or to a blocking high were subject to a progressive shrinking along the meridional direction, finally shaping in cyclonic and anticyclonic eddies that were absorbed by the block.

This idea has been further investigated in the following years. Green (1977) analyzed the strong blocking occurred in July 1976, suggesting that transient eddies were cardinal in the maintenance of the block. He assumed that the vorticity transfer from the baroclinic disturbances was able to maintain the block against the dissipation caused by friction. Austin (1980) performed a numerical simulation with a quasi-geostrophic model, confirming that the forcing by the anticyclonic eddies on the blocking structure and noting a constructive interference between the eddies and the planetary waves.

A deeper interpretation of the role of eddies was however provided by Shutts (1983). He

introduced the idea of *eddy straining*, for which the eddies propagating along a baroclinic zone (i.e. the jet stream) when they encounter a ridge are stretched in the meridional direction. Then these eddies, embedded in the blocking pattern, are subject to the reverse energy cascade, transferring energy progressively at lower wavenumbers (i.e. providing vorticity to the block). This forcing of vorticity provided by the synoptic systems would maintain the block against "being blown away by the mean flow rather than against friction" (Shutts, 1983). A simple schematic representation is given in Figure 2.3. Moreover, making use of a series of non-linear integrations of a barotropic model, he pointed out that blocking emerges naturally even in absence of orography, suggesting that eddies were able also to onset the block. The introduction of the topography only increases the split of the westerly jet at the end of the oceanic basins, facilitating the initiation of the block by the transients.

The maintenance of the blocking anticyclone by the eddies against westward advection by the mean flow rather than against friction has been subsequently confirmed (Illari and Marshall, 1983; Illari, 1984; Mullen, 1987). In addition to this, the introduction of the **E**-vector by Hoskins et al. (1983) to compute the momentum transport by the transient eddies provided a further framework that finally supported the *eddy straining* theory for the onset and the maintenance of the block. Indeed, Hoskins et al. (1983) were able to show that the elongation of the synoptic system occurring upstream the block tends to force easterly winds downstream, reinforcing the blocking structure.

The role of strong synoptic transients during the phase of onset of the block has been particularly investigated. Hansen and Chen (1982) examined two different blocking episodes over the Atlantic and Pacific basin, noting that in both the cases blocking developed downstream of intense storm activity (i.e. the so-called *explosive cyclogenesis*, characterized by cyclone onset with a very rapid decrease of the minimum of SLP).

The interaction between explosive cyclogenesis and planetary scale circulation was addressed in the following years by Colucci (1985, 1987). He argued that the formation of a block was depending mainly on the amplitude of the planetary waves and on their relative phase with the developing cyclone. Tsou and Smith (1990) found that the vorticity forcing associated with explosive cyclogenesis has a fundamental role during the onset of the block.

Similar results have been obtained by Nakamura and Wallace (1990, 1993). They highlighted that in the days before the blocking onset there was an increase in baroclinic activity, and that synoptic eddies were able to advect low potential vorticity air from the subtropics.

Colucci and Alberta (1996), making a comprehensive study over 7 winters about the relation between cyclogenesis and blocking, found that cyclogenesis may actively operate on the onset of the block only after a preconditioning by the existing planetary waves, that must be meridionally elongated with a strong southerly component.

However, Nakamura et al. (1997) showed that the feedback between eddies and synoptic perturbations may be responsible for the onset of the majority of the Pacific blocking, while the large-scale anomalies associated with the planetary waves have larger impact on Atlantic blocking. This distinction may arise from the different separation between the eddy-driven and the subtropical jet present over the Pacific and the Atlantic (Eichelberger and Hartmann, 2007).

The importance of the planetary wave dynamics moved Pelly and Hoskins (2003) to study blocking on the dynamical tropopause, and to connect it with Rossby Wave Breaking dynamics (McIntyre and Palmer, 1983). Indeed, the potential vorticity framework (Hoskins et al., 1983; Hoskins and Sardeshmukh, 1987) provides a clear view of the poleward extrusion of the subtropical low vorticity air from the subtropics, in a mechanism similar to the *eddy straining* suggested by Shutts (1983). Moreover, Rossby wavetrains over the Atlantic have been identified as a precursor for the formation of the Atlantic block (Nakamura, 1994; Woollings et al., 2008; Tyrlis and Hoskins, 2008b).

More recently, the analogies between atmospheric blocking and the North Atlantic Oscillation (Woollings et al., 2008, 2010c), the theories that relate the NAO with Rossby Wave Breaking (e.g. Benedict et al., 2004; Franzke et al., 2004) and the distinct roles that cyclonic and anticyclonic wave breaking have on the weather pattern (e.g. Strong and Magnusdottir, 2008) further emphasized the importance of the large scale dynamics.

In any case, even though some pieces are still missing to the puzzle, the interaction between the small scale and the large scale as originally hypothesized by Shutts (1983) is probably the most interesting theory concerning the blocking dynamics. Rossby waves and their "breaking" at the end of the storm track, associated with the effect of the transient eddies, operate during the onset of the block and act replacing and maintaining the low vorticity anomaly against the diabatic effects (i.e. the radiative cooling) and friction at the ground.

2.4 Conclusions and open issues

As emerged as evident in the last sections, several theories have been proposed to explain atmospheric blocking onset and maintenance. It could be argued that, even though extremely interesting and fascinating, theories coming from the most "theoretical" point of view have found less fortune in the literature. The multiple flow equilibria Charney and DeVore (1979), the modon theory (McWilliams, 1980) and the soliton theory (Malguzzi and Malanotte-Rizzoli, 1984), all proved in simplified models based on the primitive equations, have encountered difficulties to be confirmed in the real world. Conversely, wider approval by the scientific community has been obtained by theories that suggest the interaction of different components of the climate, as orography-forced waves, thermally-forced waves (Tung and Lindzen, 1979; Hoskins and Karoly, 1981; Cassou, 2008) or, above all, baroclinic eddies and their interaction with the mean flow (Shutts, 1983). The linear and non-linear interaction of different waves has emerged as important to the onset and to the maintenance of the blocking events and, more in general, in shaping the mid-latitude variability. For this reason, an increasing relevance has been obtained by the "Rossby Wave Breaking interpretation" of not only atmospheric blocking (Pelly and Hoskins, 2003; Woollings et al., 2008), but also of the North Atlantic Oscillation (Benedict et al., 2004).

However, as shown in the very beginning of this thesis (Chapter 1), there are many points still open in blocking research that do not include the inner dynamics of blocking. The major ones are listed here below:

- There is a wide controversy (and far to be solved) about what indices should be adopted and what should be discarded to detect blocking. Even if it is easy to identify on a synoptic map a blocking event, it is notably harder to find agreement when reanalyses or climate models are analyzed. Indeed, defining univocally the "blocked grid points" and therefore the "contours" of the events it is very difficult. Many methods can be proposed, several produce similar results, but a uniform technique has not been adopted yet.

- The simulation and prediction of atmospheric blocking, even if it is improving, it is not satisfactory, especially over the European region. The reasons of the biases of climate models are still unknown. For the moment, the main suspect is the ability to resolve the small-scale eddies. Therefore great efforts are carried out to improve the horizontal

and vertical resolution of climate models, even though it is possible that could exist other explanations for this bias.

- Atmospheric blocking is characterized by a large inter-annual variability and by an interesting correlation with extreme events. Understanding what external or internal forcing of the Earth's climate system drives this variability it is mandatory but not straightforward. Moreover, atmospheric blocking is connected with other elements of mid-latitude climate system, and these relationships still must be explored in detail.

In the rest of this thesis, we will try to tackle these three above-mentioned points. While Chapter 3 presents a new comprehensive blocking climatology trying to provide a new blocking index able to improve the benefits and reduce the caveats of the preexisting ones, Chapter 4 will be especially focused on the last of these issues, aiming at unveiling the connection between atmospheric blocking, the North Atlantic Oscillation and the jet stream variability. Finally, Chapter 5 will investigate the improvements of the last generation of climate models in representing blocking.

Chapter 3

A Northern Hemisphere blocking climatology

This chapter presents the method developed to detect atmospheric blocking and introduces the related blocking climatology. In particular Section 3.1 provides an overview of the blocking detection scheme and of the main diagnostics developed, while Section 3.2 shows the results obtained making use of three different reanalysis datasets. Finally, in Section 3.3 the properties of blocking are analyzed in order to detect different phenomenological blocking events and the variability and trends of blocking pattern are investigated.

3.1 The blocking detection scheme and the associated diagnostics

Given the large amount and the variety of different objective methods for blocking detection (as seen in Section 2.2), the choice of a specific detection scheme is everything but straightforward. Indeed, every method presents its own caveats and benefits.

Finally, we opted in this thesis for an approach based on the reversal of the meridional gradient of the geopotential height. This choice is mainly due to the largest amount of authors that in literature make use of this "family" of indices, which facilitates the comparison and the assessment of our index. Furthermore, the accessibility to this meteorological field (i.e. geopotential height) makes the retrieval of this quantity for analyzing climate simulations notably easier.

We hence added some spatial and temporal constraints to the canonical definition of meridional gradient reversal, in order to preserve the quasi-stationarity of the blocking and its persistence. The quasi-stationarity is ensured by a spatial filter that require a minimum longitudinal dimension but that allows for a small spatial displacement (both longitudinal and meridional) for each day. This is done because blocking is a stationary pattern, but it typically moves a few degrees during its lifecycle. Finally, the persistence is granted by a minimum of 5 consecutive days.

Together with the blocking index we developed a series of different diagnostics. Two of them are focused on the intensity of the blocking events, while another one is dedicated to the analysis of the Rossby Wave Breaking associated with the blocking events.

A detailed description of the blocking index is reported in the Appendix: a short summary is however presented in the following sections.

3.1.1 The blocking algorithm

In order to objectively identify blocking, the bidimensional extension of the Tibaldi and Molteni (1990) index developed by Scherrer et al. (2006) is adopted. The index is extended from 30° N to 75° N. It provides a measure of the frequency of large-scale reversals of the meridional gradient of the geopotential height, measured at 500 hPa. The index requires that the reversal of the meridional gradient (i.e. the presence of easterly winds) south of the considered grid points is observed simultaneously with the presence of a strong positive meridional gradient (i.e. strong westerly winds) to the north of the same grid point.

Formally, for every grid point of coordinates (λ_0, Φ_0) we define:

$$GHGS(\lambda_0, \Phi_0) = \frac{Z500(\lambda_0, \Phi_0) - Z500(\lambda_0, \Phi_S)}{\Phi_0 - \Phi_S}, \tag{3.1}$$

$$GHGN(\lambda_0, \Phi_0) = \frac{Z500(\lambda_0, \Phi_N) - Z500(\lambda_0, \Phi_0)}{\Phi_N - \Phi_0} \tag{3.2}$$

where Φ_0 ranges from 30°N to 75°N and λ_0 ranges from 0° to 360°. Φ_S= Φ_0 - 15°, Φ_N= Φ_0 + 15°. Therefore an Instantaneous Blocking (IB) is identified if:

$$GHGS(\lambda_0, \Phi_0) > 0 \qquad GHGN(\lambda_0, \Phi_0) < -10m/^\circ lat \tag{3.3}$$

However, this definition does not provide any information about the spatial or temporal extension of the phenomena which are the main constraints to define a blocking event (Rex, 1950a).

In order to introduce spatial persistence, Large Scale Blocking (LSB) events are defined as IB extended for at least 15° of continuous longitude, a spatial constraint analogous to the one usually seen in the literature (e.g Tibaldi and Molteni, 1990; Pelly and Hoskins, 2003). This allows the detection of large scale blocking events and ensures that the spatial scale of the events is larger than the Rossby radius of deformation.

A Blocking Event is finally defined if a LSB occurs within a box of 10° lon x 5° lat centered on that grid point for at least 5 days. Such criteria ensure that the detected episodes have both significant meridional and zonal extension, are quasi-stationary and persist for sufficient time to be considered as real blocking events. Furthermore, it is possible to compute the duration of every single event for every grid point.

It is worth noting that the Blocking Index described here shows weak sensitivity to changes of the spatial and temporal extents of the definition (i. e. LSB longitudinal extent, box area and time persistence), especially with respect to the localization of the spatial distribution of the Blocking Events. The different methodologies that have been tested during the development of this work suggest that changes in the blocking detection scheme lead only to quantitatively different values of blocking frequency, but they are unable to significantly modify the spatial patterns.

3.1.2 Intensity indices

Two different indices providing a measure of the intensity of the blocking are computed: the Meridional Gradient Intensity (MGI), which is simply the value of the reversed meridional gradient at Z500 as measured by the algorithm of blocking detection, and the Blocking Intensity (BI), a bidimensional extension of the method developed by Wiedenmann et al. (2002). While the former gives a measure of the intensity of the easterly wind to the south of the blocked point, the latter indicates how the meridional circulation is affected by the presence of blocking.

3.1.3 Associated Rossby Wave Breaking

A measure of the direction of rotation of the Rossby Wave Breaking associated with blocking is also obtained. Even if RWB events are usually detected using the reversal of potential temperature gradient at the 2-PVU surface, by exploiting the similarities between them and blocking events presented in the Introduction, we compute a Wave Breaking Index (WBI) in order to detect whether the blocking is associated with a cyclonic or with an anticyclonic wave breaking. More in detail, using the horizontal gradient of geopotential height measured 7.5° south of the blocked grid point, we are able to compute the WBI that distinguishes between anticyclonic IB events (Z500 decreasing eastward) and cyclonic IB events (Z500 increasing eastward). This method, similar to the one adopted by Masato et al. (2011), appears to be consistent with the areas of wave breaking defined in literature (Tyrlis and Hoskins, 2008b; Strong and Magnusdottir, 2008). Moreover, as shown in the Appendix, it is a geostrophic approximation of the method adopted by Kunz et al. (2009b) based on the horizontal stretching deformation.

It is worth highlighting that BI, MGI and WBI are all computed only for Instantaneous Blocking events.

3.1.4 Data

The data used in this Section is the Northern Hemisphere daily geopotential height at 500 hPa. Unless otherwise specified, the data analyzed are from NCEP/NCAR Reanalysis (Kalnay et al., 1996) from which the 60-year period from 1951 to 2010 was selected. Winter season (DJF) data for a total number of 5415 days have been selected.

Data from the European Centre for Medium-Range Weather Forecast (ECMWF) ERA-40 (Uppala et al., 2005) and ECMWF ERA-INTERIM Reanalysis (Simmons et al., 2007) have also been used. The periods analyzed are the DJF 1958-2002 and the DJF 1980-2010 respectively. All data are at the reduced resolution of 2.5° x 2.5°.

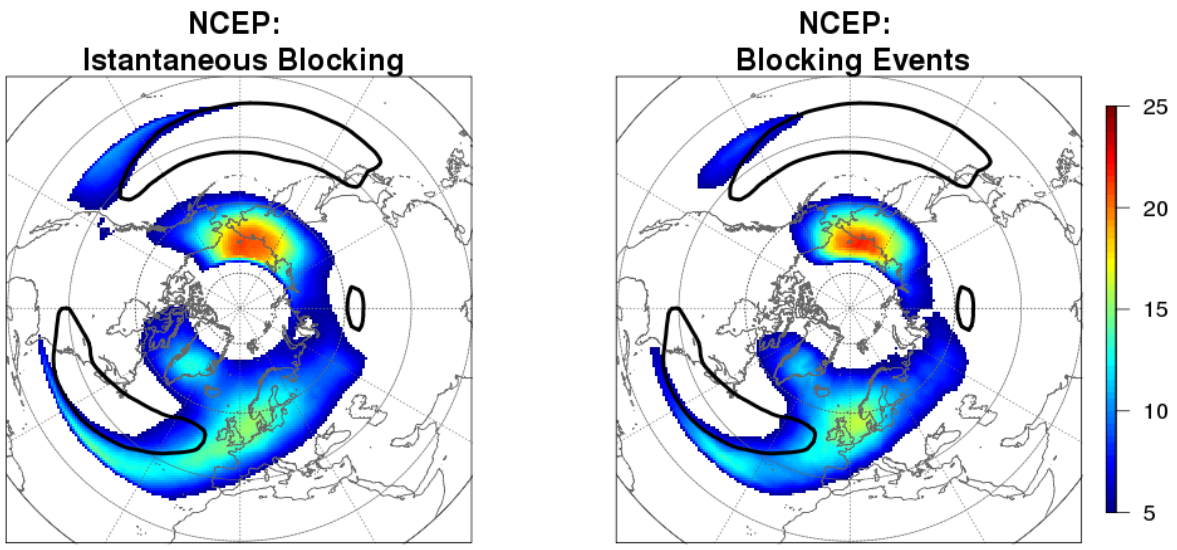

Figure 3.1: *NCEP/NCAR Reanalysis (DJF 1951-2010) Instantaneous Blocking frequency (left panel) and Blocking Events frequency (right panel). Colours are representative of percentage of blocked days with respect to total days. Contours show the eddy driven jets as climatological zonal wind speed higher than 8 m/s at 850 hPa.*

3.2 Blocking Climatology and its assessment with different Reanalyses

The Instantaneous Blocking (IB) climatology is reported in Figure 3.1 (left panel), and it is measured as the percentage of blocked days in the 60-year period examined in the NCEP/NCAR Reanalysis (1951-2010). The well-known high frequency area present over Europe is evident, with a maximum placed between the British Isles and the North Sea. However, IB frequency is dominated by high-latitude events occurring over the North Pacific/Eastern Siberia and over Greenland (defined as High-Latitude Blocking, HLB, Berrisford et al. 2007). A strip of high values of IB develops from the British Isles to the south-west up to Florida at very low latitudes. A similar but less noticeable region of blocking is seen over the Subtropical Eastern Pacific.

The Blocking Events frequency is reported in the right panel of Figure 3.1. Interestingly, the distribution of the blocking frequency is only slightly affected by the introduction of the spatial and temporal constraints. A small reduction of blocking frequency is observed over

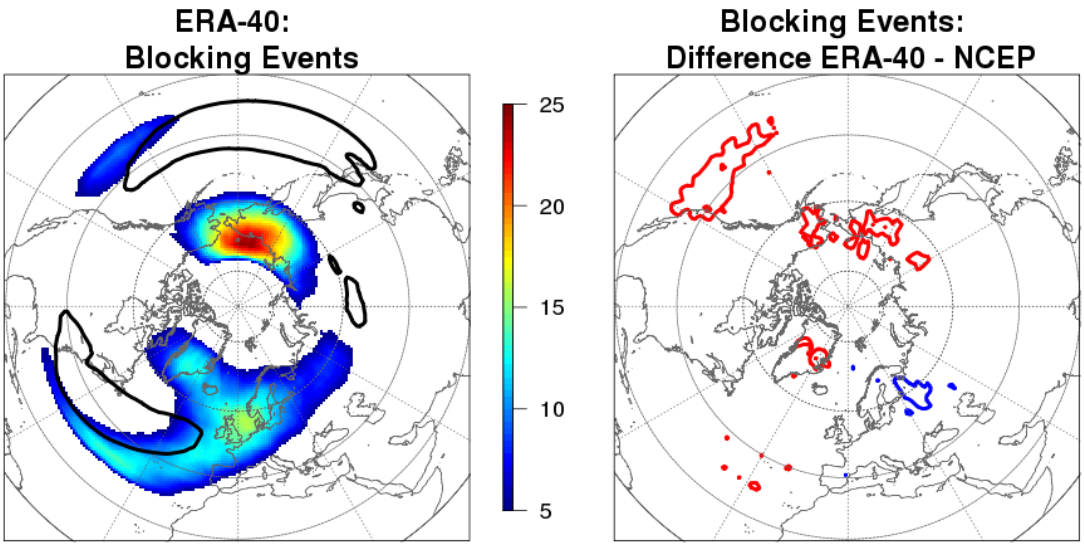

Figure 3.2: *ERA-40 Reanalysis (DJF 1958-2002) Blocking Event frequency (left panel) and difference for the corresponding period of NCEP/NCAR Reanalysis (right panel). Colours are representative of percentage of blocked days with respect to total days. In left panel, black contours show the eddy driven jets as climatological zonal wind speed higher than 8 m/s at 850 hPa. In right panel, red contours indicate positive bias and blue ones negative bias. They are drawn every 1 %.*

Greenland and over the Central Eastern Atlantic (i.e. off the coast of Portugal, suggesting that blocking over this area is smaller in extent and short-lasting) but, overall, the patterns remain unchanged. The adoption of different spatial and temporal constraints just partially affects the distribution of blocking.

In order to strengthen our analysis, other Reanalysis datasets have also been used. In the left panels of Figure 3.2 and Figure 3.3 are reported the Blocking Event climatologies for ERA-40 Reanalysis (DJF 1958-2002) and ERA-INTERIM (DJF 1990-2010) respectively, while in the right panels the differences with respect to the corresponding period of the NCEP/NCAR Reanalysis are shown.

The biases between the different Reanalyses considered are generally very small, of the order of 1% of blocked days. This means relative differences lower than 5-10% in the areas where blocking occurrence is higher. Likely due to the lack of observations, larger differences are recorded over the Pacific Ocean and the Subtropical Atlantic. In any case, the Pearson's

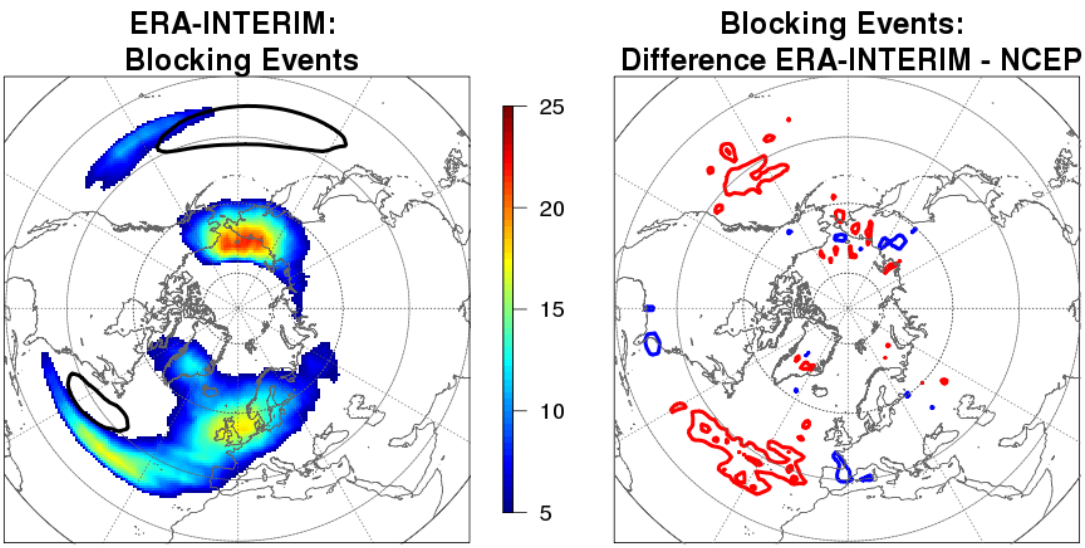

Figure 3.3: *As in Figure 3.2 but ERA-INTERIM Reanalysis (DJF 1980-2010).*

correlation between the 2D blocking daily maps among the different datasets is extremely high (0.9 for both ERA-INTERIM/NCEP and ERA-40/NCEP respectively), confirming the high agreement between the datasets, even on a daily basis.

Recently, Barnes et al. (2011) compared (using the ERA-40 Reanalysis) different blocking indices based on the reversal of the meridional gradient of geopotential height, zonal wind and potential temperature. They concluded that a few differences were emerging among the different indices. Therefore, given the consistency among the reanalyses, the results of Barnes et al. (2011) and the small change in blocking pattern and frequency obtained changing spatial and temporal constraints (see Section 3.1.1), we can state that the blocking index adopted here is robust.

Looking again to the Atlantic region, it is possible to see that the both the ERA-INTERIM and the ERA-40 Reanalyses confirm the existence of two distinct relative maxima, placed over Subtropical Eastern Atlantic and Central Europe. This point will be addressed in the next section.

3.3 Characteristics, variability and trends of Northern Hemisphere blocking

Once the quality of the index and the main characteristics of the climatology has been assessed, it is extremely interesting to analyze the properties of the different sectors of blocking seen in the climatology. Making use of the above-presented diagnostics, in the following section blocking events of the Northern Hemisphere will be studied in order to distinguish them in different categories.

3.3.1 Low Latitude Blocking

As was shown in Section 3.2, the introduction of the Blocking Event definition reduces the climatological frequency of occurrence of blocking over the Central Eastern Atlantic. This reduction acts to distinguish between events over Central Europe and events over the Subtropical Atlantic, suggesting that these latter events may have different properties. This anomalous region of blocking will be hereafter defined as Low Latitude Blocking (LLB), and will include blocking over the Subtropical Eastern Atlantic and the similar events over the Subtropical Eastern Pacific. This new definition is introduced in order to distinguish them from the canonical blocking sectors currently studied in the literature. Since these LLB events have never been discussed in previous works, can they be considered as actual blocking events?

In the literature, long-lasting high-pressure systems over the Eastern Atlantic (40N-50N, 40W-5E) have been defined as Strong Persistent Ridge Events (SPREs) by Santos et al. (2009). LLB events presented here share some features with SPREs (such as persistence and the barotropic anticyclone associated with it), but are detected over a wider area extending equatorward and are less localized and less persistent than SPREs. On the other hand, due to their positioning close to the subtropics, they resemble as well the Rossby Wave Breaking events measured along the subtropical tropopause by Postel and Hitchman (1998).

A foremost characteristic of LLB events can be found by analyzing the Blocking Intensity (BI) index and the Meridional Gradient Intensity (MGI) index. Climatology of these indices are reported in Figure 3.4. MGI, that measures the intensity of the easterly winds south of the block, reaches higher values at high latitudes and very small over the subtropics, with maximum values observed coincidently with the blocking frequency maxima. Conversely,

BI, which provides information on the impact of the blocking on the meridional circulation, shows higher values at the exit regions of the jet streams. Blocking events occurring in those regions strongly divert/block the flow, causing notable circulation anomalies on both the meridional and zonal direction. Concerning Low Latitude Blocking events, since BI and MGI are both small, it is possible to infer that blocking detected south of 40°N are often events with negligible impact on the circulation. Similar considerations can be drawn when the ERA-40 and the ERA-INTERIM dataset are considered (not shown).

Moreover, it is interesting to note that there exists a relationship between the location of LLB events and the average position of the eddy-driven jet stream (shown by the black contour in Figures 3.1, 3.2 and 3.3): in both the Atlantic and Pacific basins, the jet tilts northward toward the end of the storm track in correspondence with the maximum of LLB events. This is evident over the Subtropical Eastern Atlantic, where the frequency of LLB is higher.

Composites of zonal wind and geopotential height during Atlantic LLB events show an increased northward tilt of the jet (not shown) and an enhanced Atlantic Ridge (Figure 3.5, lower left panel). In this panel the composites of the Z500 field (black contours) and their anomalies (red and blue colors) during blocked days during Atlantic LLB are reported. Therefore, the detection of LLB events can be probably interpreted as the development of a strong ridge configuration associated with the poleward displacement of the subtropical

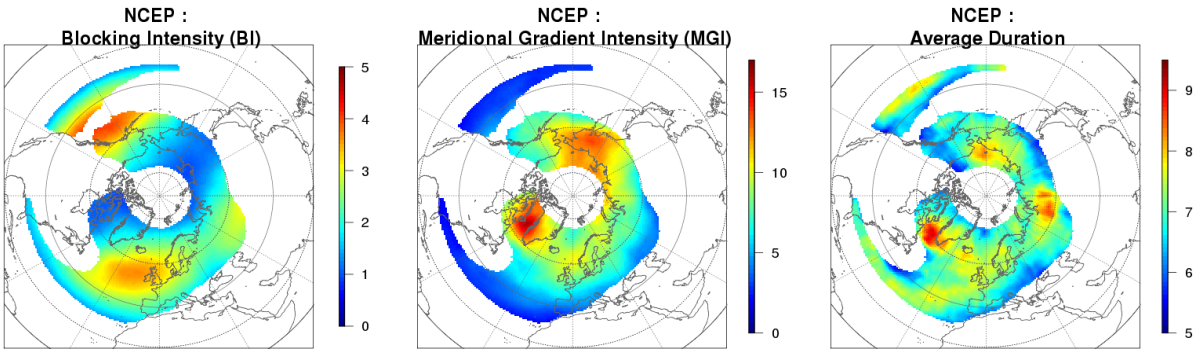

Figure 3.4: *NCEP/NCAR Reanalysis (DJF 1951-2010) diagnostics. From left to right: average Blocking Intensity (BI) index, average Meridional Gradient Intensity (MGI) index and average blocking duration. Only values where Blocking Events frequency exceeds 2% are plotted.*

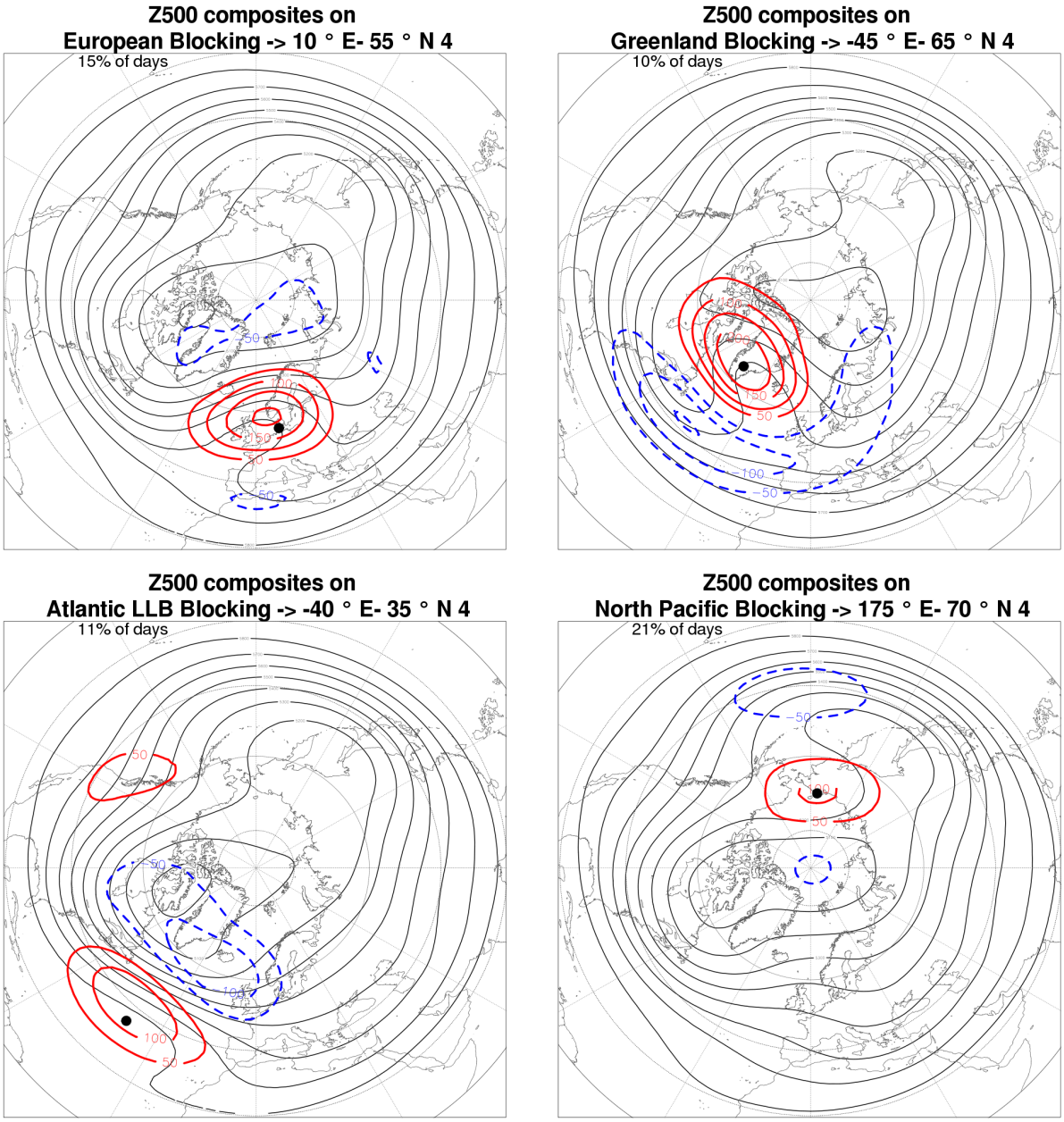

Figure 3.5: *Composites on blocked days of geopotential height at 500hPa. From upper left, clockwise: European blocking, Greenland Blocking, Atlantic LLB and North Pacific Blocking. Positive anomalies are contoured in red, negative anomalies in blue and they are drawn every 50 m. Dots marks the points on which composites are computed.*

easterlies located south of the blocked area. Our interpretation is that LLB represents the transition between the westerly wind regime and the easterly regime typical of the subtropics and it is a consequence of the definition of the blocking index. LLB events are thus generated by fluctuations of the subtropical high pressure systems and do not configure as real blocking events because they are unable to block or divert the flow.

Finally, a supplementary analysis with a slightly modified blocking index was performed (not shown). A further constraint to the south was added: the meridional gradient of the geopotential height between 15° and 30° south of the blocked grid point must be negative (i.e. between 15° and 30° south of the blocked grid point there must be westerly winds). This constraint aims at excluding all blocking events connected with a northward shift of the subtropical easterlies since they are unable to modify the mid-latitude flow. As expected, by applying this modified blocking index, events detected south of 40°N are totally excluded while the global patterns remain unchanged. This confirms the hypothesis that LLB events are linked to northward displacements of the subtropical high.

However, we prefer to keep the original version of our index for two main reasons: firstly, we would like to address more in detail the role and properties of the LLB events and try to investigate their phenomenological differences with respect to blocking over Europe. Secondly, we want to make our work comparable with other previous works (Scherrer et al., 2006; Buehler et al., 2011).

3.3.2 Unique characteristics of the European Blocking

Atmospheric blocking and its impact over the Atlantic basin has been historically analyzed as a unique phenomenon (Tibaldi and Molteni, 1990; Trigo et al., 2004). This point of view has been changing in the last years, when a distinction between the two Atlantic relative maxima, one placed over Central/Northern Europe (European Blocking, EB hereafter) and the one over Greenland (Greenland Blocking, GB hereafter) have been pointed out. The latter one has been recently investigated in many works (e.g Woollings et al. 2008). GB events have been defined as High-Latitude Blocking (HLB) since they divert the main westerly flow rather than blocking it.

The analysis of our diagnostics are consistent with this interpretation: it can be noticed in Fig. 3.4 that GB events show very low values of BI and, even if they present very high values of MGI, they are located about 20° north of the jet stream. This implies that, even

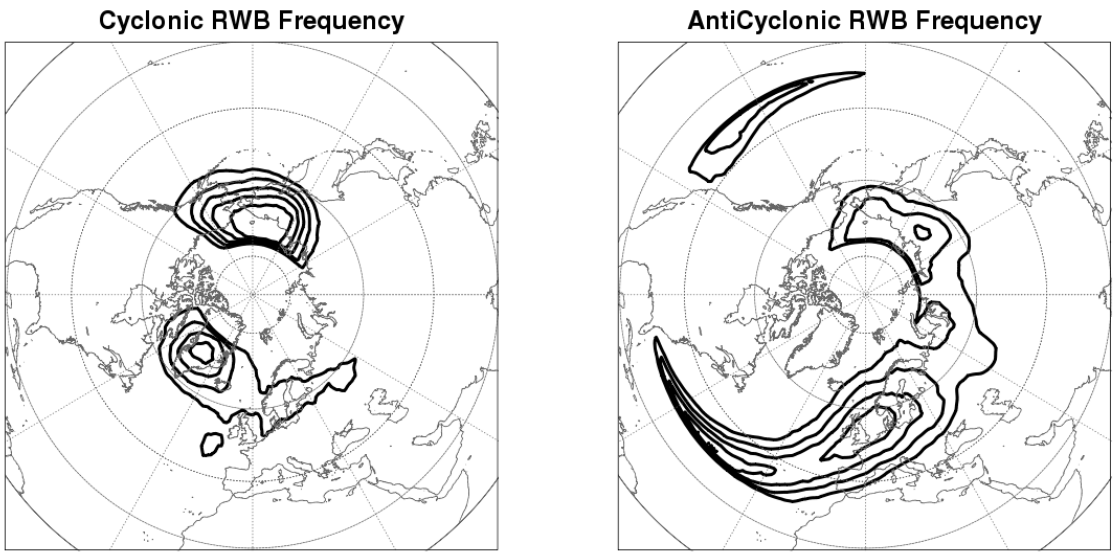

Figure 3.6: *Cyclonic Rossby Wave Breaking (left panel) and Anticyclonic Rossby Wave Breaking (right panel) as defined by Wave Breaking Index (WBI), represented as percentage of wave breaking days with respect to total days. Contours are drawn from 4% every 2%.*

though they are associated with strong easterly winds, GB events are not able to block the westerly flow because they occur too far north of the jet stream.

Our diagnostics highlight other important distinctions between EB events and GB events. Clear differences are visible if the dominant wave breaking type detected by the Wave Breaking Index (WBI) is examined (Figure 3.6). WBI highlights that GB events are dominated by cyclonic wave breaking while EB ones are dominated by anticyclonic wave breaking. It is important to notice that a sharp transition zone between cyclonic and anticyclonic events cannot be easily demarcated: over Scandinavia and Northern Europe both events are detected (Fig. 3.6). Extremely similar patterns are obtained analyzing ERA-40 and ERA-INTERIM Reanalysis (not shown). This likely occurs since both EB and GB develop from strong Atlantic Ridge configuration (Tyrlis and Hoskins, 2008b; Woollings et al., 2008). As a matter of fact, GB events originate from the retrogression of an anomalous strong Atlantic ridge and they are often anticipated by EB (about half of the cases, not shown).

Looking at the composites shown in Figure 3.5 (GB, upper right panel, and EB, upper left panel), the deformation of the geopotential height field is different, with the clear predominance of the cyclonic wave breaking for GB (Northwest-Southeast axis of the trough-ridge

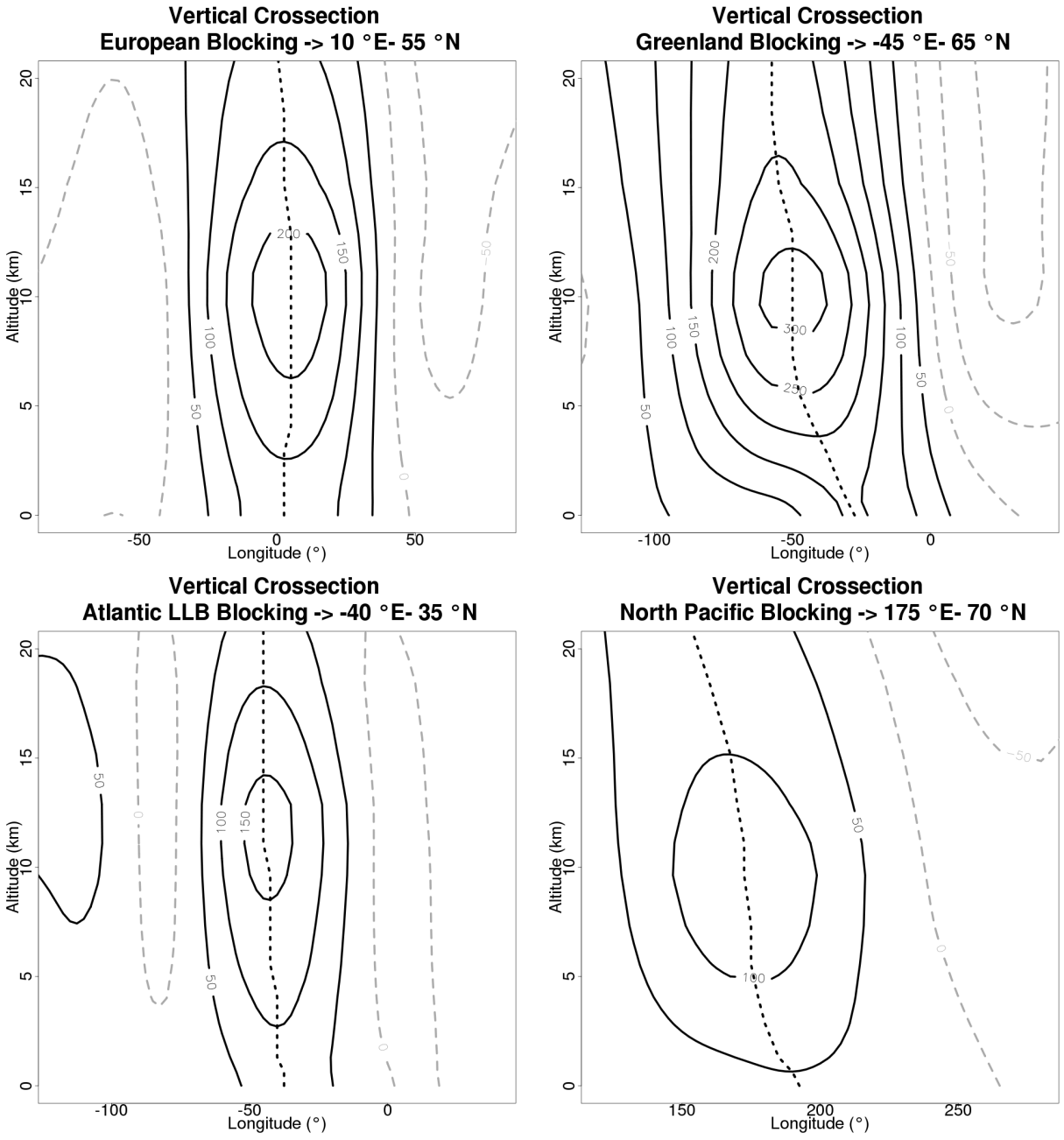

Figure 3.7: *Longitudinal cross section of geopotential height anomalies composited on blocked days. From upper left, clockwise: European blocking, Greenland Blocking, Atlantic LLB and Pacific Blocking. Positive anomalies are contoured in black, negative anomalies in dashed grey and they are drawn every 50 m. The black dotted line shows the maximum positive anomaly at each level.*

system) and the anticyclonic breaking for EB (Southwest-Northeast axis of the trough-ridge system). The former one is dominated by a dipolar structure while in the latter one the positive anomaly over Central Europe is notably stronger than the double negative anomalies over the Mediterranean and the Arctic Sea.

The average duration of the events (Figure 3.4, right panel) provides further differences between EB and GB: even if long lasting events are detected also over North Pacific/Eastern Siberia, longer duration are observed over Greenland (with high values, higher than 9 days, over the Labrador Sea). European Blocking and Atlantic LLB events tend to be shorter. An area of large (about 9 days) average duration is detected over inner Central Siberia, in a region where in any case few blocks are detected ($< 4\%$). These events can be a consequence of the oscillation of the high-pressure system present over Central Siberia during Northern Hemisphere winter.

In any case, the average duration of blocking events appears to be the most sensitive field to the choice of the period among the ones analyzed up to now. When compared among each other on the same period (1958-2002 for NCEP vs. ERA-40 and 1980-2010 for NCEP vs. ERA-INTERIM, not shown), the datasets show strong similarities, even though NCEP/NCAR Reanalysis presents slightly higher values over Greenland. On the other hand, marked differences are reported among the datasets when the whole period is examined (not shown). This suggests that the long-term variability may play an important role in determining the pattern of this field.

It is worth remarking that the distribution of the duration of the Blocking Events is not Gaussian, but it is sharply decreasing with increasing duration (not shown, Wiedenmann et al. 2002; Barriopedro et al. 2006). In some cases the distribution is "exponential-like", but for many regions the obtained PDF is more irregular (not shown). Therefore it is important to point out the mean value reported is not providing information about the upper tail of the distribution and the related extreme events. Similar considerations may be drawn for the MGI. However, the study of the extreme values is beyond the scope of this study.

Additional differences between EB and GB emerge when the meridional cross-section of geopotential height anomalies during the Blocking Events is studied (Figure 3.7). EB cross-section shows an equivalent barotropic structure while the GB one is definitely tilted (upper left and right panel respectively), similarly as can be observed for blocking over Eastern Siberia/North Pacific (lower right panel). This baroclinic-like feature over North Pacific

and Greenland may be connected to the presence of the underlying Greenland/Siberian landmass that may impact the pressure field at lower levels. Alternatively, it can be possible that blocking associated with cyclonic wave breaking presents a tilted vertical cross-section conversely to blocking associated with anticyclonic wave breaking. Anyway, to shed light on this couple of hypotheses a more detailed case-study-oriented analysis (that goes beyond the goal of this climatological analysis) should be performed.

Interestingly, an analogous distinction of blocking events, as the one discussed up to now between EB and GB over the Atlantic basin, cannot be drawn for the Pacific basin. Here the blocking index detects a single maximum placed over Eastern Siberia (defined as North Pacific Blocking, NPB hereafter). NPB possesses the same features observed for GB, even though it has less impact on the wind field (this latter point is due to the southern position of the Pacific eddy jet stream, which is lying about 10° to the south with respect to its Atlantic counterpart). In fact, GB and NPB events both lie to the north of the eddy-driven jet and both are dominated by cyclonic wave breaking (Fig. 3.6). Moreover, they both show long duration, low values of BI and high values of MGI (Fig. 3.4), and they both have a tilted nature when the geopotential height anomalies cross-section is analyzed (Fig. 3.7, lower right panel). As GB, NPB usually appears as a dipole of high and low pressure systems on the northern flank of the jet stream (Fig. 3.5, lower right panel) and originates from the amplification and the subsequent retrogression of the local ridge (i.e. the Alaskan Ridge).

These findings lead to two important considerations: firstly, it emerges clearly that North Pacific Blocking is unable to block the westerly flow and it acts only in diverting it. Therefore, as its Atlantic counterpart GB, it must be considered as a group of High Latitude Blocking events. Secondly, it is possible to conclude that no Pacific counterpart of EB exists. This striking difference between the two basins may have its origin in the separation between the eddy-driven jet and the subtropical jet present over the Atlantic basin, probably arising from the orographic effect of the Rocky Mountains (Brayshaw et al., 2009), that cannot be found over the Pacific. Here eddies are trapped by the subtropical jet, suppressing the meridional wave propagation and therefore reducing the presence of mid-latitude Pacific blocking. (Nakamura and Sampe, 2002; Eichelberger and Hartmann, 2007).

The bulk of events over the Pacific are indeed HLB-like, and the actual blocking, the one that is really able to block the flow, is instead occurring farther south and east, as shown also by Pelly and Hoskins (2003). This region is detected by the large values of both

intensity index, BI and MGI, and it is found over Eastern Pacific, at the end of the storm track (Fig. 3.4). These blocking events show in any case very low climatological frequency ($< 4\%$): therefore, we conclude that the European Blocking can be considered as the "real" mid-latitude blocking event (i.e. the only able to block the westerly flow), whereas the other ones can be interpreted as HLB.

This conclusion partially conflicts with past climatological analysis of blocking carried out with 1-dimensional indices (Tibaldi and Molteni, 1990; Barriopedro et al., 2006). These indices, which traditionally measure blocking at 60°N, usually detected two maxima of blocking activity, one over Central Europe and the other one over the North Pacific (around 160° - 180° E). We argue that Pacific HLB events rarely onset and develop a few degrees south of the climatological maximum (around 70°N), thus generating the false mid-latitude peak reported by 1-dimensional blocking indices.

It must be highlighted that the proposed distinction between HLB and EB events is not merely geographic, but, as presented above, is based on strong phenomenological differences: different durations, wave breaking type, intensities and cross-section all suggest that the distinction between HLB and EB events could be due to different physical mechanisms operating in blocking development.

3.3.3 Inter-annual Variability and Trends

Since blocking can have a large impact on the weather pattern and sometimes can lead to the occurrence of extreme events, quantifying the variability and the possible changes in the preferred location of blocking occurrence is a high priority. For this reason, in the last part of this work the analysis of the inter-annual variability and of the related trends of blocking is presented. This was done by adopting the 60-year period of the NCEP/NCAR reanalysis and averaging the considered fields on a yearly basis.

The inter-annual variability of the Blocking Events, which is expressed through the standard deviation of the yearly frequency of occurrence for each grid point, is reported in the upper right panel of Figure 3.8. Large values are recorded (> 7 % of blocked days, that considered an average 15% of blocked days per season means almost a 50% of relative variation) over the main sectors of blocking. Interestingly, slightly smaller values are present over Central Europe, shaping the high-value pattern over the Atlantic basin in two main bands on the two sides of the jet stream, broadly corresponding with the areas where anticyclonic

and cyclonic wave breaking dominates.

In the upper left panel of Fig. 3.8 the linear trends of the yearly blocking frequency are shown. Due to the high year-to-year variability, just few areas show significance at the 90% level (shown by the black contours). However, a marked increase is observed for the Atlantic LLB (0.2 % per year, which means in 60 years almost a 80% relative increase of blocking occurrence in that area). Over Siberia a general reduction of blocking frequency is observed. In addition to this, an increase/decrease dipole associated with an Eastward shift is seen over Pacific, and a similar but weaker pattern is notable over Greenland. Indeed, the general low level of significance observed suggest that is likely that no trends are present, especially for mid-latitude blocking. The only region where the trend is significant is the Atlantic LLB region. As shown by Ndarana et al. (2012) for the Southern Hemisphere, Rossby wave breaking trends are associated with displacements of the jet streams. Therefore, this increase is consistent with the observed poleward displacement of the Atlantic jet (Archer and Caldeira, 2008; Woollings and Blackburn, 2012).

A similar analysis was carried out by studying the variability and the trends of the Blocking Intensity index (lower panels, Fig. 3.8). The variability appears to be smaller with respect to blocking frequency, and interestingly higher values are recorded about 10° north of the climatological maximum. Likely due to the smaller inter-annual variability, the trends of the BI index are clearer and more robust. In the Pacific basin there is an evident eastward shift of the area of maximum intensity, towards British Columbia (shown by the blue/red dipole). A weaker dipole is evident also over the Atlantic sector, where it is observed a stronger increase over Europe suggesting the possibility of an increase rather than a shift.

The BI maximum values are recorded in the exit region of the jet streams and, by definition, the BI measures how much the circulation is affected by the blocking. Therefore, we argue that this observed change could be associated with a trend in the strength and the zonal extension of the jet stream. In any case, deeper investigation of this hypothesis goes beyond the scope of this study. Finally, it is worth noting that the same procedure has been carried out with the MGI index. However no significant trend was detected with this diagnostic (not shown).

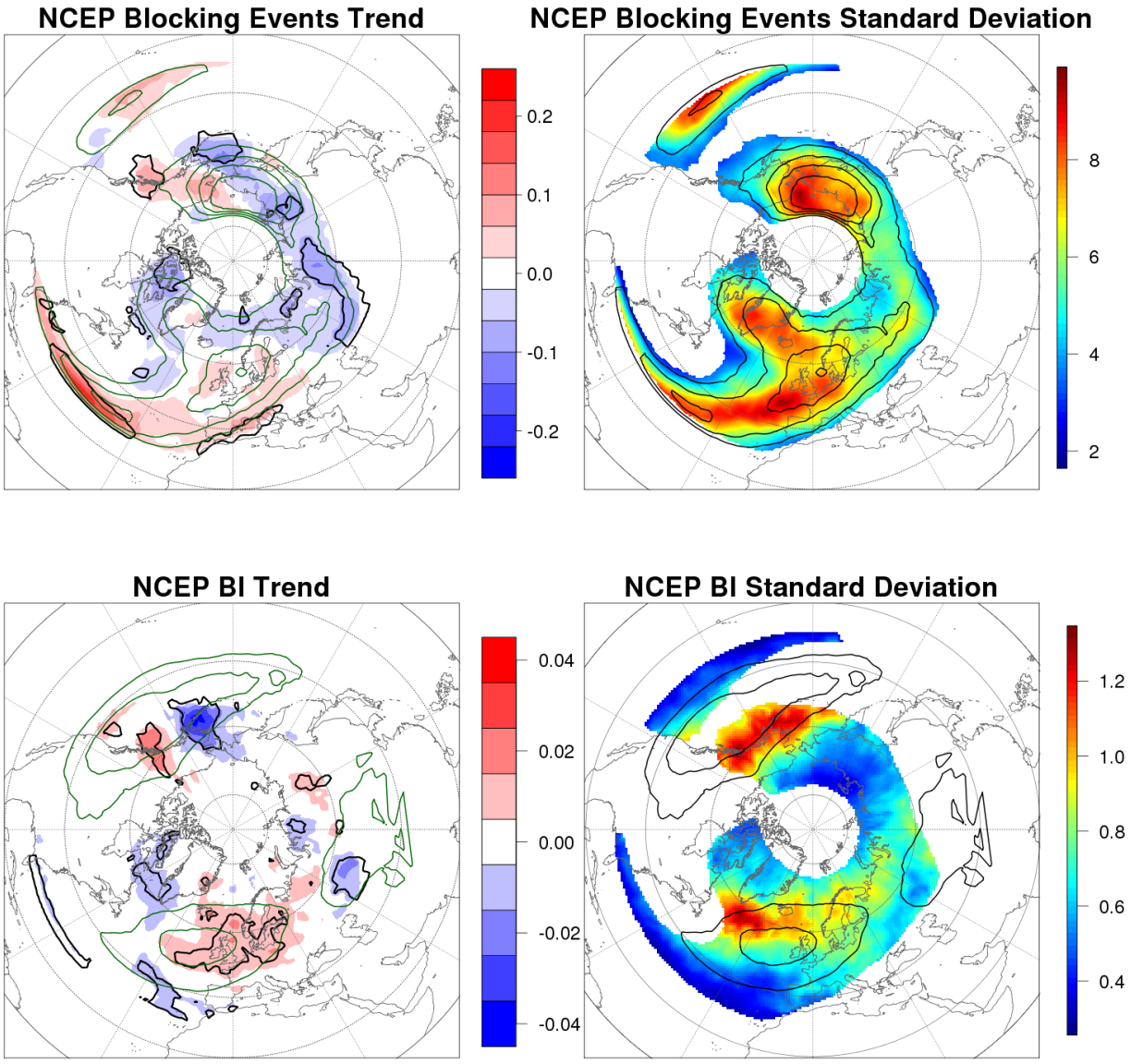

Figure 3.8: *Left: Blocking Events (upper panel) and Blocking Intensity (lower panel) trends in the NCEP/NCAR Reanalysis (DJF 1951-2010) computed on yearly basis. Units are percentage of blocked days per year and BI value per year respectively. Black contours show the 90% significance level and dark green contours are the climatologies. Right: Blocking Events (upper panel) and Blocking Intensity (lower panel) standard deviation. Black contours are the climatologies. In all figures, only values where Blocking Events frequency exceeds 2% are plotted.*

3.3.4 Discussions

In this chapter a new bidimensional blocking climatology based on the reversal of the meridional gradient of the 500-hPa geopotential height was presented. An analysis of NCEP/NCAR Reanalysis was carried out using data for the winter season (DJF) throughout 60 years (1951-2010). Data from the ECMWF Reanalysis (ERA-40 and ERA-INTERIM) have been adopted as well in order to increase the robustness of the results. Several diagnostics providing information about characteristics of blocking have been computed: blocking intensity, its duration and the type of wave breaking associated with it.

The set of diagnostics presented here provides a large source of information that allows us to define 3 main categories of blocking events. The first case, blocking occurring on the poleward flank of the jet stream was defined as High Latitude Blocking. HLB events occur mainly over Greenland (Greenland Blocking) and over Eastern Siberia (North Pacific Blocking). They represent the largest number of events detected by the blocking index adopted here, and they are characterized by the fact that they are just able to divert the jet stream equatorward (instead of blocking it) and by the cyclonic Rossby wave breaking associated with them. Moreover, their longitudinal geopotential cross section is tilted showing a baroclinic feature.

A second category of blocking-like structure was defined as Low Latitude Blocking: this category contains all events adjacent to the subtropics, approximately south of 40°N. LLB are signatures of the oscillations of the subtropical high and the corresponding flow reversal. These events, occurring mainly over Central Eastern Pacific and Atlantic, are unable to block the flow and they seem also unable to divert it, thus having an almost negligible impact on the mid-latitude weather pattern. They are barotropic and associated with anticyclonic Rossby Wave Breaking, and their signature is an enhanced subtropical ridge.

The last group of blocking events is the one that splits the flow and typically occurs at the mid-latitudes. Our analysis suggested that only events over Central Europe could be defined as "real" mid-latitude blocking events; these events are classified as European Blocking (EB). EB shows a signature similar to Atlantic LLB events, with an enhanced barotropic ridge associated with an anticyclonic-wave breaking. Interestingly, this region of blocking (lying on the equatorward side of the jet stream north of 40°N) is not confined into a small region but originates from the breaking of the Atlantic ridge, which can occur from 30°E to 20°W. Therefore even though EB events appear to have similar phenomenological

characterization with our diagnostics, they can have various effects on the weather pattern. Moreover, we argue that also the Atlantic LLB events over the Azores can be originated by the same kind of wave breaking as the EB, but those events are associated with wave breaking occurring too equatorward to effectively impact the mid-latitude westerly flow.

It is worth highlighting that the phenomenological differences here discussed among LLB, EB and HLB are evident also in the ERA-40 and ERA-INTERIM dataset, and that the relative differences among datasets are in the order of the 5-10%. This provides a proof of the robustness of the diagnostics adopted. However, the long-term variability of the blocking activity leads to evident differences if the whole datasets are compared (as for instance in the case of ERA-40 and ERA-INTERIM).

In the last section of the work a strong inter-annual variability emerged from the analysis of the Blocking Events yearly timeseries. Even though such variability does not allow an easy detection of significant trends in Blocking Events frequency, a marked increase is observed for Atlantic LLB events, while at high latitudes several areas of decreased blocking frequency are identified. The trends reported for the Blocking Intensity are more evident, suggesting an increased intensity of Blocking Events over Central Europe and British Columbia. This last feature could potentially have some influence on the extreme events over those regions.

In conclusion, this new blocking climatology offers a detailed phenomenological characterization of blocking behavior, but other main aspects still need to be investigated to gain a more complete understanding of blocking.

For instance, the climatologies and the associated diagnostics presented here can be used to investigate in detail the relationship among the main teleconnection patterns (in first place the North Atlantic Oscillation) and the effect that blocking has on the Atlantic and Pacific eddy-driven jet stream. These latter points will be examined in the following Chapter.

Chapter 4

Euro-Atlantic blocking and its impact on mid-latitude climate

The Euro-Atlantic region shows a great amount of natural variability, characterized by several atmospheric phenomena acting on different spatial and temporal scales, ranging from synoptic scale cyclones up to large-scale planetary wave oscillations.

This is due to the fact, as pointed out in Chapter 3, that the Euro-Atlantic region is characterized by a peculiar atmospheric circulation. It is the only part of the Northern Hemisphere where it is possible to observe a clear separation between the eddy-driven and the subtropical jet streams. This configuration is very likely responsible for the high frequency of the observed atmospheric blocking over Europe, that makes this region the only one where it is possible to observe a significant mid-latitude blocking frequency in the Northern Hemisphere. The presence in the same basin of European, Atlantic LLB and Greenland blocking makes the analysis of this sector extremely challenging.

Moreover, Euro-Atlantic blocking can have large impacts on the weather pattern of the European continent, leading to strong anomalies in both temperature and precipitation. These anomalies are particularly strong during the winter season, when the thermal contrasts between land/sea and high/low latitudes are strongest.

Therefore it is of undoubted importance to analyze the properties of Euro-Atlantic blocking and how it relates with other main elements of the climate. In this chapter we will focus on the relationships existing among atmospheric blocking, the Atlantic jet stream variability and the North Atlantic Oscillation. In Section 4.1 a special attention will be awarded to the

relationship between European blocking and the displacements of the eddy-driven jet stream. Hence Section 4.2 will be focused on the coupling between the negative phase of the NAO and Greenland Blocking, with a special regard to the spatial variability of the NAO pattern.

4.1 Blocking and the Atlantic eddy-driven jet stream

The Atlantic eddy-driven jet stream is one of the main components of the mid-latitude climate and its oscillations and displacements are a major source of variability for the whole Northern Hemisphere. The fundamental dynamics concerning its existence have been described in Section 1.2.2. However, many works in the literature devoted a special attention to the characteristics of its variability and to its relations with the Euro-Atlantic teleconnection patterns.

In recent years, many works studied the latitudinal position and the persistence of the Atlantic eddy-driven jet stream (Barnes and Hartmann, 2010b; Barnes et al., 2010; Kidston and Vallis, 2010) and the association between the jet shifts and the North Atlantic Oscillation (Strong and Davis, 2008; Athanasiadis et al., 2010).

Much of the wintertime Euro-Atlantic variability can be associated with the low-level westerly winds blowing over the Atlantic ocean. Woollings et al. (2010b) analyzed the displacements of the Atlantic jet stream in association with the occurrence of Rossby Wave Breaking (and consequently, with blocking). They found a trimodal distribution of the latitudinal position of the eddy jet stream, detecting a central "non-perturbed" state of the jet and two different equatorward and poleward preferential positions. While the equatorward one seems to be tightly coupled to the occurrence of GB events, it is harder to find a blocking region clearly linked to northward jet displacements. Indeed, they suggested that European Blocking is decoupled from the Atlantic jet stream.

Starting from the work of Woollings et al. (2010b) and exploiting the climatology developed in Chapter 3, the purpose of our work is to address the relationship between atmospheric blocking and Atlantic jet stream displacements with a special focus on the role played by European Blocking. This relationship will be investigated using daily data from the NCEP/NCAR Reanalysis (Kalnay et al., 1996) and from the climatology presented in Chapter 3. The period analyzed spans over 55 years, for the winter seasons (DJF) from 1951 up to 2005, in order to be compared with the historical simulations of the models participating

to the CMIP5 project (see Chapter 5).

4.1.1 The Jet Latitude Index

To study the daily changes of the position of the eddy-driven jet stream, we introduce the Jet Latitude Index (JLI) following Woollings et al. (2010b). The JLI is used to study the influence of blocking events occurring in different region of the Euro-Atlantic basin on the position of the jet stream. The JLI expresses the latitude of the zonally averaged maximum of the zonal wind speed between 60° W and 0° longitude. The zonal wind speed is vertically averaged from 925 hPa to 700hPa. The daily values of the JLI is a measure of the latitudinal position of the Atlantic eddy-driven jet, each day. For our work a slightly different version of this index is adopted, based on 5-day running-mean data and on absolute latitude values. In addition to the daily latitudinal position, we will make use of the daily value of zonally averaged maximum of zonal wind speed in order to provide information on the jet strength.

Figure 4.1 (left) shows the DJF blocking climatology over the Euro-Atlantic region for

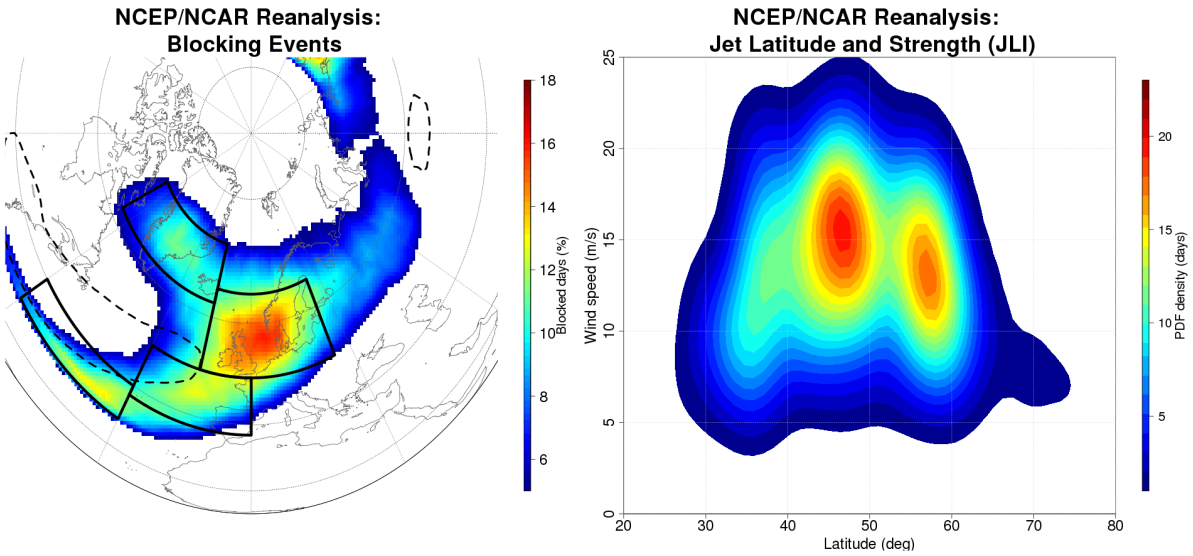

Figure 4.1: *Left panel: blocking events frequency. Colours are representative of percentage of blocked days per season. Dashed black contours show the eddy driven jets as climatological zonal wind speed higher than 8 m/s at 850 hPa. Filled black contours show the Atlantic LLB, European, Greenland and Iberian Wave Breaking sectors as defined in Table 4.1. Right panel: 2D PDF of JLI and jet strength. PDF is multiplied by the number of days of the dataset.*

Table 4.1: Sectors for blocking analysis.

Azores (Atlantic LLB)	Europe (EB)	Greenland (GB)	Iberian Wave Breaking (IWB)
60W-30W	15W-25E	65W-15W	30W-0W
30N-40N	50N-65N	62.5N-72.5N	37.5N-50N

the 1951-2005 NCEP/NCAR Reanalysis expressed as the percentage of blocked days. The blocking climatology is extremely similar to the one shown in Figure 3.1 in Chapter 3. It is reported only for completeness since with respect to Fig. 3.1 only the last 5 years of the dataset are not included.

The right panel of Figure 4.1 shows the climatology for the same period for the Atlantic eddy-driven jet stream, expressed via the JLI. It is reported as a bidimensional PDF showing the JLI on the x-axis and the jet speed on the y-axis. With respect with the 1-dimensional JLI PDF reported in Figure 1 of Woollings et al. (2010b) some minor differences can be seen in the proportion of the peaks, with the southern one not clearly evident. However, the trimodal nature of the Atlantic JLI PDF is preserved. The most interesting thing emerging from Fig 4.1 is the higher values of jet speed for the central peak, in the order of 2-3 m/s higher than for the poleward and equatorward peak.

4.1.2 Jet Variability and the role of European Blocking

In order to analyze the relationship between the Atlantic jet stream and the blocking events, we focused our analysis on four lat-lon sectors, whose coordinates are reported in Table 4.1 and whose areas are shown in the left panel of Figure 4.1. Those sectors have been defined as boxes centered around the relative maximum of Blocking Events frequency in the considered area. In addition to the already mentioned GB, EB and Atlantic LLB, a further sector defined as Iberian Wave Breaking (IWB) is introduced. This sector, over Eastern Atlantic off the coast of Western Europe, is similar to the one defined in previous works (Woollings et al., 2010b, 2011) and it covers the blocking area on the equatorward side of the jet that is not included in the EB and LLB sectors.

Using daily data, a sector is considered as blocked when at least one blocked grid point

is detected within the box. Therefore it is possible to create a daily binary timeseries (that provides the blocked or non-blocked state of the sector) for each sector.

Composites on blocked days for the position and strength of the Atlantic jet-stream are computed for each sector and they are shown in Fig 4.2. The upper left panel shows the well-established relationship linking the occurrence of Greenland Blocking with southward displacement of the jet stream (Woollings et al., 2010b). A clear association between blocking and northward jet displacement is found for blocking events occurring over the Eastern Atlantic (IWB, lower left panel)

The 2D PDF for the European Blocking (upper right) is also associated with a northern-most occurrence of the jet, even though the jet can still be found the other positions, with a secondary preference for the equatorward position.

Moreover, excluding the days when a blocking is detected in these three reference regions (EB, GB and IWB), the JLI distribution becomes almost unimodal, as shown by lower right panel of Fig. 4.2. This distribution is very likely representative of the "neutral mean state" of the jet that resembles the "non-perturbed state" proposed by Woollings et al. (2010b). Moreover, when LLB is occurring the JLI PDF (not shown) is very similar to the "no blocking" situation, confirming that these events are unable to divert the jet.

Overall, these findings are partially contrasting the results from Woollings et al. (2010b, 2011), even though they used a different blocking index. They found the same coupling between GB and southward displaced jet, and similar results between IWB region and poleward displaced jet. However, they stated that European Blocking is "remarkably decoupled" from the jet stream, but the results presented here shows that European Blocking is associated with the poleward displacements of the jet.

The reason behind this apparent inconsistency between these two analyses must likely be searched in the different index adopted for the analysis. Indeed, the climatology obtained with the θ-on-2-PVU index, shown in Figure 2 in Woollings et al. (2008), is characterized by a maximum of European Blocking frequency centered over Central and Eastern Europe. Conversely, as can be seen in Figure 4.1, the maximum of European Blocking for the geopotential height index is placed over the North Sea, about 20° westward and 10° northward. It is therefore possible that the events detected in the present work can be associated more actively with jet stream displacements.

The major role played by European Blocking during poleward displacements of the jet is

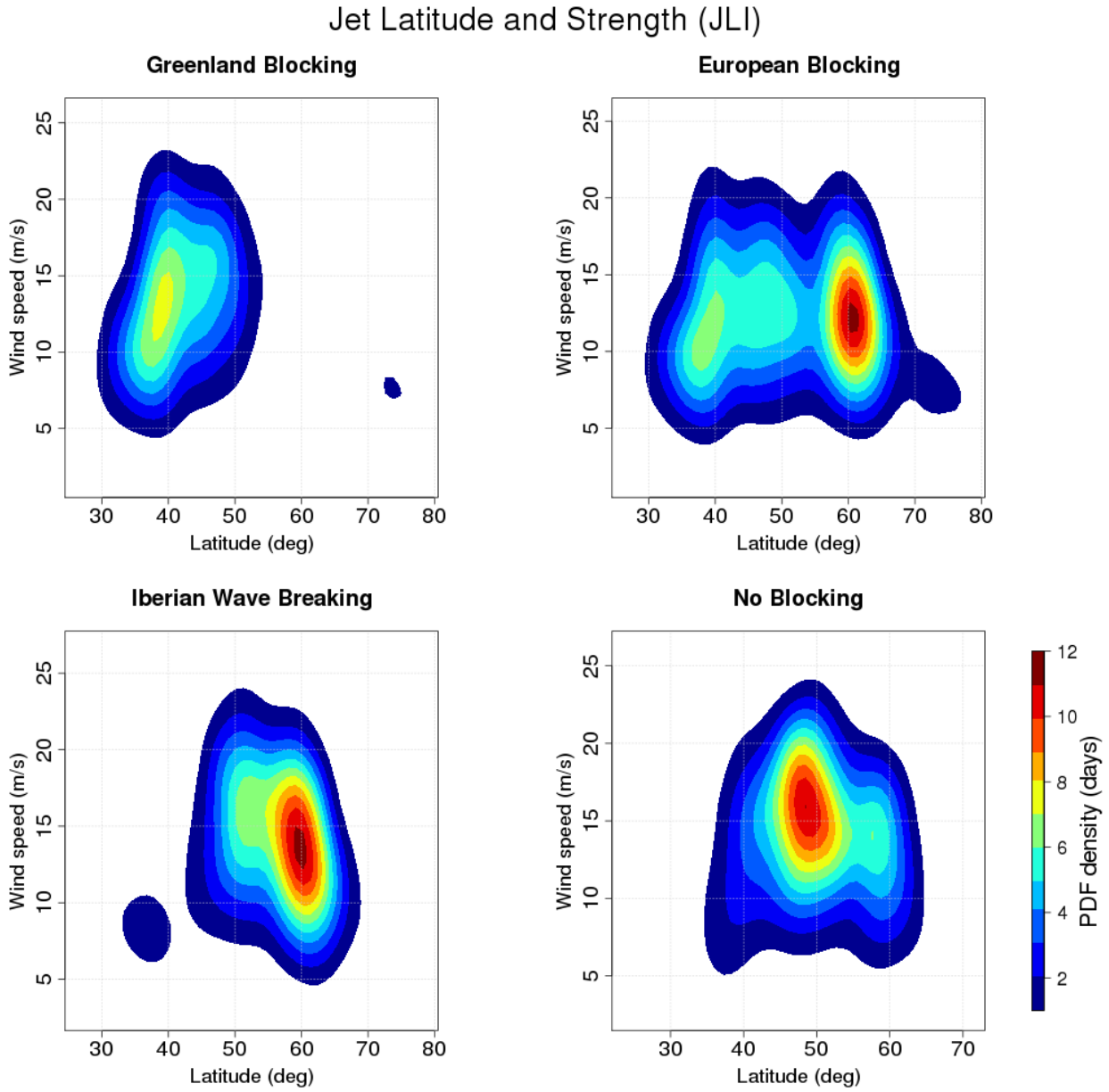

Figure 4.2: *2D PDF of JLI and jet strength composed on blocked days occurring in different sector. From lower left, clockwise: IWB, Greenland, European blocking. Lower right panel shows when no blocking is occurring in neither of the three above-mentioned sector. PDFs are multiplied by the number of days of the dataset.*

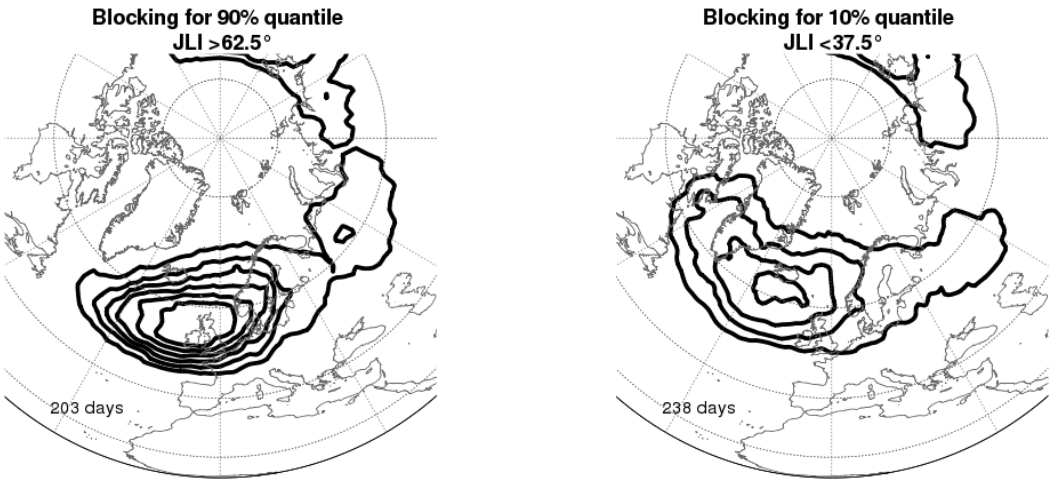

Figure 4.3: *Blocking frequency for days of occurrence of the extreme deciles of the JLI PDF. Left panel is upper tail of the PDF, right panel is the lower tail. Contours are drawn every 10%*

confirmed by the results reported in Figure 4.3. Here the approach is reversed, compositing blocking events frequency on the jet latitudinal position. In left panel the upper tail of the JLI PDF is chosen (maximum poleward displacements) and in the right panel the lower tail is adopted (maximum equatorward displacements). The two tails have been defined as a function of the deciles of the JLI PDF. Similar results have been obtained adopting the extreme quartiles as threshold (not shown). The coupling between the northward jet displacements and the EB events is therefore evident, since the blocking frequency of occurrence for the JLI upper decile reach values around the 80%. These findings strengthen the idea that the displacements of the jet stream in the Atlantic basin are associated with blocking events, and more specifically, that EB is a fundamental element during the northward displacements of the jet stream. More importantly, without blocking occurrence the variability of the jet is confined around its central position (or vice-versa, without jet variability no blocking is occurring).

Looking back at the climatological values of blocking frequency (left panel Fig. 4.1) it is possible to notice that the distinction between the boxes labelled EB and IWB is arbitrary. The area of relative maximum, shaded in light blue, does not present any relative minima that may suggest the presence of different preferential blocking regions. This region is spread

uniformly over Western and Central Europe and has its maximum between Norway and the British Isles. Chapter 4 showed that blocking in this region is all characterized by anticyclonic wave breaking, a barotropic cross-section and similar values of duration. Since in the previous analysis we noticed that both IWB and EB sectors are associated with poleward displacements of jet, we speculate that no phenomenological difference exists between these two sectors.

In order to validate this hypothesis and to understand how much this blocking-jet coupling can be considered linear in space, further analyses have been performed. In the left panel of Figure 4.4, the position of the jet along the region of anticyclonic wave-breaking is studied, as indicated by the red line in the plot crossing South-Eastern Atlantic and Europe. For each longitude, the PDFs of the JLI during blocked days are constructed. The LLB reflects the "non-perturbed" state of the jet, where the jet lies generally around 50° N. This is more or less its average position (Fig. 5.3). While we move along the blocking region (which is associated with anticyclonic wave breaking) the jet is forced to shift northward almost linearly, reaching maximum latitudes of about 65° N, until the EB occurs over the British Isles (about 0° W). Those events split the flow in two branches, one generally lying at about 60° N and the other one at 40° N. However, the jet keeps its preferential position to the north of the block. This last feature very likely occurs because of the nature of the blocking itself, which is generally originated from subtropical air moving north-eastward (not shown) and it is associated with the jet moving farther north. Since the JLI is computed as a zonal average between 60° W and 0°, blocking events occurring further east are independent from the jet.

On the other hand, the behavior of the blocking events at high latitudes, the ones dominated by cyclonic wave breaking, is totally different (right panel in Fig. 4.4). Here the PDF along the red line moving over Greenland and Iceland is computed. During Blocking Events the jet is always constrained to stay equatorward, at about 40°N. Maximum effect is obtained in the areas next to Greenland, but as seen in Fig. 4.3 an important role is played by blocking over Iceland.

The idea that the European Blocking region is dominated by an unique category of Rossby Wave Breaking events fits well with works that highlight the short-persistence of northward displacements of the jet stream in comparison with its southward displacements (Barnes and Hartmann, 2010b). Since the European Blocking occurs in a wide region which extends across several thousands of kilometers, it could act in various ways on the jet position, shifting it

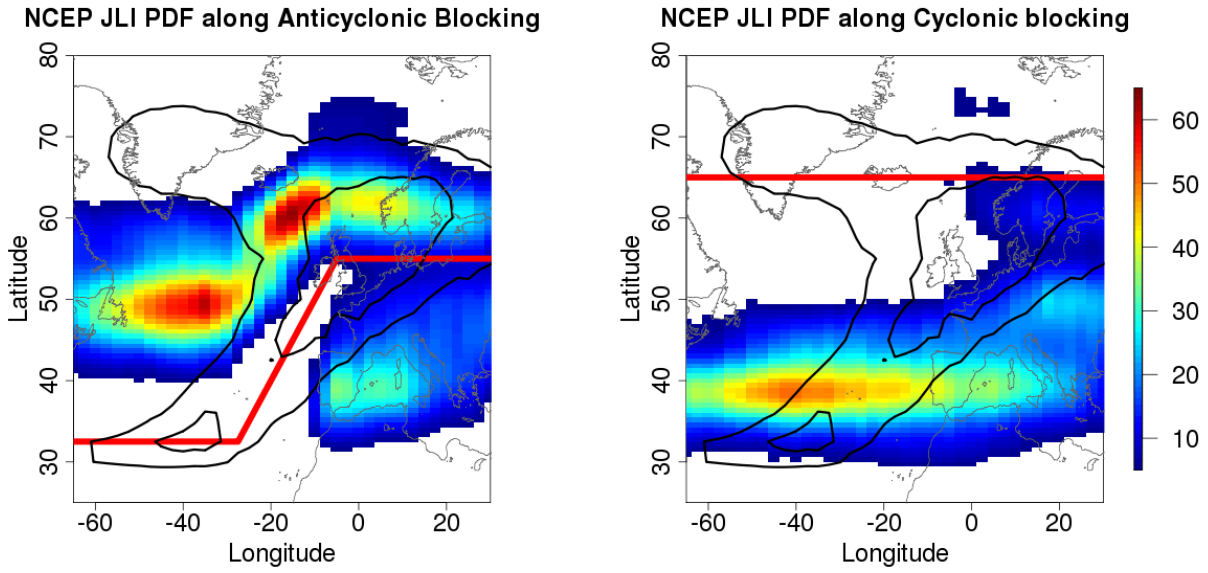

Figure 4.4: *Upper panels: PDFs of JLI during blocked days (colours) for NCEP/NCAR Reanalysis computed for each grid point along the red line. The red line depicts the region of preferential cyclonic (left) and anticyclonic (right) wave-breaking (see text for details). The Blocking Events climatology is represented by contours, drawn at 8% and 12%. PDFs are multiplied by the number of days of each dataset*

northward or splitting it. A new developing blocking in this sector (i.e a new Rossby Wave Breaking) will hardly fall in the same position as the previous one. Therefore, it will not reinforce the previous position of the jet, but will rather tend to move the jet into another position.

Conversely, Greenland Blocking is associated with a more confined jet probably because the event is usually more localized over the Greenland landmass: a new wave breaking will reinforce the preexistent jet position.

This issue is further confirmed by the blocking duration seen in Chapter 3 and plotted in Figure 3.4. Again, the longer duration of Greenland Blocking events with respect to the European ones agrees with the interpretation of Barnes and Hartmann (2010b).

A different approach leading to similar conclusions is shown in Fig. 4.5. The average values of JLI during blocking days over the whole Euro-Atlantic basin is analyzed together with its associated standard deviation for every grid point. Here it is again possible to see that if blocking is detected at 40° N (i.e. LLB events), the jet is placed about ten degrees to

the north with very small variability. Looking poleward of 40°N, it is evident the that more to the north the blocking develops, the more to the north the jet is found. This occurs from the Azores up to the British Isles, where the standard deviation becomes very large abruptly, suggesting very high variability (or more probably a split flow, according to what is shown in Fig. 4.4). On the contrary, the blue colors and small standard deviation at higher latitudes show that blocking over Greenland, Iceland and Eastern Canada favor the southward jet position.

Therefore, from our analysis it emerges as impossible to distinguish blocking events occurring over the whole European area (ranging from the Azores up to Scandinavia). This suggests that the whole anticyclonic wave breaking occurring equatorward of the eddy driven jet is responsible for the northward displacement of the jet and, sometimes of the European Blocking events. Since the jet penetration over Europe can have large variations, it is reasonable to assume that if wave breaking is occurring farther east and north, the subtropical air is able to penetrate over central Europe and the anticyclonic circulation becomes independent

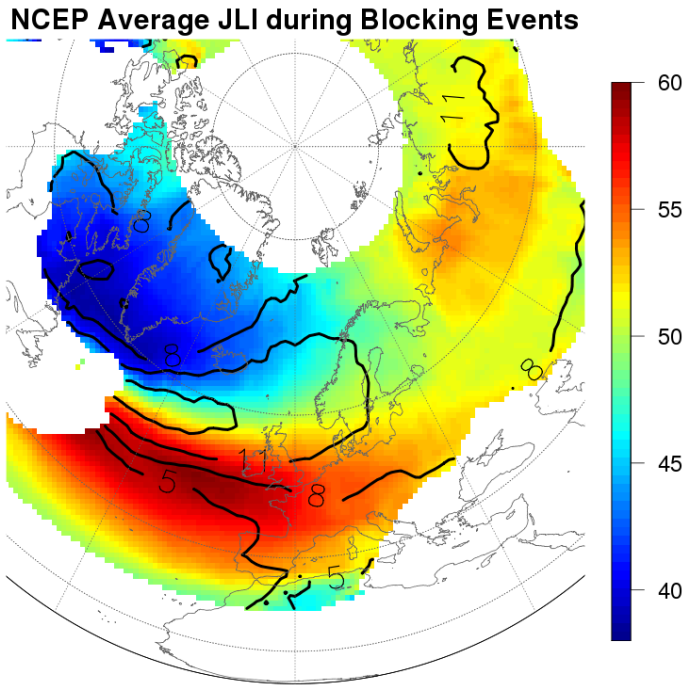

Figure 4.5: *Average JLI for blocked days for each grid point (color) and its standard deviation (contours).*

from the jet, causing the "classical" type of European Blocking.

These findings partially conflict the idea of the four weather regimes over the Atlantic basin (3 jet positions + European blocking; Cassou et al. 2007; Woollings et al. 2010b). The "southward displaced jet / Greenland blocking regime" and the "not perturbed jet / no blocking" are extremely evident also in our analysis. However, with the diagnostics here adopted it is harder to distinguish between the "poleward displaced jet" and the "European/Scandinavian blocking" regimes. We do not state that such distinction is not reliable, since it is demonstrated by several methods of analysis (i.e. EOFs and cluster analysis, Wallace and Gutzler 1981; Cassou et al. 2007), but we argue that, unlike the first two regimes we analyzed, these latter have the same physical origin. Indeed, they are both consequences of the Rossby Wave Breaking on the equatorward side of the jet.

A last consideration regards the JLI during the blocking lifecycle (not shown). We observed on average about two days lag between the beginning of the jet displacement and the onset of the blocking, with the former leading. However, this feature does not provide any information about any cause-effect mechanism, since it is well-known that before blocking onset (i.e. the occurrence of a wave breaking) the Z500 anomaly and its associated wave must amplify and grow. During this stage the jet is already shifting, whilst the reversal of the meridional gradient is not yet observed.

4.2 Blocking and the Euro-Atlantic teleconnection patterns

The North Atlantic Oscillation (NAO) is a major regional pattern of wintertime variability in the Northern Hemisphere. The NAO index describes a dipolar oscillation in surface pressure between the subtropical high-pressure and the mid-latitude low-pressure in the North Atlantic (Hurrell et al., 2003). A more complete description of the NAO has been carried out in Section 1.2.4.

Traditionally, the NAO index has been measured as the pressure difference between the Azores and Iceland (Walker and Bliss, 1932). More recently, following the concept of teleconnection patterns, it has been defined as the Principal Component (PC) timeseries of the leading Empirical Orthogonal Functions (EOF) in Euro-Atlantic sector mean sea level pressure (Wallace and Gutzler, 1981).

Observations show a recent positive trend in the wintertime NAO index, especially through the 1980s and 1990s (Hurrell, 1995). Furthermore, the NAO pattern as represented by different methods (e.g. rotated and non-rotated EOFs analysis, regression analysis, etc.) shows an eastward displacement (e.g Hilmer and Jung, 2000; Jung et al., 2003; Peterson et al., 2003; Zhang et al., 2011), and other studies investigate the origin of this migration (e.g. Luo and Gong, 2006; Luo et al., 2010).

The origin of the NAO remains a widely debated question. Recent studies have reconnected the origin of the NAO to Rossby Wave Breaking (RWB) events, defined as the reversal of the potential temperature gradient measured at the tropopause level (McIntyre and Palmer, 1983). RWB can be classified into cyclonic and anticyclonic events according to the tilt and the direction of rotation of the trough-ridge pair (Thorncroft et al., 1993; Peters and Waugh, 1996). In the same years, RWB have been associated with blocking events (Pelly and Hoskins, 2003; Tyrlis and Hoskins, 2008a).

This emerging linkage between RWB and blocking provides further interest on the works focused on the role of RWB in modulating the North Atlantic Oscillation. Many authors found evidence of a relationship between the NAO and Rossby Wave Breaking (Benedict et al., 2004; Franzke et al., 2004; Riviere and Orlanski, 2007; Kunz et al., 2009a,b). These works suggest that the cyclonic RWB is tightly associated with the negative phase of the NAO, while anticyclonic RWB depicts a positive phase. According to those works, RWB acts as a driver to the NAO, and contributes significantly to determine its phase. However, Strong and Magnusdottir (2008) proposed that in addition to the direction of rotation of the RWB the latitude where the event is occurring is important as well.

In addition to this, a group of recent papers (Croci-Maspoli et al., 2007a; Woollings et al., 2008, 2010c) showed that the phase of the North Atlantic Oscillation is strongly linked with the presence or absence of blocking over Greenland. This interpretation of the NAO as a dualism between a "blocked" and a "non-blocked" state fits notably well, both statistically and physically, with observational data (Woollings et al., 2008). The negative phase of the NAO is largely correlated with the presence of blocking over Greenland (Greenland Blocking), and with an associated southward shift of the eddy driven jet stream, which merges with the subtropical jet.

The NAO phase has also been connected with displacements of the tropospheric jet streams. Woollings et al. (2010b) observed a trimodal variability of the low-level jet stream

and showed that the southward displacements of the jet stream are tightly coupled with the occurrence of blocking over Greenland and with the NAO. In Section 4.1.2 we showed that blocking occurring on the equatorward side of the jet is linked to the northward displacements of the jet.

In the following sections we will address the relationships between blocking, North Atlantic Oscillation and the secondary teleconnection patterns. In Section 4.2.1 we will address the main connection between Euro-Atlantic blocking and the first three teleconnection patterns. In Section 4.2.2 the relationship emerging between the frequency of Greenland Blocking and the pattern of the North Atlantic Oscillation will be addressed in detail. Finally, Section 4.2.3 will provide a statistical interpretation of the eastward shift of the NAO related to the variability of Greenland Blocking occurrence.

4.2.1 North Atlantic Oscillation and Blocking

As mentioned in the Introduction of Section 4.2, several recent works have linked the occurrence of atmospheric blocking to the phase of the North Atlantic Oscillation (NAO). In order to investigate this relationship, we performed an Empirical Orthogonal Function (EOF) analysis of the monthly mean Z500 over the North Atlantic sector (90°W-40°E, 20°N-85°N) and we use the Principal Component of the leading mode of variability to define the NAO index.

The NAO pattern, computed as the linear regression onto the Z500 field, is reported in contours in Figure 4.6. Colors represent the blocking frequency.

In order to compare the NAO index and the blocking frequency, the analysis is focused on the same four lat-lon sectors, whose coordinates are reported in Table 4.1 and whose areas are shown in Figure 4.1 and have been introduced in Section 4.1.

The daily binary timeseries (that provides the blocked or non-blocked state of the sector) for each sector is compared with the daily NAO index timeseries. The Pearson's Correlation coefficients between the daily blocking timeseries and the daily NAO index (and the second and third EOFs) are reported in Table 4.2. Results show a negative correlation between the NAO and the GB measured as -0.53 (significant at 99%,) and a smaller but also significant (99%) positive correlation between the NAO and the LLB/IWB sector (0.37/0.33). Correlation values increase if the monthly and yearly timescales are used instead of the daily ones (not shown). Even though the time averaging reduces the number of degrees of freedom, the

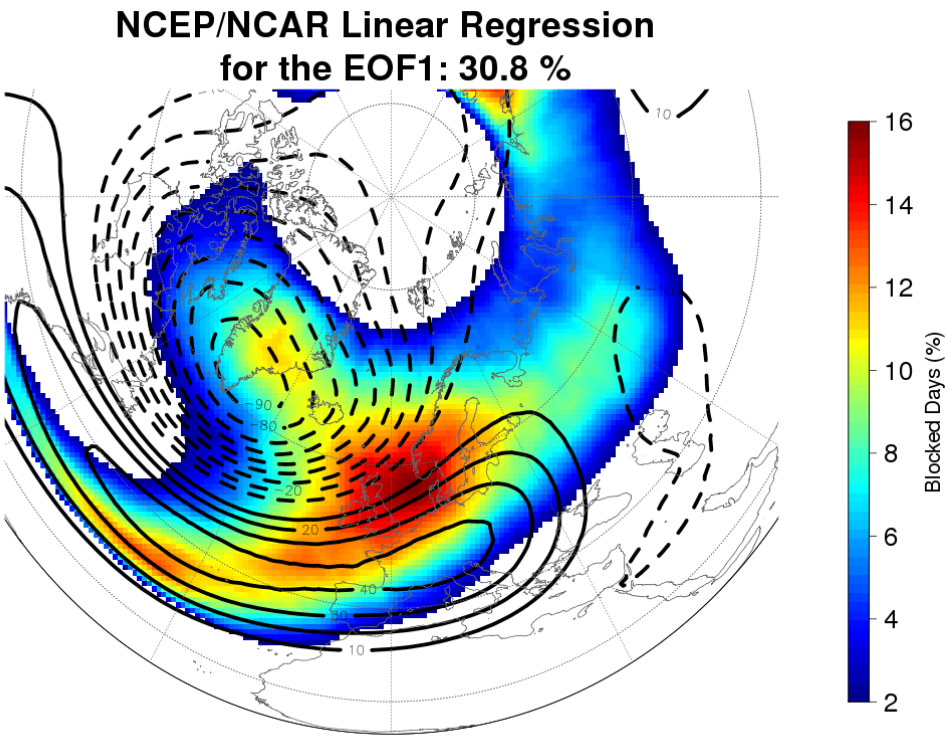

Figure 4.6: *North Atlantic Oscillation pattern shown as the linear regression of the Atlantic (20N-85N, 90W-40E) monthly Z500 EOF1 (contours) for NCEP/NCAR Reanalysis. Blocking Events frequency is shown by colours.*

level of significance remains high (99%). On the other side, no significant correlation (-0.1) is found between the European Blocking and the NAO.

The negative correlation found between GB events and the NAO index is in agreement with the "blocking-dependent" interpretation of the NAO presented by Woollings et al. (2008). They found a correlation between Greenland Blocking and NAO of -0.47.

A further confirmation of the strong link between GB and NAO comes out when the duration of the NAO phases is considered: it is longer for the negative than for the positive phase (Barnes and Hartmann, 2010a). The right panel of Fig. 3.4 shows that blocking over Greenland lasts on average about 2 days more than over other parts of the Euro-Atlantic basin.

Composites on the main fields again indicate that, at least in the NCEP/NCAR Reanalysis, it is hard to distinguish between the negative NAO phase (and its associated weather regimes) and the Greenland Blocking events. To perform such a comparison, the negative

and positive NAO terciles have been used to define a binary daily timeseries. When the daily NAO index exceeds the terciles threshold, the day is considered in the composites, otherwise it is discarded. The resulting timeseries, filtered with a 5-day persistence filter, have been used to compute the 2-m Temperature composites shown in Figure 4.7. The central and right upper panels show how the pattern of 2-m Temperature composites of GB and NAO- are very similar. EB events, reported in the upper left panel, present a weaker impact on the 2-m Temperature, with patterns considerably different compared to those associated with both the NAO phases.

The positive correlation found between IWB events and positive NAO phase is notably larger than the one shown in Woollings et al. (2008) (0.33 vs. about 0.2, see their Fig. 18). This probably occurs because the adoption of Z500 surface to define the blocking index (as done in this work) allows the detection of events at low latitudes, whereas the index based on θ at the 2-PVU surface does not (Woollings et al., 2008). The positive correlation is well reflected by the composites on 2-m Temperature anomalies (Fig. 4.7, lower panels): both the blocking over the IWB sector and the Atlantic LLB 2-m Temperature anomalies patterns are similar to the positive NAO case, though weaker.

It is interesting to point out that the anomalies for the four blocking cases are widespread over the Northern Hemisphere. This is very likely due to the associated displacements of the Atlantic jet stream, which forces a redistribution of the heat by the zonal winds. Since the disturbances on the jet position is more uniform during IWB and GB, it is not surprising that the temperature anomalies associated with these events are larger.

This characterization of the NAO in terms of occurrence of the Greenland Blocking pro-

Table 4.2: *Pearson's correlation values of the entire DJF daily timeseries (4964 days) between blocking occurrence in different Atlantic sectors and the Principal Component of the main Atlantic teleconnection patterns (EOFs).*

Teleconnection pattern	Atlantic LLB	Europe	Greenland	IWB
North Atlantic Oscillation (1^{st} EOF)	0.37	-0.1	-0.53	0.33
East Atlantic Pattern (2^{nd} EOF)	0.03	-0.01	-0.23	0.43
Mid Latitude Anomaly (3^{rd} EOF)	-0.22	0.58	0.06	0.13

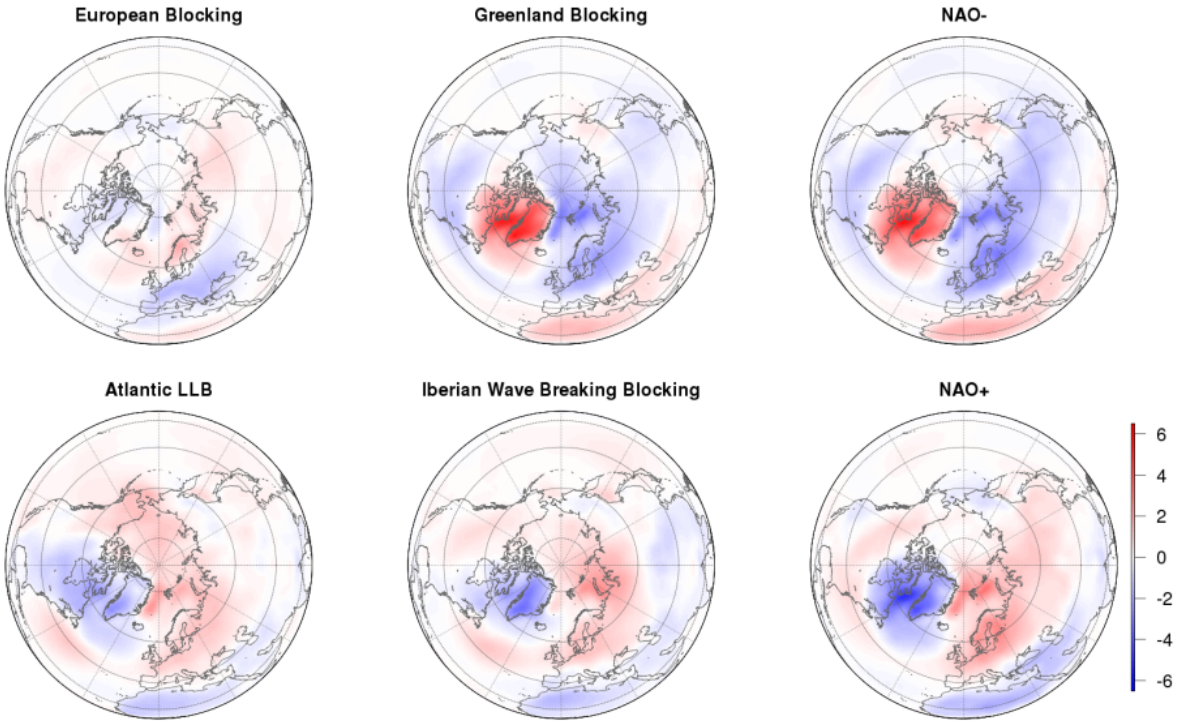

Figure 4.7: *Composites of 2-m Temperature in NCEP/NCAR Reanalysis for different Blocking Events and NAO phases. Clockwise, from upper left, European Blocking, Greenland Blocking, NAO negative tercile, NAO positive tercile, Iberian Wave Breaking Blocking and Atlantic LLB. Red are positive anomalies, blue negative anomalies.*

posed by Woollings et al. (2008) and here confirmed with a different methodology, it is not surprising if we consider the NAO pattern and the Blocking Events frequency together, as in the left panels of Figure 4.6. Figure 4.6 shows the regression pattern of monthly Z500 on the leading North Atlantic EOF (contours) and the Blocking Event frequency (colours). Here the link between GB and NAO is well reflected by the geographical overlap between the Greenland relative maximum of blocking frequency and the negative center of action of the NAO (placed over Greenland and the Labrador Sea).

Interestingly, the link is less evident when the NAO is computed with SLP (not shown). In this case the negative center of action is placed over Iceland. This can be explained by the strong baroclinicity associated with the Greenland blocking (shown in the upper right panel of Fig. 3.5). It is therefore possible to infer that the SLP anomalies associated with the Greenland Blocking are placed about 20° to the East of the blocking maximum. It is also worthwhile to note that this region is very close to Iceland, where the Stykkisholmur station

is located, i.e. the place where the NAO index is historically measured at surface.

On the other hand, the Atlantic LLB is lying in correspondence of the positive center of action of the NAO, consistently with the positive correlation show in Table 4.2.

4.2.2 Modulation of NAO pattern by Greenland Blocking

In order to investigate the impact of the Greenland Blocking on the NAO patterns, we define the Greenland Region as a box placed between 70°-20°W and 62.5°-72.5°N, centered on the climatological blocking frequency relative maximum over Greenland. For each day, if at least a single grid point in the box is blocked, the whole sector is considered blocked. In this way, a daily binary timeseries can be defined and compared with the NAO index. From this timeseries a large and significant anticorrelation (-0.7 on monthly basis) emerges, which is in agreement with Woollings et al. (2008).

After computing the total number of blocking days from the daily blocking index for each DJF season, we split the database into three different categories according to the index terciles. We define "High Greenland Blocking" years (HGB, blocked days over Greenland >30 days, 18/55 years), "Low-Greenland Blocking" years (LGB, blocked days <15 days, 16/55 years) and "Neutral Greenland Blocking" years (NGB, when the blocking frequency is in between the two thresholds).

For convenience, the case in which no selection has been applied (i.e. the whole dataset) has been defined as Original Greenland Blocking (OGB). Since results for the NGB and OGB category are very similar for every analysis performed here, we decided to report the OGB case only.

The blocking climatology and the main Euro-Atlantic EOFs are again computed according to the subset defined as OGB, HGB and LGB. Results are shown in Figure 4.8. The first column shows the EOF and blocking for the OGB case (DJF 1951-2005). The North Atlantic Oscillation and the East-Atlantic pattern are clearly evident in the upper and lower panels (contours), while the blocking frequency (shading) shows the canonical blocking pattern already seen in previous chapters.

The second column reports the patterns for the HGB case. As expected the blocking frequency is almost doubled over Greenland. Moreover, blocking frequency is also higher at all high latitudes suggesting a strong linkage in wave breaking activity on the poleward side of the jet. The pattern of the first EOF is pretty similar to the OGB case, but it shows

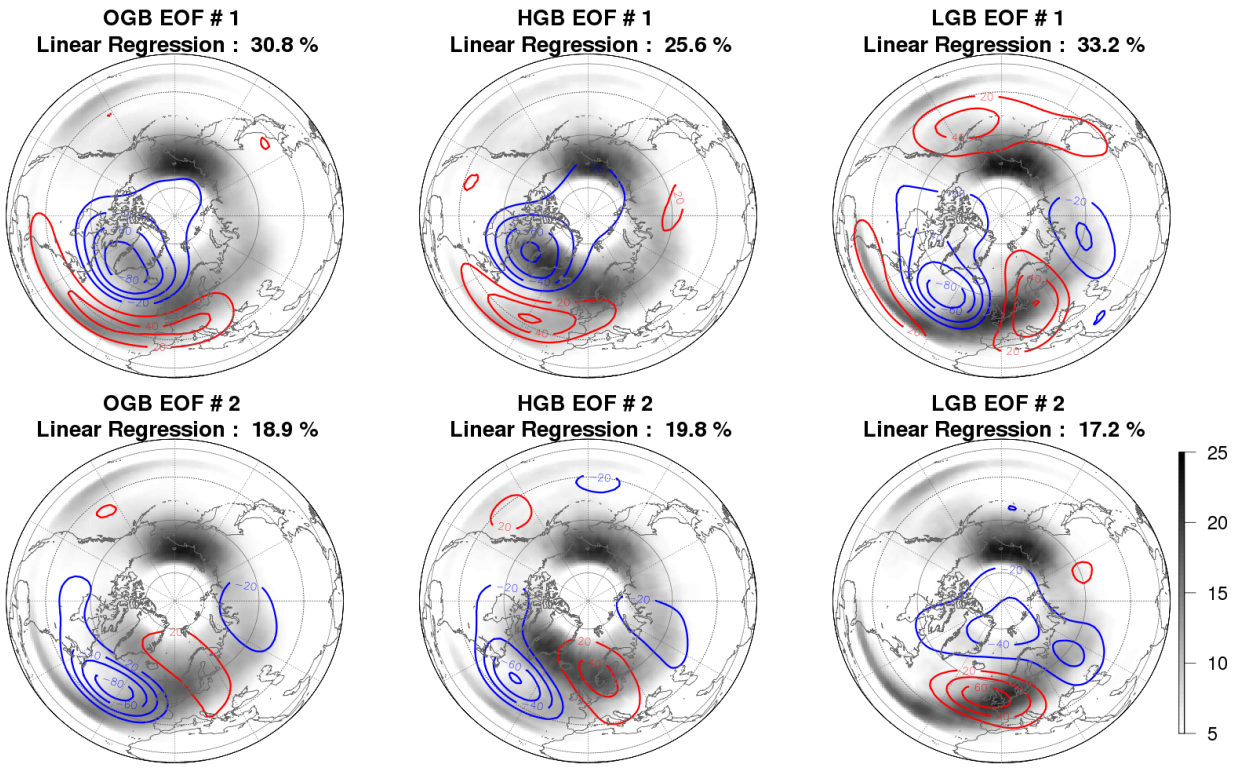

Figure 4.8: *Linear regression patterns on Z500 monthly anomalies for the first (upper panels) and second (lower panels) EOFs for the 3 different categories of GB frequency. Red contours show positive values, blue contours the negative ones. Blocking frequency, expressed as percentage of blocked days, is shown by the gray scale.*

a westward shifted shape, with smaller zonal extensions especially for its positive center of action. The EA pattern is remarkably similar to the one of the original case.

The EOFs of the LGB case reveal a very different NAO-blocking relationship. In particular the first EOF pattern is no longer NAO-like. Such pattern broadly corresponds to the EA pattern shown in the OGB case, but some significant differences are present (larger global teleconnectivity, tripolar anomalies and northward displacement). Interestingly, a NAO-like pattern is detectable in the second EOF, even though it is notably north-eastward shifted, weaker and no longer linked to the occurrence of Greenland Blocking (monthly correlation coefficient between NAO and GB is -0.07).

Therefore, in the absence of Greenland Blocking, the NAO-like pattern associated with the zonal variability is no longer the dominant mode of regional variability over the Euro-Atlantic.

Obviously, the stratified sampling of the dataset performed in order to compute the subset is by construction affecting the EOF-based NAO patterns. It is important to point out that, if the NAO is defined as the one present in the OGB case, the HGB case represents years with negative NAO index while the LGB case represents years with positive NAO phase. This is due to the strong anticorrelation present between the NAO and GB.

It is useful to highlight how this approach shares some features with the one used in (Croci-Maspoli et al., 2007a). They excluded from their dataset the days when blocking is occurring over the Euro-Atlantic sector (80°W-60°E, 20°N-80°N) and then they performed an EOF analysis. They found that the first two EOFs were switched, with the EA pattern explaining more variance. Consequently, they linked the blocking occurrence to the NAO. Our approach provides further information on the localization of this blocking-NAO dependence, suggesting that without GB blocking the NAO is no longer the first EOF.

Adopting the JLI, Woollings et al. (2010b) showed the presence of a strong link between NAO, GB and jet displacements. We apply the same methodology in order to shed light on the connection between the EOF-related statistical variability and the dynamical variability of the jet stream. We especially aim at investigating the behaviour of the Atlantic jet stream under the anomalous EOF1 present in the LGB case. The JLI PDF for the three Greenland blocking categories (OGB, HGB and LGB) during the different phases of the NAO and EA is hereafter analyzed. The positive and negative phases have been defined as the days exceeding the positive and negative terciles of the PC timeseries of each EOF (with a 5-day persistence criteria). The JLI PDFs for the three categories are reported in Figure 4.9. It shows that the variability of the Atlantic jet is lead by a trimodal PDF in latitude (black line). The NAO phase distinguishes between the central peak and the equatorward-displaced peak (blue and green lines), while the EA variability distinguishes between the central peak and the poleward displacement of the jet (orange and red dashed lines). This analysis is consistent with Woollings et al. (2010b), in which they showed that both leading EOFs are needed to completely describe the jet variability. Similar conclusions have been obtained by Athanasiadis et al. (2010) adopting the EOFs of the upper tropospheric zonal wind.

The JLI PDF for the HGB case is shown in the central panel of Figure 4.9. This confirms the link between the negative phase of the NAO and the southern latitudinal position of the jet stream, as pointed out by many studies (e.g. Woollings et al., 2010b). Increased GB frequency is associated with increased equatorward displacements of the jet. On the other

hand, the JLI variability related to the EOF2 (i.e. EA) is similar to the OGB case, here again distinguishing from the central peak and poleward displaced peak.

The LGB case (lower panel, Figure 4.9) shows that with few Greenland Blocking events the equatorward displacements completely disappear. Interestingly, the first and the second

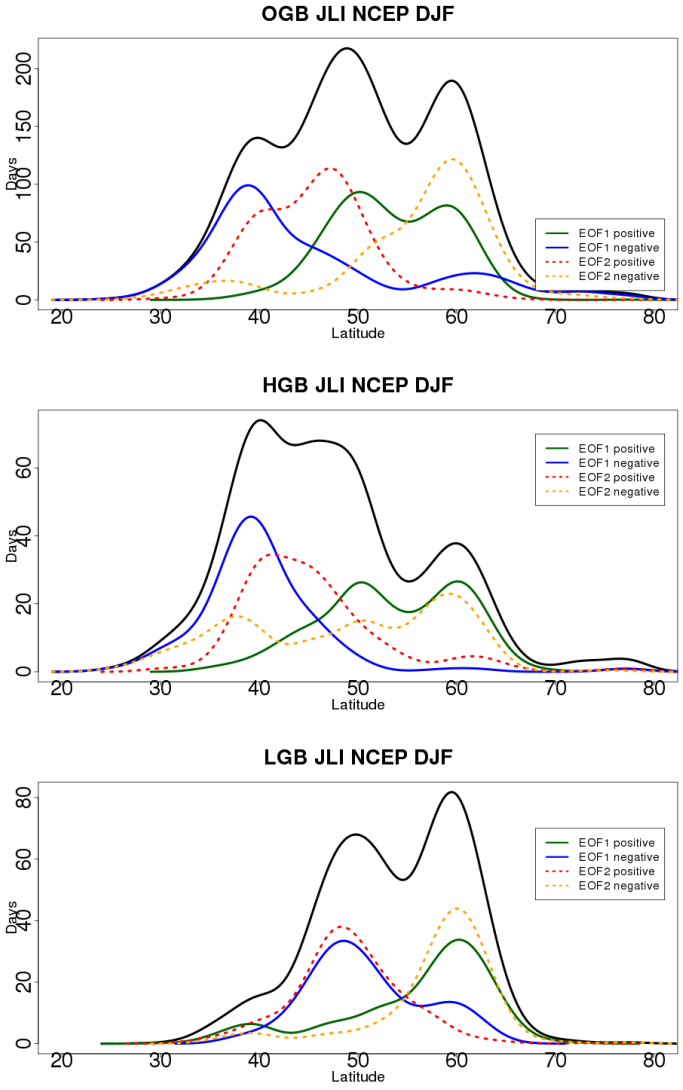

Figure 4.9: *JLI PDF for the three different categories of GB frequency. A gaussian kernel-density estimator with standard deviation of 2° lat has been applied to compute the PDFs. Black lines represent the climatological values of the JLI. Blue line represents the JLI PDF for days during the EOF1 negative tercile, green line for days during the EOF1 positive tercile. Orange and red lines represent the negative and positive tercile respectively for the EOF2.*

EOFs both describe the variability between the neutral state of the jet and the poleward displaced ones. This implies that without Greenland Blocking the variability over the Euro-Atlantic is no longer trimodal, but it is limited to a bimodal pattern. Importantly, this more limited mode of variability precludes the existence of a zonal NAO-like pattern (lower panels of Figure 4.9).

4.2.3 Eastward shift of the NAO

This approach to analyze NAO variability is especially relevant to the numerous studies that have suggested the presence of a recent north-eastward displacement of the NAO, (e.g. Jung et al., 2003; Luo and Gong, 2006). In comparing the EOF1 pattern of the HGB case and the OGB case it is possible to notice that in the latter both the centers of action are shifted eastward with respect to the HGB case. Moreover, the zonal extension of the positive center of action of the OGB case is wider and extends into Western Europe. We speculate that the eastward shift of the NAO pattern is connected with the reduction of the Greenland Blocking frequency.

In order to confirm this hypothesis, we created 35 subsets of 20 years each from the yearly timeseries of GB (covering the 55 years), characterized by decreasing values of the average yearly GB frequency. The subset with the highest average GB frequency (about 45 blocked days) has been created choosing the 20 years with the highest GB frequency (i.e. it is similar to the HGB case) in the whole dataset. We created the other subsets in the following way: first, we removed the highest-frequency GB year from the previous subset. Then, we added the highest-frequency GB year that was not part of the previous subset in order to still have 20 years in the new subset. This was repeated 34 times in order to span the whole 55 years. We finally obtain 35 subsets of 20 years each. The last subset created has an averaged GB frequency of about 9 days, and it is similar to the LGB case.

For each subset we performed an EOF analysis and we identified the location of the minimum and maximum of the linear regression of EOF1. Therefore we were able to detect the geographical shift of the center of action of the NAO as a function of the GB frequency.

In the upper panel of Figure 4.10 it is clearly evident that with progressively higher GB frequency the NAO shifts to the West, especially for its negative center of action that becomes centered over the Labrador Sea (similar to the HGB case).

When the GB frequency is reduced, the negative center of action shifts to the East,

reaching Iceland and then moving to the South. The overall Eastward shift is about 30°.

The movement in the positive center of action is more complex. With high values of GB, it is placed approximately over the Azores. With decreasing values, it is subjected to a small westward displacement but its position remains almost stationary over the Central Atlantic. When a threshold value is reached (about 20 blocked days) it abruptly moves to Central Europe. At this stage, EOF1 is no longer representing a zonal mode of variability, but rather a teleconnection pattern more similar to the classical EA.

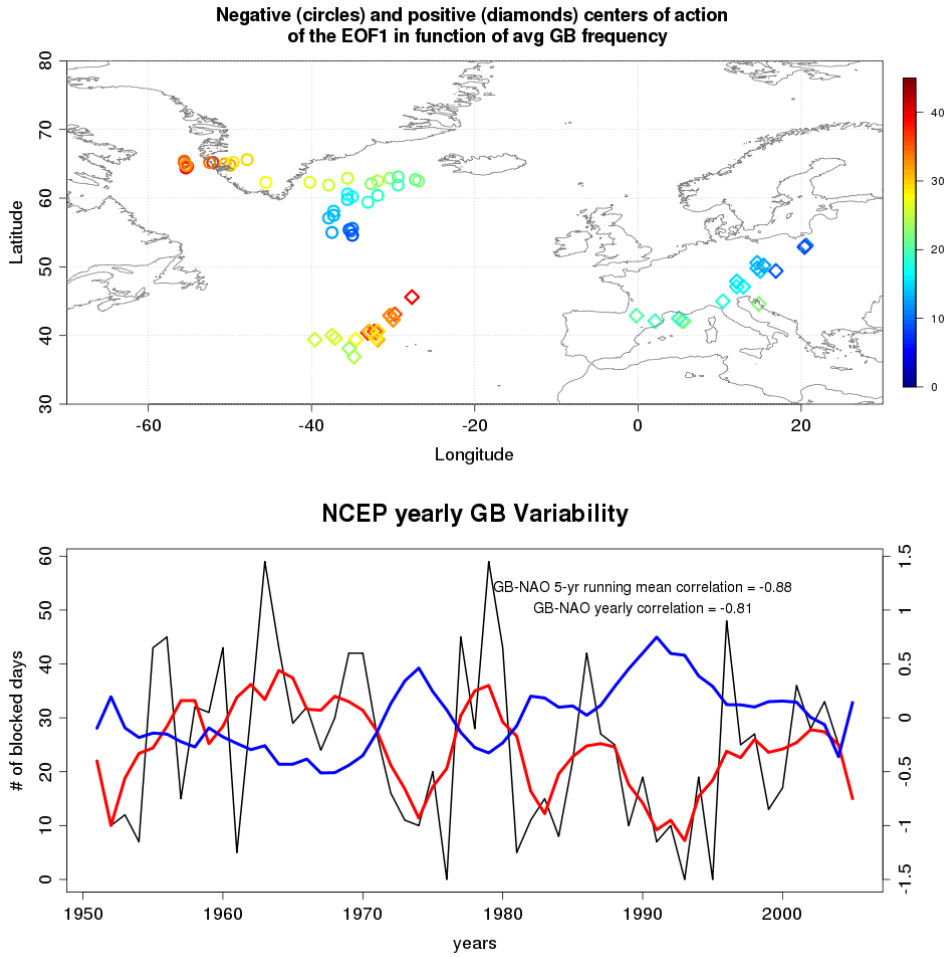

Figure 4.10: *Upper panel: EOF1 centers of action shift as a function of the GB frequency. Circles represent the position of the negative center of action, diamonds the position of the positive one. See text for details. Lower panel: GB yearly frequency measured as number of blocked days (black line) and its 5-year running mean (red line). The blue line is the 5-year running mean of the yearly averaged NAO index.*

Consequently, we argue that the EOF-based North Atlantic Oscillation may be interpreted as the statistical result of the succession of different GB events, and that its pattern and intensity are primarily linked to the frequency of the GB itself. If GB events are more frequent, the incidences of an equatorward-displaced jet are also more frequent and hence the main mode of variability over the Euro-Atlantic sector is mainly associated with the GB occurrence. Alternatively, when the GB frequency decreases, other phenomena become more relevant in determining the NAO pattern and sign.

A logical consequence of this geographical dependence of the NAO pattern to the occurrence of the Greenland blocking may be an explanation of the observed eastward shift during the 1980s and the 1990s. Figure 4.10 (lower panel) shows the Greenland Blocking yearly frequency, its 5-year running mean and the 5-year running mean of the NAO index. It is evident that GB frequency has been affected by a small but constant reduction in the number of blocked days. Even though blocking is a very noisy and variable field, it is evident that GB has reached a minimum during the 1980s and 1990s. Since the reduction of the GB frequency leads to an eastward shifted NAO, the variability in the GB activity observed in the NCEP/NCAR Reanalysis suggests that this eastward shift of the NAO is very likely related to the GB variability.

4.2.4 Discussions

In this chapter we analyzed the relationship among the blocking activity, the eddy-driven jet stream displacements and the main teleconnection patterns over the Euro-Atlantic sector. This was carried out using data from the NCEP/NCAR Reanalysis during the winter season (DJF) throughout 55 years (1951-2005).

Making use of the Jet Latitude Index (JLI) introduced by Woollings et al. (2010b), we showed that the majority of blocking events lying on the equatorward side of the Atlantic jet, characterized by an enhanced Atlantic ridge and by an anticyclonic-wave breaking, are associated with a poleward-displaced jet. Only a few European Blocking (EB) events are clearly associated with a split flow.

Therefore we argue that the whole blocking region, lying on the equatorward side of the jet stream north of 40°N, from Azores up to Scandinavia, must be considered as a unique region when the Euro-Atlantic variability is studied. We also argue that the Atlantic LLB events over Azores can be the same manifestation of the EB, but those events are associated with

wave breaking occurring too equatorward for effectively impacting the mid-latitude westerly flow. These results are consistent with the phenomenological analysis presented in Chapter 3. Finally, it is shown that when no blocking is occurring over the Euro-Atlantic sector, the jet stream is not perturbed and it is found in the central peak of the PDF.

Overall, these findings are partially contrasting the works of Woollings et al. (2010b), where it is concluded that European Blocking is "remarkably decoupled" from the jet stream. From the results we present here, European Blocking appears to be mostly associated with the poleward displacement of the jet.

We can summarize by depicting a trimodal blocking-dependent Euro-Atlantic variability: when no blocking is occurring (but also during LLB events, since they cannot affect the jet stream), the Atlantic eddy driven jet is in its central "neutral" position. The equatorward jet position is linked to the occurrence of Greenland blocking (and associated cyclonic wave breaking), while the poleward jet position is linked to the European blocking (and associated anticyclonic wave breaking). EB is not confined in a small region but is originating from the breaking of the Atlantic ridge, which can occur from 30°E to 20°W (even more to the west if LLB are also considered as a part of EB events).

Therefore EB events can have various effects on the weather pattern. Although generally EB is associated with a poleward shift of the jet, sometimes the wave breaking associated with it occurs farther East and North leading to the formation of jet-isolated strong high-pressure systems that are commonly defined as European Blocking.

This trimodal variability partially conflicts with the idea of 4 weather regimes usually detected over the Euro-Atlantic basin. Indeed, we showed that the "poleward displaced jet" and "European blocking" mode are substantially identical under a phenomenological point of view (i.e. vertical cross-section, associated wave-breaking orientation, duration, effects on the jet stream, etc...). In any case, we do not disagree with the classical 4-state distinction, since it is demonstrated by several methods of analysis (i.e. EOFs and cluster analysis, Wallace and Gutzler 1981; Cassou et al. 2007). We argue that, unlike the first "southward displaced jet / Greenland blocking" and the "central jet / no blocking" regimes we analyzed, the "poleward displaced jet" and the "European blocking" regimes have the same physical origin. This hypothesis is also supported by the fact that they are both associated with the Rossby Wave Breaking on the equatorward side of the Atlantic jet.

We also showed that the area of highest frequency of EB, placed between the British

Isles and the North Sea, is not correlated with the North Atlantic Oscillation. Therefore, a straight EOF approach to the climate variability over the Euro-Atlantic sector is not able to fully explain the blocking variability.

Hence, starting from the anticorrelation observed between the NAO phase and Greenland Blocking (Woollings et al., 2008), we analyzed the relationship between the GB occurrence and the NAO pattern, showing that in years with high GB frequency (i.e. negative NAO index) the NAO signal is strengthened and shifted westward. Additionally, we showed that with low GB frequency (i.e. positive NAO index), the first EOF of the Euro-Atlantic sector no longer represents a zonal mode of variability and is more similar to the East-Atlantic pattern.

We were able to reconcile these findings with the Atlantic jet stream displacements. With a high frequency of GB, the increasing number of observed southward jet displacements suggests that the NAO, canonically defined as a zonal mode of variability, is strongly linked to the GB occurrence and its associated jet displacements. Conversely, if the number of GB days is smaller than average, the southward displacement of the jet no longer exists. We were finally able to relate the variability of the NAO pattern and its recent eastward shift with the changes of the Greenland blocking frequency.

This GB-dependent interpretation of the North Atlantic Oscillation, suggested by Woollings et al. (2008), is in agreement with studies that connect the NAO to the occurrence of cyclonic and anticyclonic wave breaking (e.g. Benedict et al., 2004). Due to the strong similarities between the RWB and the blocking (Pelly and Hoskins, 2003) and the predominance of cyclonic wave breaking over Greenland seen in Chapter 3, our interpretation is also consistent with the NAO-RWB mechanism. Therefore we conclude that the Greenland blocking (and the associated Rossby Wave Breaking and southward displacement of the jet) is the primary physical mechanism leading to the North Atlantic Oscillation.

Since the EOF defines the main mode of variability over the defined sector, we speculate that the NAO is obtained by the combination of GB and the blocking on the equatorward side of the jet. This area, characterized by blocking and associated anticyclonic RWB, extends from the Azores up to Scandinavia and it is associated with poleward displacements of the jet stream, as seen in Section 4.1.2. In the HGB case, GB is able to explain the majority of the variance of the low frequency Z500 field. Therefore, the pattern of the first EOF is very similar to the pattern of anomalies associated with GB days.

As the GB frequency decreases, GB is no longer dominating the Euro-Atlantic variability, and therefore loses its centrality in the EOF1-NAO pattern. The EOF1 pattern appears zonally elongated and it is subjected to an eastward shift because it is also affected by the blocking at the equatorward side of the jet. Finally, if GB events almost disappear, the variability of the jet is then only linked to the blocking on the equatorward side of the jet. It is then assumed that the new NAO pattern takes the shape of the northward-eastward displaced anomalies as the EOF2 does in the LGB case. This suggests that the NAO pattern is obtained by the combination of GB and by the equatorward RWB, but with different weights. Quantifying how the NAO index is related to the two different events is beyond the scope of this study, but we argue that in any case the GB components notably dominate the shaping of the pattern. Other phenomena not included in this study may also affect the sign and the shape of the NAO.

To summarize, caution should be used when studying the NAO via EOF analysis as it may lead to misleading results, especially in climate models. Many models (e.g. Gillett et al., 2003) show a shifted first EOF pattern and significant bias in blocking activity (Scaife et al., 2010). Therefore, we argue that a biased blocking representation in climate models, especially over Greenland, can totally offset the pattern of the North Atlantic Oscillation and lead to the analysis of a mode of variability which is fundamentally different from the one observed in the Reanalysis.

Chapter 5

Blocking in climate models

This chapter addresses the representation of blocking by the latest generation of climate models, with a special regard to the Centro Euro-Mediterraneo sui Cambiamenti Climatici (CMCC) climate simulations and to the models involved in the Coupled Model Intercomparison Project - Phase 5 (CMIP5). While Section 1.3 has already given a brief introduction to the complex world of climate models, here we introduce an analysis of the performance of different climate models in the simulation of blocking. Section 5.1 will provide an introduction to the CMIP5 project and to the CMCC climate model. Then, Section 5.2 shows the results of the analysis of the CMCC climate model. More in detail, the relationship between atmospheric blocking and the Atlantic jet stream in a fully coupled simulation and in an atmosphere-only one is studied. Comparing the two runs, a discussion about the role of Sea Surface Temperatures (SSTs) is carried out. Finally, Section 5.3 is focused on models involved in the CMIP5 project. Here atmospheric blocking and both the Atlantic and Pacific jet stream climatologies resulting from more than 20 different climate models are analyzed and evaluated together. Moreover, an assessment of the CMIP5 climate projections for the next century under a high-emission scenario is provided.

5.1 CMIP5 simulations and the CMCC climate model

The Coupled Model Intercomparison Project (CMIP) is a standard experimental protocol to evaluate the outputs of coupled General Circulation Models. It was established in 1995 by the World Climate Research Programme (WCRP) and provides a wide community infrastructure for sharing and comparing data from GCMs of different climate and meteorological institutes.

Phase 3 of the CMIP project (CMIP3), started in 2004, has been part of the Assessment Report 4 (AR4) by Intergovernmental Panel on Climate Change (IPCC), including simulations for both past and present climate forcing. In 2008, involving more than 20 different climate modeling groups from all over the world, WCRP launched Phase 5 of the CMIP project, called CMIP5[1].

The CMIP5 protocol includes different typologies of experiments, with standard outputs and predefined forcing, based on two main goals: on the one side, long-term simulations (century time scale), on the other near-term simulations (10-30 years), often defined as decadal predictions. Since the predefined set of experiments is wide and not all the modeling groups have the possibility to perform them all, a scale of priorities has been defined.

Historical simulations and long-term simulations lay in the "core" of the experiments demanded to the modeling groups. Historical simulations can be briefly divided into fully coupled experiments (defined as historical) and into atmosphere-only experiments (AMIP[2]). The external forcing for the historical and AMIP runs is specified by the CMIP5 protocol. Specifically, well-mixed greenhouse gases are specified individually to the radiation code as CO_2, CH_4, N_2O, CFC-11, CFC-12 and HFC-134-equivalent; anthropogenic three-dimensional sulphate aerosol concentrations are specified considering the direct and first indirect effect; the total solar irradiance (TSI) and the percentage of irradiance in each of the shortwave model radiation bands vary with an 11-year solar cycle (for the TSI an anomaly is added to the 1367 Wm^{-2}); specified monthly-mean ozone fields include variations associated with the solar cycle. For the AMIP runs, the imposed Sea Surface Temperatures (SSTs) are the HadISST (Rayner et al., 2003).

Additionaly, future simulations are divided into an a high emission scenario (RCP8.5) and a midrange emission scenario (RCP4.5)[3].

In the following sections we will also analyze in detail two different runs from the the Centro Euro-Mediterraneo sui Cambiamenti Climatici Climate Model with a resolved Stratosphere (CMCC-CMS). The two CMCC-CMS runs here used are involved in CMIP5 project and therefore respect all the above-mentioned specifications.

[1]for further details, see the official website `http://cmip-pcmdi.llnl.gov/cmip5/` and Taylor et al. (2012).

[2]The Atmospheric Model Intercomparison Project (AMIP) is a standard for atmospheric model evaluation based on monthly mean observed Sea Surface Temperature and Sea Ice Concentrations.

[3]For details on the Representative Concentration Pathways (RCPs), see Moss et al. (2010)

CMCC-CMS is based on the MA-ECHAM5 (Middle Atmosphere ECHAM5) atmospheric component (Roeckner et al., 2006; Manzini et al., 2006), the OASIS3 coupler (Valcke, 2006; Fogli et al., 2009) and the OPA8.2/LIM ocean and sea-ice components (Madec et al., 1998; Fichefet and Morales-Maqueda, 1997). The oceanic component has a constant resolution of about 2 degrees in horizontal and 31 vertical levels. The atmospheric configuration adopted here (T63L95) has a high vertical resolution (95 levels), a high top (up to 80 km) and a horizontal resolution of about 1.8 x 1.8 deg (Manzini et al., 2012). This version of MA-ECHAM5 includes the parameterization of momentum conserving orographic and non-orographic gravity wave drag. The shortwave radiation scheme covers the 185-4000 nm spectral interval with a spectral resolution of 6 bands separating the UV and visible ozone absorption (Cagnazzo et al., 2007).

Data from two different experiments will be used. The first one is a historical numerical experiment of the CMCC-CMS climate model, while the second one is the corresponding AMIP run. Different from the CMIP5 recommendations, the historical ozone concentrations are extended to the top of the model (0.01 hPa, whereas the CMIP5 data stopped at 10 hPa).

The model outputs are all interpolated on the 2.5°x 2.5° grid in order to facilitate the comparison with NCEP/NCAR Reanalysis.

5.2 CMCC-CMS results

The following section will analyze the CMCC-CMS historical and AMIP runs. The first one, hereafter called HIST, is a historical numerical experiment for the DJF 1951-2005. The second one, hereafter named AMIP, is the corresponding AMIP run for the DJF 1951-2005.

5.2.1 Blocking, Atlantic jet stream and NAO in the CMCC-CMS climate model: a climatological overview

A first step to perform the analysis of the blocking and jet stream variability in the CMCC-CMS model is to assess its climatological bias, for both the HIST and the AMIP runs. In order to simplify the treatment of these biases, we adopted the same time window (DJF 1951-2005) as in Chapter 4 in order to compare two experiments with the NCEP/NCAR Reanalysis.

Figure 5.1 shows the blocking events climatology for the DJF 1951-2005 for the HIST simulation (upper left panel) and the difference with respect to the same period of the NCEP/NCAR Reanalysis (upper central panel). The NCEP/NCAR Reanalysis climatology is shown in Figure 4.1. The simulation exhibits a large underestimation of the European Blocking, associated with an eastward displacement of the blocking on the equatorward side of the jet (blue/red dipole over Eastern Atlantic). Moreover, the HIST run presents a slight overestimation of the events over Greenland, whereas over the Pacific the representation of the blocking is more accurate. However, also in this case a little eastward shift is visible, with a moderate increase of the events over the Eastern Pacific at the edge of the storm track region. Fig. 5.1 also shows the same diagnostics for the AMIP run (lower left and central panels), showing that with imposed SSTs, a noticeable increase in blocking frequency is obtained almost everywhere. This leads to an overestimation of blocking over the Eastern Pacific and the Atlantic LLB area, but it provides also a decrease in the bias over Europe. On the other hand, over the Atlantic, the blocking frequency is slightly reduced over Greenland and more generally at high latitudes.

In addition to this, it is possible to see that in the HIST run the climatological Atlantic eddy-driven jet stream is stronger (not shown), broader and more penetrating over Europe than in NCEP/NCAR Reanalysis and in AMIP run (dashed contour in the left panels of Figure 5.1 and in Figure 4.1, respectively). This feature is very likely connected to the low blocking frequency reported over the Eastern Atlantic: under a climatological point of view an increased (decreased) number of blocking events will imply a weaker (stronger) jet at the end of the storm track, confirming once more the tight relationship between the climatological jet stream position and the blocking frequency. This conclusion is in agreement with the findings obtained in Chapter 3 with different Reanalysis datasets.

Fig. 5.1 also reports the 2D PDF for the JLI and the jet strength (right panels). While HIST shows an evident negative bias in the poleward displaced peak and a positive one in the equatorward displaced peak, AMIP presents a smaller bias in both peaks (compare with right panel of Fig 4.1). With respect to the the NCEP/NCAR Reanalysis PDF, both simulations show an equatorward displaced central peak (3-4°). However, the poleward and equatorward peaks are approximatively placed at the same latitudes seen in the Reanalysis.

Interestingly, the meridional position of the three peaks is approximately the same in both the HIST and the AMIP experiments, whereas minor changes can be observed in the

jet speed. This suggests that the impact of different SSTs can change the frequency of occupancy of the three peaks, but not their latitudinal position. Therefore, it is reasonable to argue that the position of the peaks depends on the dynamics of the atmospheric model, and SSTs can only modulate their amplitude.

Moreover, the speed values of the central peak are also well represented by both the simulations, even if the climatological means show (especially for HIST) a stronger and broader low level Atlantic jet stream (not shown). This suggests that the variability in the Atlantic region is extremely important in the representation of the mean state, and that the mean state may be not representative of the "non-perturbed" state of the jet stream.

The main diagnostics of the model are in agreement with the NCEP/NCAR Reanalysis,

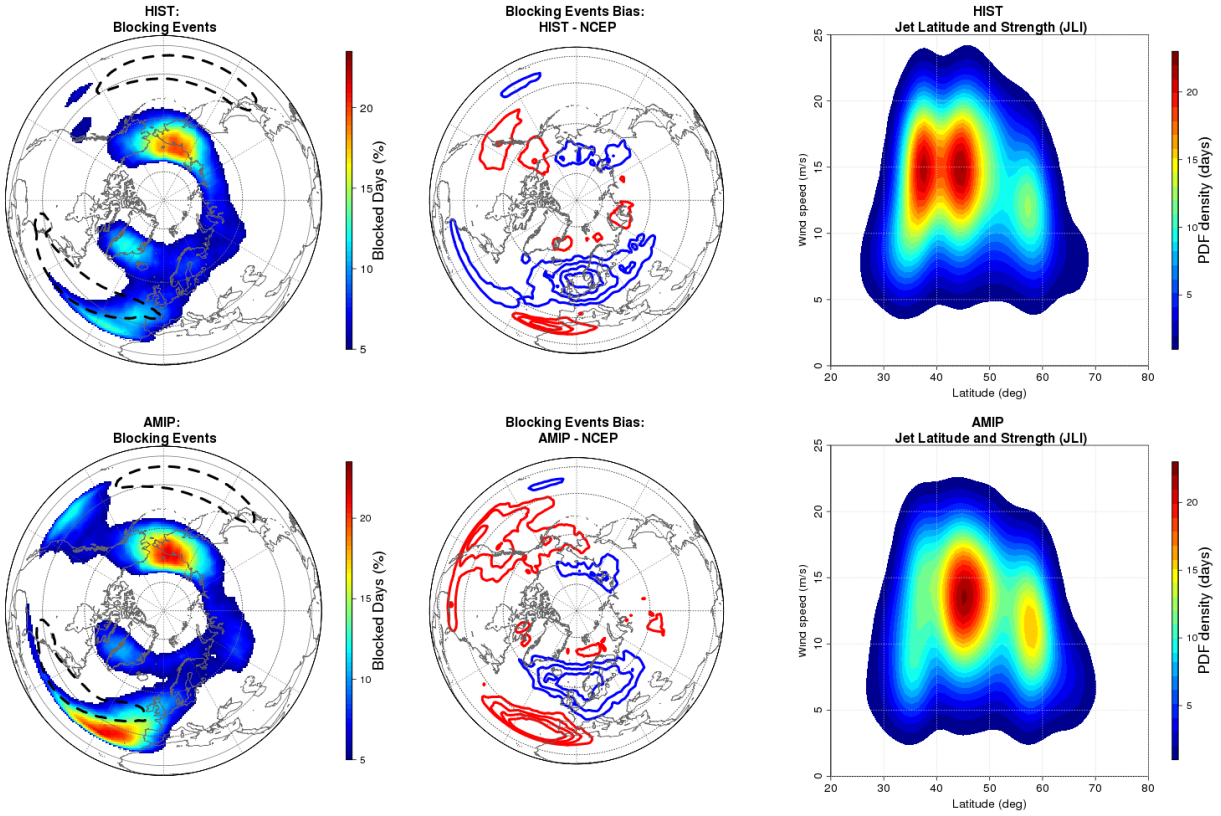

Figure 5.1: *Left panels: Same as Fig. 4.1 but for CMCC-CMS HIST/AMIP runs (upper/lower panel). Central panels: Difference between HIST/AMIP and NCEP-NCAR Reanalysis (upper/lower panel). Blue contours shows negative bias, red contours show positive bias and they are drawn each 2%. Right panel: 2D PDF of JLI and jet strength for HIST and AMIP (upper and lower panel). PDF are multiplied by the number of days of the dataset.*

especially for the blocking intensities and the pattern obtained in the composites analysis (not shown). Detected regions of cyclonic and anticyclonic wave breaking are the same (not shown). However, the model shows a general underestimation of the blocking duration of about 1 to 2 days (not shown). Overall, these results suggest that blocking and Atlantic jet phenomenology are reasonably well represented by the model, even if duration and frequency are both underestimated over Europe.

The NAO pattern of the CMCC-CMS model is reported in the central and bottom panels of Fig. 5.2. In both simulations the NAO shows a westward displacement of the negative one (from Iceland to Greenland) and a poleward/eastward displacement of the positive center

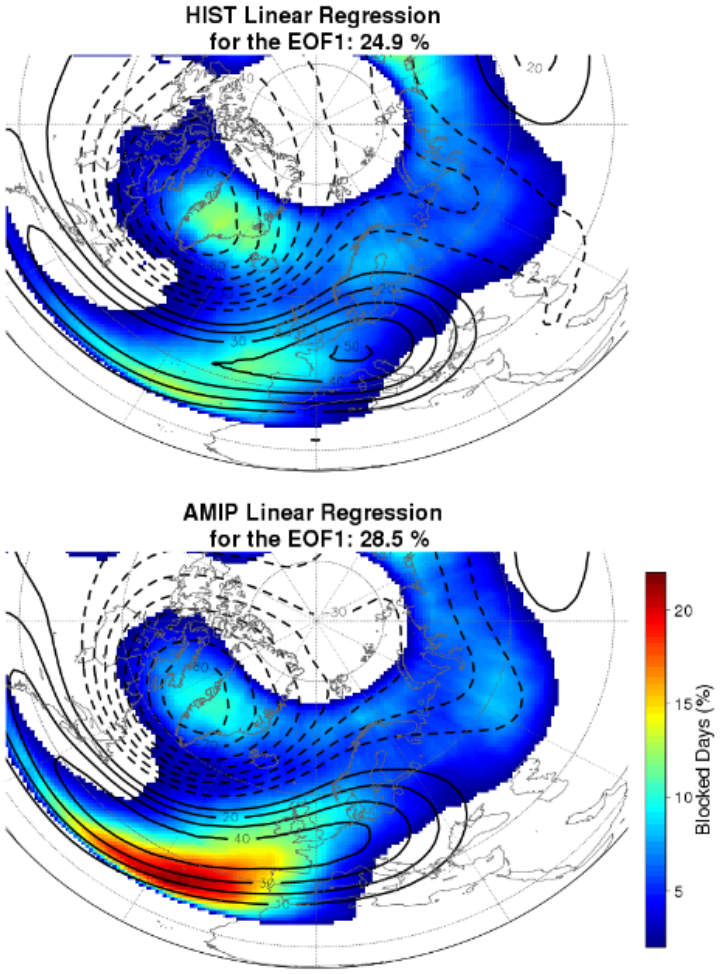

Figure 5.2: *North Atlantic Oscillation pattern shown as the linear regression of the Atlantic (20N-85N, 90W-40E) monthly Z500 EOF1 (contours). Blocking Events frequency is shown by colours. From top to down CMCC-CMS HIST and CMCC-CMS AMIP.*

of action (from Azores to Bay of Biscay), more marked for the HIST simulation. Overall, there is good agreement between the NCEP/NCAR Reanalysis (described in 4.2.1) and the CMCC-CMS model. This is likely connected to the good representation of the blocking over Greenland: both simulations present small bias over Greenland and significant (at 99%) negative correlation coefficient (-0.49 for HIST and -0.51 for AMIP). On the other hand, both simulations show no correlation between European Blocking and NAO index (-0.07 for HIST and 0.11 for AMIP), in agreement with the results for the NCEP/NCAR Reanalysis.

5.2.2 European Blocking and the Atlantic jet displacements: the role of SST in the CMCC-CMS climate model

After having assessed the main elements of the Euro-Atlantic variability, it is interesting to study together the biases in the blocking frequency and in the JLI distribution in the CMCC-CMS model. In fact, as shown in Figure 5.1, both simulations present significant underestimation of blocking frequency over Central Europe. As we have shown, this region of blocking seems to have notable impact on the jet distribution, since it is coupled with the northernmost position of the jet. Therefore we investigate the model biases in the JLI to see if it is in agreement with the model biases in the blocking frequency.

To simplify our approach, we used the 1-dimensional JLI PDF as done by Woollings et al. (2010b). This technique, even though it might omit some information concerning the jet speed, is used to assess the quality of the representation of the eddy-driven jet stream and its relationship with blocking in climate simulations. Figure 5.3 shows the JLI distribution for NCEP/NCAR Renalysis (upper panel), HIST (central panel) and AMIP (lower panel). The blue, green, orange and dotted lines are constructed as for the 2D PDF in Fig. 4.2. The upper panel shows similar results to that of Fig. 4.2, and it is reported only for comparison. HIST shows the above-mentioned trimodality, with the northward peak smaller and the southward peak notably larger. These results are consistent with the findings reported above (Figure 5.1): the large southern peak of the JLI PDF is associated with the intense simulated GB activity, while the less frequent modeled EB and IWB events are reflected by a smaller northernmost peak of the JLI distribution. The lack of events in HIST over Europe is particularly evident in the EB and IWB region. On the poleward side of the jet, a slight overestimation of the blocking frequency is present over Greenland.

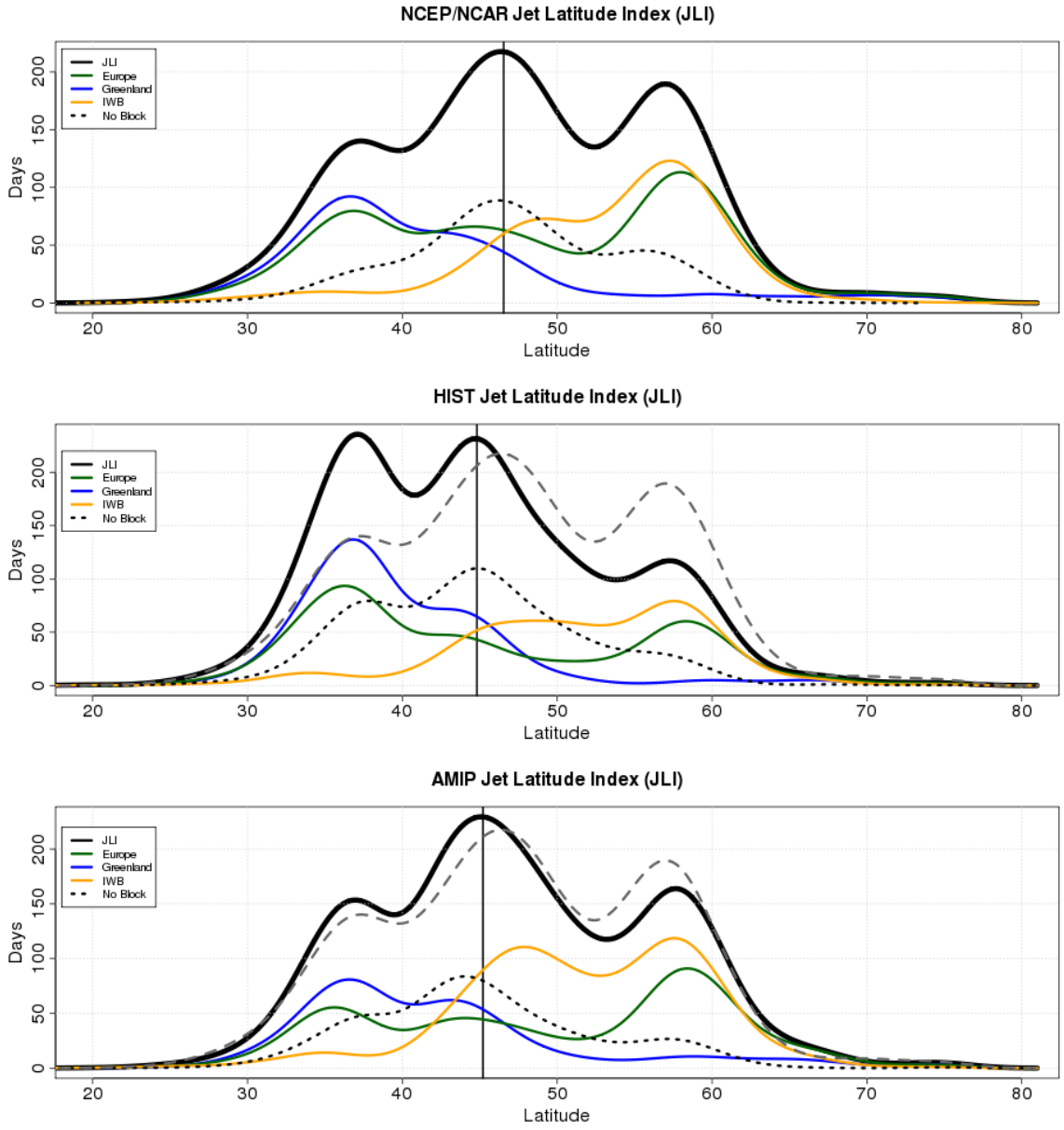

Figure 5.3: *Upper panel: Jet Latitude Index PDF for NCEP/NCAR Reanalysis, where black line represents the climatological distribution, blue line represents GB days, green line EB days and orange line IWB blocking days. Dotted line represents JLI when no blocking in three sectors are detected. Black vertical line shows average JLI value. PDFs are multiplied by the number of days of each dataset. Central and lower panels: the same as upper panel but for CMCC-CMS HIST and CMCC-CMS AMIP respectively. Dashed lines is the JLI PDF for the NCEP/NCAR Reanalysis.*

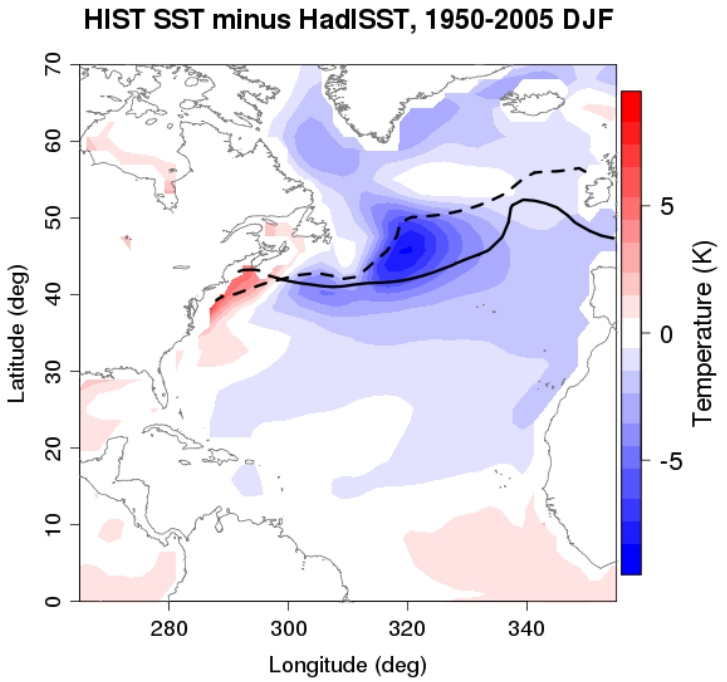

Figure 5.4: *SST bias between the coupled CMCC-CMS HIST and the HadISST used for the AMIP run, for the DJF 1951-2005. The solid and dashed lines represents the position of Atlantic current as the 10°C isotherm for HIST and the AMIP respectively.*

Evident improvements are obtained with the AMIP experiment. A small bias is still present in the northernmost peak, but, overall, the PDF is now close to the one obtained from the NCEP/NCAR Reanalysis. We speculate that this improvement may be due to the wrong reason. The positive blocking bias (lower central panel in Fig. 5.1) present in the Eastern Atlantic (i.e. the IWB sector) very likely compensates the negative bias still present in the EB events. This can be seen in the lower panel of Fig. 5.3, where the orange line is almost doubled with respect to the HIST. This suggests that the right proportion of the northward peak of the JLI PDF may be connected mainly to the overestimated numbers of IWB blocking events.

The first reason behind the strong difference seen between HIST and AMIP must be searched in the different SSTs. We thus investigated the climatological SST field, shown in Figure 5.4. The evident cold bias present over the whole Atlantic basin, with a maximum of about -10 K in the central Atlantic may be responsible for the differences in the blocking activity at low latitudes and the wrong representation of the Atlantic jet stream variability.

Such results are only partially agreeing with the work by Scaife et al. (2011). They showed a significant improvement in blocking frequency over Europe with improved simulation of the Atlantic ocean and with imposed SSTs. They were also able to reduce the positive bias in the jet stream speed. Concerning blocking, here we report an increase in the blocking over Eastern Atlantic/Western Europe (with a marked overestimation) but only a small reduction of the bias of blocking over Northern and Central Europe (Fig. 5.1). On the other hand, bias in the simulated jet stream is reduced, and this is due mainly to a change in the occupation of its mode of variability.

The difference between Scaife et al. (2011) and our results may be connected to the different climate models analyzed. The possibility that the differences were arising from the different blocking indices used was also tested, but since not even the 1-dimensional Tibaldi and Molteni (1990) index was able to detect improvement in the European Blocking frequency, this hypothesis has been dropped.

Unfortunately, the observed SSTs bias is large and therefore understanding what influences the most the blocking and jet stream representation is not straightforward. The main suspect is the simulation of the Gulf Stream and the associated mid-latitude front in SST that impacts the surface baroclinicity (Brayshaw et al., 2008). Fig. 5.4 shows that in HIST the 10°C isotherm, representative of the Atlantic current, is almost 10° to the south with respect to the HadISST. This southward displacement may affect the variability of the Atlantic eddy-driven jet stream.

5.3 Climate change in CMIP5 models

In the following sections we will analyze the representation of blocking in the set of the CMIP5 models. We will make use of the historical and the RCP8.5 experiments. The first ones will be used to define the ability of climate models to reproduce the atmospheric blocking climatology and the jet stream variability in the present-day climate. The second ones will be used to evaluate the change and trend of blocking frequency and jet stream position in the next century, supposing an important increase in human-related emissions.

To detect atmospheric blocking and define the daily jet latitudinal position, we will make use of the indices presented in Chapter 3 and 4. For reason of convenience, only the Instantaneous Blocking (IB) index will be used to define the blocking frequency. However,

we will introduce a Jet Latitude Index not only for the Atlantic but also for the Pacific jet stream. Conversely from its Atlantic counterpart, the Pacific JLI is computed from 15°-65°N, in order to avoid the orographic effects by the Alaskan topography. It is measured from 120°-180°W. Due to availability of data, only the 850-hpa zonal wind is used. Zonal wind data are interpolated onto the regular 2.5°x 2.5° grid before performing any analysis.

Table 5.1 shows the models from the CMIP5 archive included in the analysis and some of their most relevant characteristics. For not all the models it has been been possible retrieve both zonal wind and geopotential height fields, since some of the data was missing from the web archive at the moment of the retrieval (June 2012). This yields to 23 models available for blocking analysis, and 19 for the jet stream assessment.

All the results here after reported refer to the winter season (DJF) and they are adapted from Anstey et al. (2013a) and Anstey et al. (2013b).

5.3.1 Bias in blocking and jet stream

Climatological blocking bias for the 23 CMIP5 analyzed models is reported in Figure 5.5. The Instantaneous Blocking index, i.e. without any spatial and temporal filtering, is reported for all the models. Anyhow, as it has been shown in Chapter 3, blocking frequency and patterns show weak sensitivity to those filtering. The bias is expressed as the wintertime (DJF) difference between the model ensemble mean (the number of ensembles is reported in bracket close to the model name) and the ERA-40 climatology for the 1961-2000 period. Statistical significance is determined by a two-sided t-test applied to inter-annual distribution of the seasonal mean blocking frequency for each grid point. The last two panels (lower right) show the Multi Model Mean (MMM) and the inter-model standard deviation.

Overall, CMIP5 models show significant bias only in areas where blocking generally occurs (i.e. they do not simulate blocking in region far away from the jet streams). However, strong bias is observed over the Atlantic basin, with a general underestimation of blocking over Europe at least in some degree. This bias was also a common feature for the previous generation of climate models, for both models from the 90s (D'Andrea et al., 1998) and even for the more recent CMIP3 models (Scaife et al., 2010). Sometimes the underestimation reaches extremely high values, with some models (e.g. GFDL-ESM2M) showing less than one fourth of the observed blocking frequency. Anyhow, some models (as the HadGEM2 family) show reduced bias over Europe.

Table 5.1: List of models from the CMIP5 archive used in the analysis. The column "runs" indicates the number of ensemble members for the historical simulations and for the RCP8.5 ones.

Model Name	Institute	Country	Hor. Res.	Lid	Runs	JLI
bcc-csm-1	BCC	China	T42	3.54 hPa	1,1	yes
CanESM2	CCCMA	Canada	T63	1.03 hPa	5,5	yes
CCSM4	NCAR	USA	1.25 x 0.94	3.54 hPa	1,0	yes
CMCC-CM	CMCC	Italy	T159	10 hPa	1,1	yes
CMCC-CESM-LOW	CMCC	Italy	T31	10 hPa	1,1	yes
CMCC-CESM	CMCC	Italy	T31	0.01 hPa	1,1	yes
CMCC-CMS	CMCC	Italy	T63	0.01 hPa	1,1	yes
CNRM-CM5	CNRM-CERFACS	France	T127	10 hPa	1	yes
EC-EARTH	ECMWF	EU	T159	4.94 hPa	2,1	no
EC-EARTH-HT	ECMWF	EU	T159	0.01 hPa	1,0	no
GDFL-CM3	NOAA-GFDL	USA	2 x 2	0.02 hPa	1,0	no
GFDL-ESM2M	NOAA-GFDL	USA	2.5 x 2	5.02 hPa	1,0	yes
HadGEM2-CC	MOHC	UK	1.88 x 1.25	0.006 hPa	3,3	yes
HadGEM2-CC-LT	MOHC	UK	1.88 x 1.25	3.67 hPa	3,3	yes
HadGEM2-ES	MOHC	UK	1.88 x 1.25	3.67 hPa	4,4	yes
IPSL-CM5A-LR	IPSL	France	3.75 x 1.9	0.04 hPa	5,3	yes
IPSL-CM5A-MR	IPSL	France	2.5 x 1.25	0.04 hPa	1,1	yes
MIROC-ESM-CHEM	MIROC	Japan	T42	0.004 hPa	1,1	yes
MIROC5	MIROC	Japan	T85	2.9 hPa	4,3	yes
MPI-ESM-LR	MPI	Germany	T63	0.01 hPa	3,3	yes
MPI-ESM-MR	MPI	Germany	T63	0.01 hPa	3,1	no
MRI-CGCM3	MRI	Japan	T159	0.01 hPa	1,1	yes
NorESM1-M	NCC	Norway	2.5 x 1.9	3.54 hPa	3,1	yes

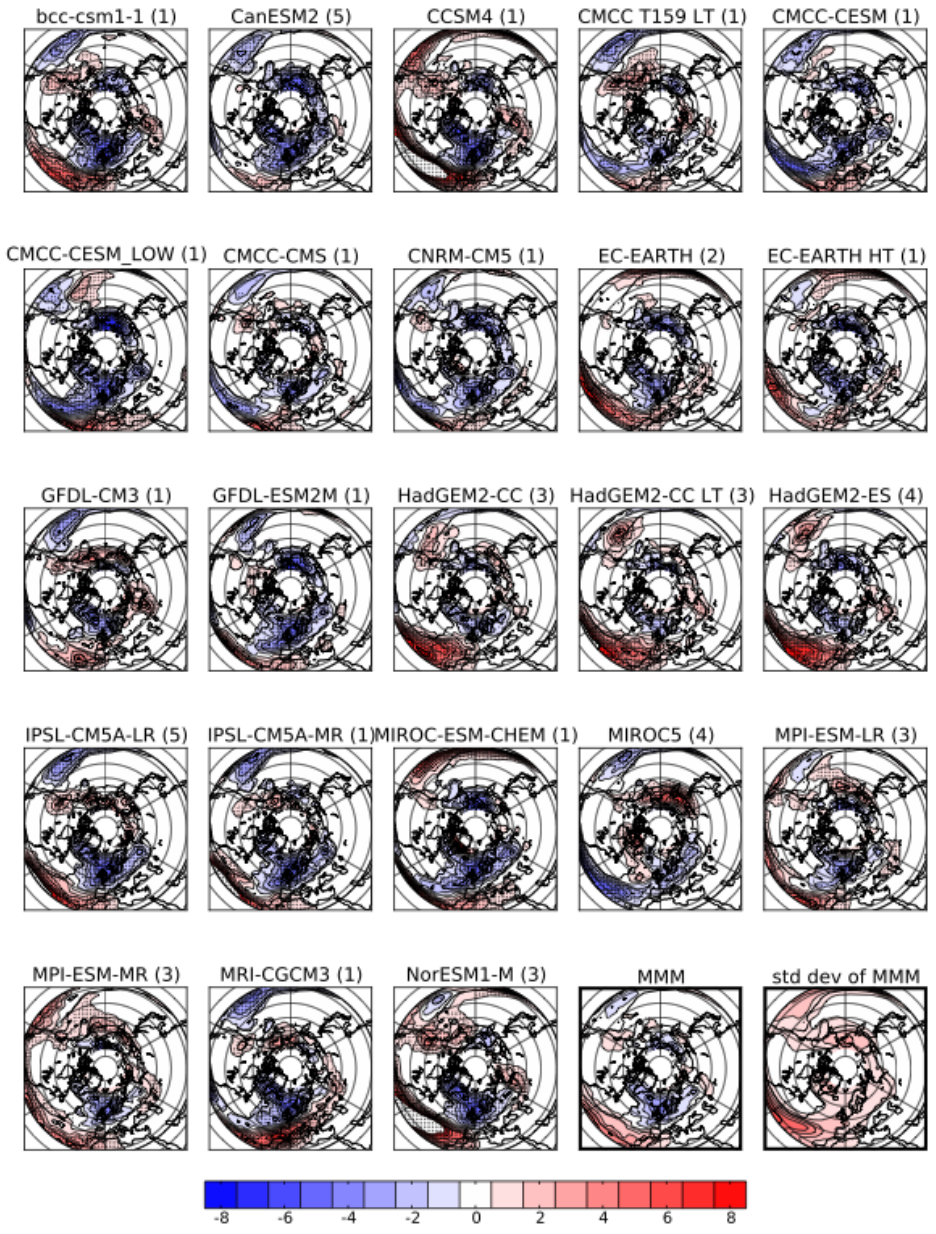

Figure 5.5: *Wintertime (DJF 1961-2000) climatological biases for the historical runs of the CMIP5 models with respect to ERA-40. Values are expressed as percentage of blocked days per season. Positive differences are shown in red, negative in blue with respect to the ERA-40 climatology. Stippling shows area of statistical significance (at 95% level with a two-side t test). The number of ensembles for each model is indicated in brackets in every caption. Lower right panels indicate the Multi Model Mean (MMM) and the standard deviation of the MMM. Adapted from Anstey et al. (2013a)*

The underestimation of European Blocking is not the only bias over the Euro-Atlantic sector, since several models also underestimate the Greenland Blocking frequency. This bias is smaller with respect to the one over Europe, but considered the importance of Greenland blocking in the weather pattern of the Atlantic basin, it is notably relevant. Indeed, as shown in Chapter 4, the coupling between the North Atlantic Oscillation and Greenland Blocking is extremely evident, therefore a significant underestimation of Greenland blocking by climate models may result in a misinterpretation of the NAO. Conversely, blocking frequency at lower latitudes is usually overestimated. This dipolar bias between low and mid-latitude suggests that many models simulate too much blocking (and associated Rossby Wave Breaking) at low latitudes and too little at higher latitudes.

Over the Pacific the situation is slightly different, and the results are definitely more encouraging. There is a weak tendency for models to show reduced high-latitude blocking (over Eastern Siberia), but often they overestimate not only the Low Latitude Blocking (LLB) but also blocking over the Western coast of the American continent.

The MMM bias and its standard deviation (lower panels in Figure 5.5 summarize the above-mentioned features: the Atlantic basin shows a deficit of blocking over Europe and Greenland, and the small inter-model standard deviation confirms that this is a common feature of the most of the CMIP5 models analyzed. The overestimation over the Atlantic LLB region is conversely associated with high standard deviation, suggesting that models disagree on the Atlantic LLB frequency. Bias over the Pacific is smaller, associated with a smaller standard deviation.

We can summarize this part stating that the issue of the underestimation of European blocking has not been overtaken by the CMIP5 models. On the other hand, promising results are obtained over the Pacific. However, an important caveat that must be explored concerns the negative bias that many models have over Greenland.

Due to the evident blocking-jet relationships emerging in Chapter 4, the Jet Latitude Index distributions for both the Atlantic and the Pacific jet streams reflect the bias discussed for blocking. Figure 5.6 shows the results. Upper panels show the JLI PDF for the DJF 1961-2000 for the Atlantic (left) and the Pacific (right). Lower panels show the biases between the models and the ERA-40 distribution for Atlantic (left) and the Pacific (right), expressed as a pure difference between the two PDFs.

At a first look, what it comes out is the the evident spread among the CMIP5 models in

representing the Atlantic jet stream variability. Some of them are unable to represent the trimodality of the PDF, and in some cases not even the bimodality is achieved (e.g. IPSL-CM5A-MR or CCSM4). Overall, the model variability, showed also by the MMM (black line), is unrealistically low. Moreover, the central peak of the MMM PDF is few degrees equatorward with respect to the ERA-40 PDF. This may suggest that the Atlantic jet stream represented by the CMIP5 models is too close to the subtropical jet, constraining the transient

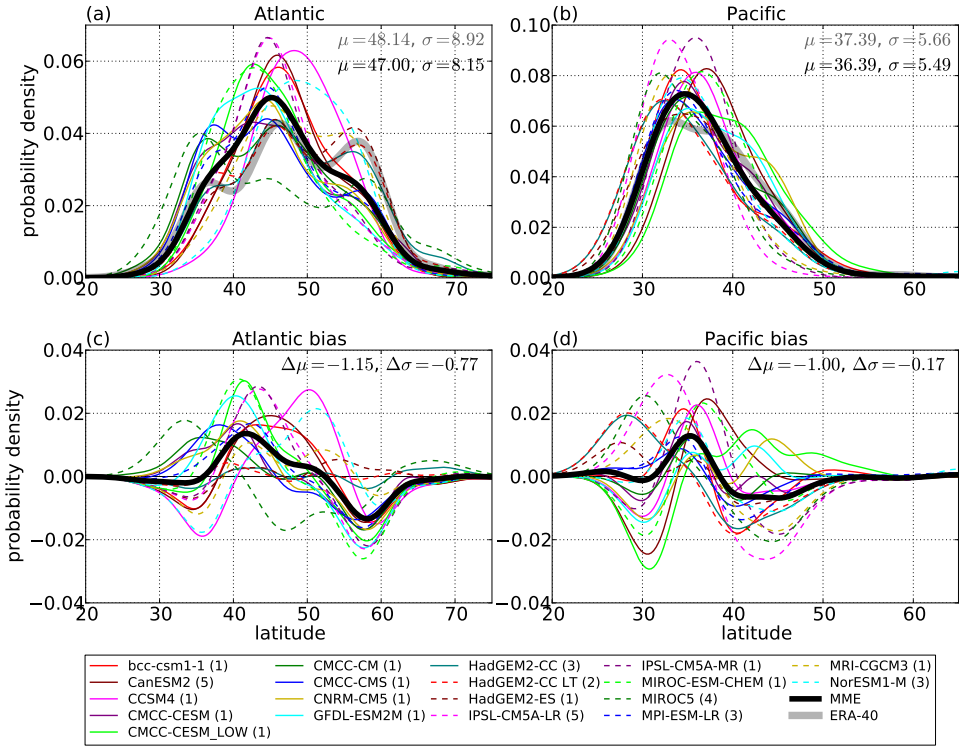

Figure 5.6: *Jet Latitude Index (JLI) for the Atlantic (left panels) and the Pacific (right panels) for CMIP5 historical runs in the DJF 1961-2000 period. Upper panels show the climatalogical PDF, lower panels the bias expressed as differences between the model ensemble mean and the ERA-40 PDF. The ERA-40 distribution is shown in grey and the Multi Model Mean is represented by the solid black line. In the upper right corner of the upper panels are reported the mean μ and the standard deviation σ for the ERA-40 (black) and MMM (grey) PDF. In the upper right corner of lower panels are shown the differences between ERA-40 and MMM. The number of ensemble members is shown in brackets in the legend. Adapted from Anstey et al. (2013a)*

eddies at lower latitudes in a more "Pacific-like" jet configuration (as proposed by Nakamura and Sampe, 2002). This can be explain why many GCMs show a reduced variability and underestimation of European Blocking. However, confirming this interpretation goes beyond the scope of this thesis.

Overall, the biases in the JLI PDF are in agreement with the bias for the blocking frequency. As shown in Chapter 4, European and Greenland blocking are the events that most impact the jet stream. The lack of these events is in accordance with a reduced poleward and equatorward variability of the Atlantic jet stream.

Over the Pacific, even though the bias between the MMM and the ERA-40 PDF is of the same order of magnitude, the inter model spread is smaller. The models generally agree on the average position of the Pacific jet. In any case, there are some exceptions with some model with an PDF shifted few degrees poleward (e.g. CanESM2) or equatorward (e.g. IPSL-CM5A-LR).

5.3.2 Blocking and jet changes in the RCP8.5 scenario

As seen in Section 5.3.1, the CMIP5 generation climate models exhibit large bias, especially over the Euro-Atlantic sector. Therefore it is not straightforward to understand to which degree of confidence it is possible to analyze and evaluate the trends in the future scenario.

However, since an unbiased model does not exist and, above all, not all the blocking and jet representation appear as largely biased, a study under a future high emission scenario (RCP8.5) it is not only a merely theoretical issue.

Figure 5.7 reports the trend for Instantaneous Blocking as the difference between the last 40 years of the RCP8.5 scenario (DJF 2061-2100) and the historical runs (DJF 1961-2000). As in Figure 5.5, the last two panels show the Multi Model Mean and the inter model standard deviation. The RCP8.5 runs were already available only for 18 models, hence only for them was possible to compute the trends.

The main feature emerging from Figure 5.7 is certainly the general reduction of blocking activity observed almost worldwide by all the models. However, even though there is an overall agreement on the sign, a great variety of regional trends is emerging. Some models show strong reduction (e.g. IPSL-CM5A-LR) while other models show very weak trends (e.g. EC-EARTH or MIROC5). It is interesting to notice that the trends are inevitably related to number of Instantaneous Blocking observed in the historical period. Especially in some

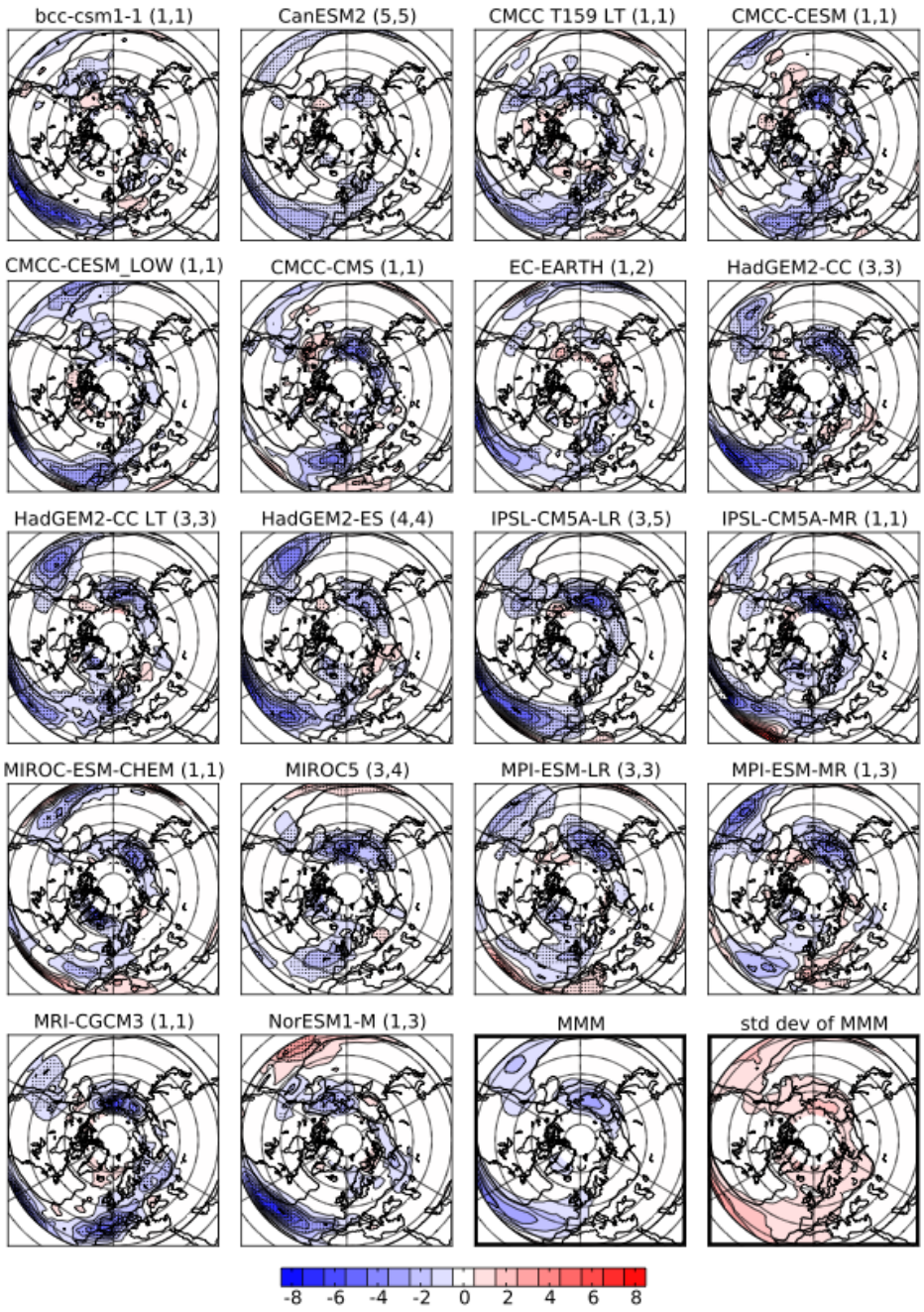

Figure 5.7: *Blocking trends (DJF) defined as the difference between the future (RCP8.5 runs, 2061-2100) and the historical period (historical runs, 1961-2000). Details as in Figure 5.5. Brackets shows the number of ensemble members for the RCP8.5 and the historical runs. Adapted from Anstey et al. (2013b)*

areas, there is an important coherence between the blocking frequency in the historical period and strength of the negative trend. For instance, models showing large positive bias over the Atlantic LLB (e.g. bcc-csm1-1, the HadGEM2 family, NorESM1-M, etc.) show very large negative trends in this region. Conversely, models showing extremely low values of European Blocking (e.g. the IPSL-CM5A family, CanESM2, NorESM1-M, etc.) show almost negligible trend over this region. Obviously, especially for European blocking, one must keep in mind that no blocking reduction is possible in region where no blocking is occurring. Indeed, other models do not reflect this behavior, with small trends associated with large positive biases (as the MIROC family).

Those results are mainly in agreement with what have been reported in literature in the recent years. An overall decreasing blocking activity has been shown occurring under different scenarios for both the CMIP3 generation models (Barnes et al., 2011) and specific coupled GCMs (Matsueda et al., 2009; Sillmann and Croci-Maspoli, 2009). Conversely, Jung et al. (2011) reported of an increased blocking frequency over the Pacific and almost negligible change over the Euro-Atlantic. Even if these results seem to contrast the results reported here, it is interesting to notice that the work by Jung et al. (2011) was carried out with the ECMWF model, which is the same atmospheric component of the EC-EARTH model here reported. Indeed, EC-EARTH is the model showing the smallest negative trend over Europe and a slightly positive trend over the North Pacific, in agreement with what found by Jung et al. (2011).

Linear trends for the Atlantic JLI are reported in Figure 5.8, and they are computed in a similar way to that performed for blocking frequency. The MMM (lower right panel) shows a reduction of the Atlantic jet variability, with an increasing frequency of occurrence for the central peak of the PDF and reduction especially evident for the poleward displaced peak. The time-mean jet shows a very small displacement equatorward of only 0.1°. All the CMIP5 models agree on the reduction of the Atlantic jet variability, increasing the reliability of this feature. Indeed, all models but MIROC5 show an increasing frequency for the central peak. This trend is in agreement with a sharpening and strengthening of the jet stream associated with a increased meridional gradient in the mid-latitudes (e.g. Woollings, 2008).

Finally, the trends for the Pacific JLI are reported in Figure 5.9. Here a more evident latitudinal trend is emerging, with a poleward shift of the distribution for most of the models. The time-mean jet for the MMM shows a 1.5° northward shift. Due to the relevance of the

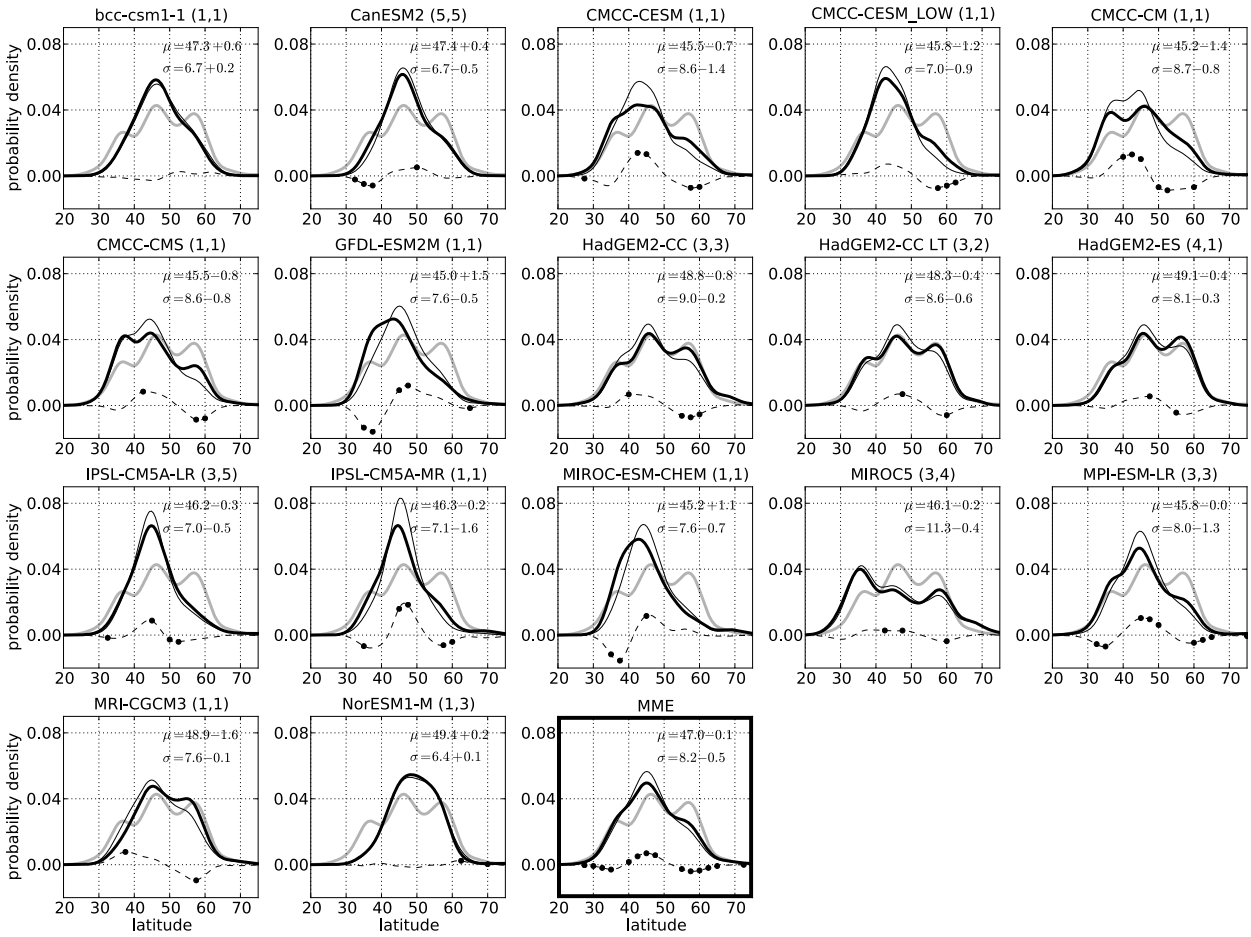

Figure 5.8: *Atlantic JLI for CMIP5 historical runs (1961-2000, thin black line), the ERA-40 Reanalysis (1961-2000, grey lines), and the future RCP8.5 runs (2061-2100, thick black line). Dotted lines show the future-minus-past differences, while the dots show where the trends are significant at 95% level. Adapted from Anstey et al. (2013b).*

thermal processes characteristic of the subtropical jet dynamics within the Pacific jet (Li and Wettstein, 2011), this poleward displacement is consistent with the expansion of the Hadley cell under condition of global warming.

Recently Barnes and Hartmann (Response of the midlatitude jets and of their variability to increased greenhouse gases in the CMIP5 models, 2012, submitted to Journal of Climate), performed a detailed and accurate analysis of the annual mean eddy-driven jet trends and variability in the CMIP5 models. They concluded showing a poleward trend for both the Atlantic and Pacific jet and a reduction of variability only for the former one. This apparent difference, somehow contrasting what have been here presented, may be explained highlight-

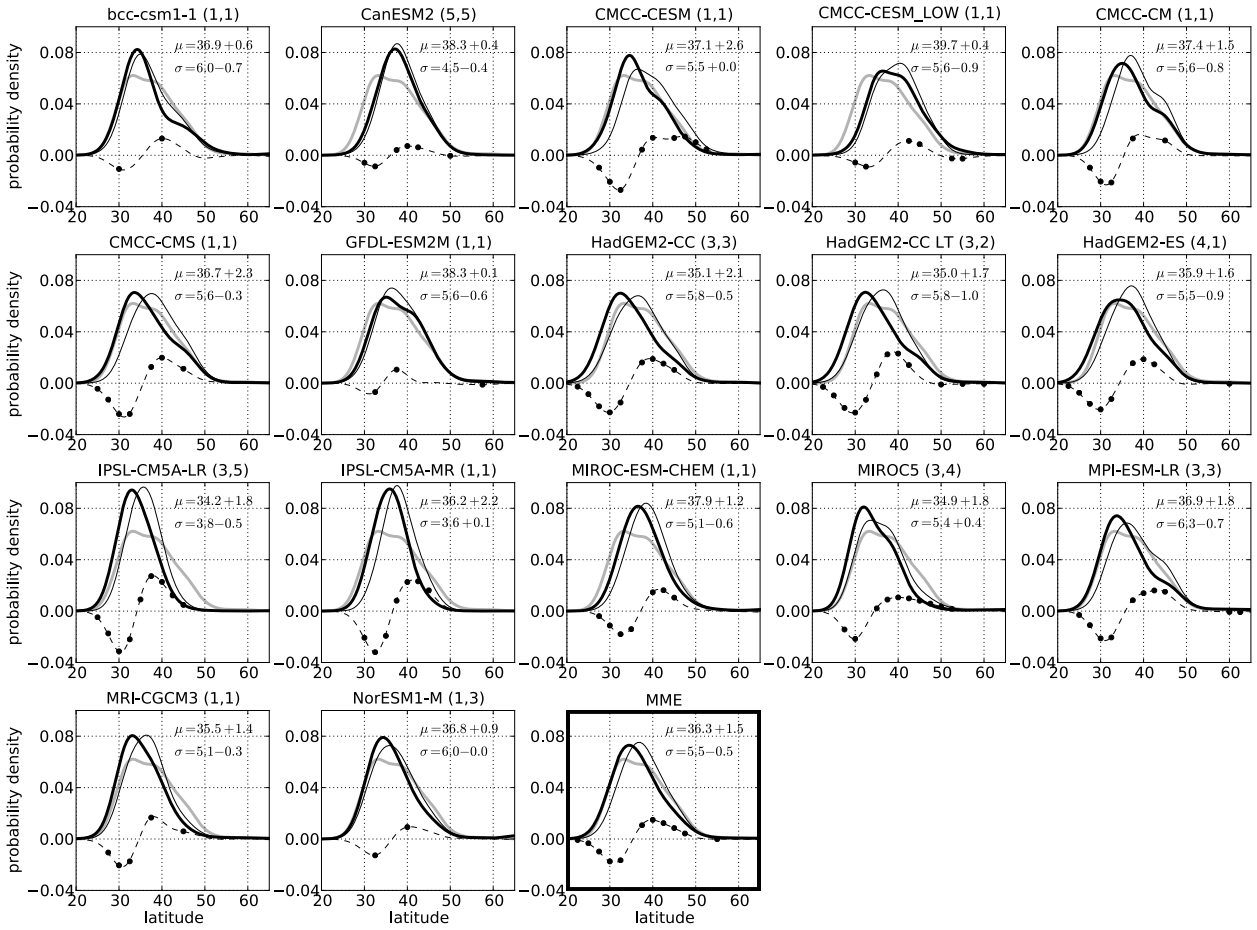

Figure 5.9: *The same as Figure 5.8, but for Pacific JLI. Adapted from Anstey et al. (2013b).*

ing that generally the jet response to GHGs increase is not equal in all the season, as pointed out by Woollings and Blackburn (2012) for CMIP3 models. However, the results of Barnes and Hartmann (2012) agree in reporting the connection between RWB/blocking frequency and jet position.

5.4 Discussions

In this chapter we provided an evaluation of the representation of atmospheric blocking and jet stream variability in several state-of-the-art climate models. The first part was devoted to the analysis of two different runs from CMCC-CMS climate model spanning over 55 years (DJF 1951-2005) and to the comparison of CMCC-CMS outputs with NCEP/NCAR Reanalysis. The two CMCC-CMS runs, an atmosphere-only (AMIP) and a historical coupled

one (HIST), show strong bias in the simulation of the blocking on the equatorward side of the jet: they both overestimate Atlantic LLB but they markedly underestimate European Blocking.

On the other hand, they show good agreement in reproducing the North Atlantic Oscillation. This is very likely associated with the small bias in the simulation of Greenland Blocking.

Interestingly, different results between the two simulations are obtained for the Atlantic jet stream: the coupled HIST run shows a bias in the trimodal distribution of the jet stream variability, while the atmosphere-only AMIP run has a smaller bias with respect to the NCEP/NCAR Reanalysis. The main improvements regards mainly the proportion of the peaks: their position in the speed-latitude space is preserved. Especially the central peak, that represents the non-perturbed jet stream, is not influenced by the different SSTs.

Overall, there is a "coherence" between the biases detected in the modeled blocking frequency and the bias of the simulated Atlantic jet representation. More GB leads to more equatorward displaced jet, more IWB/EB leads to more poleward displaced jet. This confirms the strong coupling between the two events seen in Chapter 4.

In any case, the improved jet representation of the AMIP seems to be good for the wrong reasons. The strong positive bias of the blocking activity over Eastern Atlantic (i.e. over the IWB sector) seems to compensate the negative bias over Central Europe, leading to a good simulation of the jet stream variability even though the modeled blocking frequency is still underestimated. This sort of "spurious improvement" must considered with caution when the jet stream variability is analyzed in climate models. Hence, it is possible to state that a right representation of the jet stream variability, measured via the JLI index, does not necessarily imply a realistic simulation of the patterns of variability of the Euro-Atlantic area. This can be particularly true for Iberian Wave Breaking and European Blocking, due to their association with the poleward displacements of the jet. This feature is also evident in other CMIP5 models, such as the one from the HadGEM2 family. Here an almost perfect the JLI PDF (Figure 5.6) is accompanied by an overestimation of IWB blocking and an underestimation of European Blocking (Figure 5.5). To summarize, it is possible to state that imposed SSTs over the North Atlantic Ocean lead only to improvements in the jet stream variability, but not in European Blocking simulation. This only partially confirms the work of Scaife et al. (2011), where they showed notable reduction of the bias also for

blocking over Central Europe.

Hence, in order to provide a more complete assessment of the ability of climate models of reproducing the blocking patterns and the jet variability, we extended our approach to a set of about 20 models involved in the CMIP5 project. Almost all the models present an underestimation of European Blocking frequency and a reduction of the Atlantic jet variability. More generally, a significant underestimation of High Latitude Blocking activity and overestimation of Low Latitude Blocking activity is observed over the Atlantic basin. This is well reflected by the large positive/negative bias of the Multi-Model Mean (MMM) over the Atlantic LLB/GB. This suggests the possibility that the distance between the subtropical and the eddy-driven jets is too small in many models, constraining the transient eddies along the subtropical jet and avoiding the occurrence of Rossby Wave Breaking at higher latitudes.

Moreover, the results reported by the MMM confirm the key blocking-jet relationship emerging from the Reanalysis and the CMCC-CMS data.

The last part of the chapter addressed the linear trends of the blocking and Atlantic and Pacific jet streams under a high-emission scenario (RCP8.5). This is performed comparing the DJF 2061-2100 of the CMIP5 models with the historical runs previously analyzed. The results show a general agreement among the CMIP5 models reporting a reduction of the blocking frequency almost worldwide (more marked for LLB events), associated with a reduction of the Atlantic jet stream variability and a poleward displacement of the Pacific jet stream.

Those trends are consistent with the idea of a strengthening of the equator/pole thermal gradient (leading to a stronger and less unstable Atlantic jet stream) and with the expansion of the Hadley cell (leading to poleward subtropical component of the Pacific jet).

Chapter 6

Conclusions and Perspectives

An extensive analysis of atmospheric blocking and its relationship with the main elements of the winter mid-latitude climate has been carried out throughout this thesis. In order to perform this study, we introduced a new detailed climatology of the Northern Hemisphere wintertime blocking, aimed at identifying blocking not only on a fixed latitude, but everywhere in the Northern Hemisphere mid-latitudes.

To this aim, we introduced a new bidimensional index, based on the the reversal of the geopotential height as 500 hPa. This index is an extension of the traditional index family derived from the Tibaldi and Molteni (1990). It includes both temporal and spatial constraints applied to ensure the accuracy of the detection of atmospheric blocking. The completeness and the robustness of the results obtained with our index, validated with three different Reanalysis datasets (NCEP/NCAR, ER40 and ERA-INTERIM), suggest that our choice is reliable.

However, it is noteworthy to remark that this index is not solving in any manner the controversial debate on which blocking index should be retained and what discarded. Other blocking indices, based on potential temperature or potential vorticity, may lead to similar results and must be considered with the same regard.

One of the key points emerging from our analysis is the need of overtaking the historical approach to blocking based on a 1-dimensional index, being based on either a fixed latitude or on an adjusted latitude (e.g. Pelly and Hoskins, 2003; Barriopedro et al., 2006; Scaife et al., 2011). Such 1-dimensional indices, even though they provide a simple snapshot of the main blocking features, are not able to fully capture the global picture of the blocking variability.

Indeed, we showed that it is possible to detect blocking-like events at high and low

latitudes too. To further investigate the properties of this wide range of blocking events, we introduced a series of diagnostics, measuring the intensity of the easterly winds associated with the blocking, the magnitude of the change of the meridional circulation, the orientation of the associated Rossby Wave Breaking events and the duration of the blocking events.

Making use of this large set of tools, we were able to distinguish among three main kind of blocking events:

- *High Latitude Blocking, HLB*: Placed over the North Pacific and Greenland, they represent the most frequent blocking events. They have been originally defined as blocking-like events associated with cyclonic Rossby Wave Breaking occurring on the poleward side of the stream (Berrisford et al., 2007). HLB events are characterized by a strong pressure anomaly, by strong easterly winds south of the blocking center, but by weak impact on the meridional circulation. Actually more than blocking the jet stream, they tend to divert it southward. Finally, conversely to the canonical blocking, they show a tilted baroclinic-like vertical pressure cross section and last on average around 8-9 days.

- *Low Latitude Blocking, LLB*: Placed over the Eastern Subtropical Pacific and Atlantic Oceans, generally south of 40°N. LLB are characterized by a barotropic pressure anomaly, an anticyclonic RWB event, a weak reversal of the gradient (i.e. weak easterly winds) and an almost negligible impact on the jet stream. They are more frequent over the Atlantic and their average duration is on the order of 6-7 days. They are at the same time the manifestation of two different events: by one side, the oscillation of the subtropical pressure system and the associated tropical wind reversal. By the other, weak RWB events that are unable to divert the jet stream.

- *European Blocking, EB*: As the name suggests, placed over Western and Central Europe, they represent the bulk of mid-latitude blocking events. EB events are the ones that fullfill the condition introduced by Rex (1950a), due to their barotropic vertical cross-section and the strong impact on the westerly flow that is able to block and divert the migratory cyclones. They last about 7-8 days and they are associated with an anticyclonic wave breaking. Interestingly, it is hard to find a counterpart of these EB events on the Pacific, at least under a climatological point of view. This striking

difference is very likely connected with the differences between the Pacific and Atlantic jet streams.

Perhaps, a potential consequence of these findings is a revision of the concept of atmospheric blocking itself. Historically, atmospheric blocking has been considered as the weather pattern that blocks the mid-latitude flow, diverting the storm track and displacing the jet stream. As our results showed, both HLB and LLB have many characteristics similar to the classical blocking events occurring over Europe. However, if it is clearly possible to distinguish between HLB and EB, due to their position with respect to the jet stream and to many phenomenological differences, it is very hard to trace a line that separates Atlantic LLB and EB.

In other words, it is possible to state that the classical definition of atmospheric blocking (the blocking action on the mid-latitude flow) is a small range of phenomena that can be included in a broader category of meteorological events. These events, phenomenologically similar to blocking, can occur at different latitudes and are highly connected to Rossby Wave dynamics. In this direction, the concept of Rossby Wave Breaking is notably helpful. Even though it is a feature typical of the upper troposphere and is not directly associated with blocking (for instance, two RWB events can maintain the same blocking structure), its similarities with blocking are widely appreciated in literature. Therefore a "RWB approach" to blocking can provide a more complete framework to analyze the blocking dynamics.

We also analyzed the inter-annual variability and the trends in the largest dataset available (the 60 years of the NCEP/NCAR Reanalysis). Unfortunately, the large inter-annual variability typical of atmospheric blocking (two following years can present 5% and 50% of blocked days respectively) yields to a very low significance for the trends analyzed. However, it is is possible to state that in the winter 1951-2010 period there was an increase of LLB, especially over the Atlantic, and a small decrease of HLB over Greenland. Moreover, both the North Pacific Blocking area and the European Blocking show a positive-negative east-west dipole in blocking intensity, suggesting an eastward displacement of the strongest blocking events. This is likely associated with a stronger and sharper jet streams.

The second part of this thesis has been devoted to the analysis of the complex relationships between blocking and some of the elements of the mid-latitude variability. More in detail, we focused our attention on the Atlantic basin, studying the interconnections among blocking, the Atlantic eddy-driven jet stream and the North Atlantic Oscillation.

Firstly, making use of the Jet Latitude Index introduced by Woollings et al. (2010b), we produced a climatology of the daily variability of the Atlantic eddy-driven jet stream. A trimodal distribution emerged clearly, with a more frequent central peak around 50°N and two smaller peaks at about 40°N and 60°N. We hence related the jet stream position to the occurrence of blocking in different sectors of the Atlantic basin. Atlantic LLB events are found to not influence the jet position, while a good correlation between poleward jet displacements and blocking occurring over Eastern Atlantic/Western Europe is discovered. On the other hand, the well-know relationship between blocking over Greenland and the equatorward displacement of the jet is confirmed.

Interestingly, when no blocking is occurring over both Europe and Greenland, we observed no changes in the position and speed of the jet, with the JLI PDF placed mainly on its central peak. This suggests that the "neutral mean" state of the jet stream is a slightly different thing with respect to its climatological position, since the latter is the final average of the daily variability. Indeed, the latitude of the average JLI position is lying few degrees poleward to the latitude of the central peak.

We then analyzed in detail the role of European Blocking, that is found to be only partially decoupled from the jet variability. European Blocking is associated with both poleward and equatorward displacements of the jet, with the former more frequent. However, not even this analysis was able to clearly distinguish between blocking over Western Europe and Central Europe, suggesting that both develop from the same dynamical phenomenon, i.e. the anticyclonic Rossby Wave Breaking on the equatorward side of the jet stream.

After that, following the innovative work by Woollings et al. (2008), we studied the relationship between Greenland Blocking (GB) and the North Atlantic Oscillation. The tight coupling, well expressed by a daily negative correlation on the order of -0.5, suggested that a relation between Greenland blocking and the negative NAO polarity that can go beyond a basic phenomenological similarity may exist. For instance, this correlation may affect longer timescales, as for example the ones that modulate NAO pattern.

In order to verify this hypotheses, we analyzed whether or not the NAO pattern (measured through an Empirical Orthogonal Function analysis) can be modulated by the occurrence of Greenland Blocking. Our findings suggest that Greenland Blocking is the fundamental engine of the North Atlantic Oscillation. In periods with extremely reduced Greenland Blocking frequency, the NAO pattern is altered up to the point that it presents a suppression of the

zonal mode of variability. In this configuration, the NAO as it is canonically interpreted (i.e. a pressure change associated with a north-south displacement of the Atlantic jet) no longer exists.

Moreover, it has been possible to shown that the eastward displacement of the NAO pattern observed in the 80s and the 90s (Hilmer and Jung, 2000), associated with a positive NAO phase, can be explained in terms of a reduction of Greenland Blocking activity in that season.

Such findings question the adoption of EOFs to study the North Atlantic Oscillation, since the interpretation of the NAO as the first EOF of the sector is obviously subject to the phenomenology of the sector itself. As shown in Chapter 3, Greenland Blocking is the largest geopotential anomaly of the Atlantic basin, therefore when this event is reduced, it is not surprising that a statistical method aimed at capturing the largest source of variability of a meteorological field will identify another pattern as the leading mode of variability. Therefore, the question: "does the NAO still exist in period with low Greenland Blocking frequency?" deserves a non-straightforward answer. We conclude our speculations arguing that the NAO is mainly the variability pattern associated with Greenland Blocking, and with low GB frequency the zonal mode of variability that controls the first EOF is the RWB events on the equatorward side of the jet.

The last chapter of this thesis was aimed at the analysis of the simulation of atmospheric blocking in climate models. A first part has been devoted to the analysis of two different experiments of the CMCC-CMS climate model: a fully atmosphere-ocean coupled run (defined HIST experiment) and atmosphere-only run with fixed Sea Surface Temperatures (defined as AMIP experiment). The difference between the two runs are therefore connected to the role played by the SSTs, that especially over the North Atlantic Ocean show large differences. Indeed, the HIST run presents a negative bias that reaches maximum values of about 10 K.

Both the experiments highlighted a good representation of Pacific and Greenland Blocking, with a small overestimation of LLB events and more marked underestimation for European Blocking. The main differences between the two runs is emerging when the Atlantic jet stream is analyzed, showing that, even though there is a negligible improvement of the blocking simulation over Europe, the AMIP run present a more clear trimodal JLI PDF. Interestingly, the central peak of the jet stream (i.e. the most frequent one in the both the CMCC-CMS runs) is not affected by the imposed SSTs, showing that the strength and the

latitude of the jet stream are very likely due only to the atmospheric component of the model.

Therefore, we speculate that SST differences can affect the distribution of the peaks and not their position. The main suspect for this behavior is the Gulf Stream and its related frontal zone, an area characterized by strong meridional gradient and thus high baroclinicity. The oceanic frontal zone for the HIST experiments lies about 10°northward with respect to the AMIP one. This difference may be responsible for different spatial distribution of the synoptic eddies, that may be responsible for blocking onset and maintenance (e.g Shutts, 1983).

Finally, the last section of the work has been devoted to the analysis of the models from the Coupled Model Inter-comparison Project - Phase 5 (CMIP5). Data from more than 20 models has been gathered from the CMIP5 web archive in order to provide a comprehensive analysis of the state-of-the-art climate models ability in simulating mid-latitude variability, for both the present-day climate and a high-GHG-emission scenario (RCP8.5). To this aim, both atmospheric blocking and the JLI for Pacific and Atlantic Ocean has been analyzed.

Overall, CMIP5 models present large bias over Europe, a common feature also for models from the CMIP3 generation (Scaife et al., 2010). Surprisingly, a relevant bias has been detected also over Greenland. This latter point has significant implication, due to the relationships between the NAO and Greenland Blocking, on the ability of CMIP5 model to simulate the NAO itself. Indeed, models with extremely reduced or even missing Greenland Blocking may have a main mode of variability of the Euro-Atlantic sector that can be different from the well-known NAO see-saw. This can lead to a misinterpretation of the NAO that may affect NAO-related studies on climate change.

Interestingly, the CMIP5 models confirm with large agreement that the blocking frequency will reduce in the next century. The majority of the models predict a decrease of atmospheric blocking at almost every latitude. This decrease is associated with a reduction of the variability of the Atlantic and Pacific jet streams, i.e. an increase in the central peak of the JLI PDF. Moreover, the Pacific jet observe a poleward displacement of the order of 1.5°. This scenario is consistent with the increase of the pole-to-equator thermal gradient that should increase the intensity of mid-latitude jets.

Even though we worked in the direction of dispelling some of the doubts regarding the role of blocking in the mid-latitude climate system, it is clear that many points still have to be addressed. For instance, the reason behind the underestimation of European blocking

in almost all the last generation of climate models is one of the most challenging ones. We speculate that this bias may be connected with the reduced jet stream variability, and hence to the distance between the Atlantic eddy-driven jet and its subtropical counterpart. This feature can be achieved with both a too southerly eddy-driven jet and too large Hadley cell. This configuration, that may be responsible for a "Pacific-like" jet stream over the Atlantic with the confinement of the transient eddies along the jet core, surely deserves future study.

Moreover, given the peculiar orographic and thermodynamic properties of Greenland (characterized by a high mountain with an ice core) it would be interesting to go into the details of the dynamics of the Greenland Blocking itself and investigating why this anticyclone is localized in this specific part of the North-Atlantic basin. For instance, perform and analyse a specific modelling experiment that change (or even remove) the orography of Greenland would be of notable scientific interest.

Similar attention should be reserved to the modulation of the blocking activity by other elements of the climate system, as the ENSO, the Madden-Julian Oscillation and other tropical source of Rossby Waves. Due to the importance of RWB dynamics in blocking action, the propagation of tropically-generated Rossby Waves shown by Hoskins and Karoly (1981) can impact blocking activity more than expected.

Furthermore, the connection between the NAO and Greenland Blocking suggests that also the stratosphere may influence blocking dynamics. The Baldwin and Dunkerton (2001) stratosphere-troposphere coupling showed the existence of a linkage between stratospheric anomalies and the Arctic Oscillation, a mode of variability that it is extremely connected with the NAO. Therefore, it is possible that the influence of the stratosphere would emerge not only over Greenland, but potentially would modulate the frequency of RWB in all the mid-latitudes.

Acknowledgments

I would like to thank Chiara Cagnazzo for the time and patience she dedicated to me in these two years, for the things she taught me and for the passion and the energy that she tried to pass me. A special thank is due to Andrea Alessandri, that helped me during the first steps of this Ph.D. career. I would also like to thank Silvio Gualdi, Antonio Navarra, Elisa Manzini and Stefano Tibaldi for the scientific discussions and personal suggestions that made me probably a better scientist. A huge hug and an enormous thank is mandatory to Beppe Fogli, that with his incredible skills helped me out a lot with software and server stuffs.

I would like to thank Rich Neale and Joe Tribbia for their hospitality and scientific support during my period at NCAR, and Stefano for the way he helped me to enjoy the US. I thank James Anstey for the patience and the collaboration that he had while we carried out the CMIP5 project. I acknowledge the CMCC and the Ca' Foscari University for the financial support throughout these years, the WAVACS Cost program and GCOE-ARS program that gave the opportunity to travel to the UK and Kyoto respectively. Indeed, I am indebted with Leslie Gray, Andrew Charlton-Perez and Shigeo Yoden for these amazing experiences.

I am also very grateful to Fabio D'Andrea and Tim Woollings, since with their accurate reviews they were able to help me in improving both the form and scientific content of this thesis.

Obviously, I would like to thank my "schoolmate" and friend Leone, and all the friends with whom I spend these three years, from the so-called guys of the *second floor* up to my friends and my flatmates of the *Via Mascarella* tribe. If living in Bologna has been a beautiful experience, it is mainly their merit.

Finally, a spontaneous, amazing and huge *"grazie"* goes to my parents, my brother and my family. But, above all, I need to thank Agnese, since she was the only one able to bear with me throughout this time.

Appendix A

Indices and Diagnostics

Hereafter a brief description of the main indices and diagnostics adopted in the work is reported.

A.1 Blocking Index

To detect Instantaneous Blocking (IB) the Z500 meridional gradient reversal is defined in a way analogous to Scherrer et al. (2006):

$$GHGS(\lambda_0, \Phi_0) = \frac{Z500(\lambda_0, \Phi_0) - Z500(\lambda_0, \Phi_S)}{\Phi_0 - \Phi_S}, \tag{A.1}$$

$$GHGN(\lambda_0, \Phi_0) = \frac{Z500(\lambda_0, \Phi_N) - Z500(\lambda_0, \Phi_0)}{\Phi_N - \Phi_0} \tag{A.2}$$

where λ_0 and Φ_0 represent the grid point longitude and latitude respectively. Φ_0 ranges from 30°N to 75°N and λ_0 ranges from 0° to 360°. Φ_S= Φ_0 - 15°, Φ_N= Φ_0 + 15°.

For a grid point of coordinates (λ_0, Φ_0), an IB is identified if:

$$GHGS(\lambda_0, \Phi_0) > 0 \qquad GHGN(\lambda_0, \Phi_0) < -10m/^{\circ}lat \tag{A.3}$$

A grid point is defined as Large Scale Blocking (LSB) if the Eq. A.3 is satisfied for at least 15 ° of continuos longitude.

Finally, a Blocking Event is detected if LSB is occurring within a box of 10° lon x 5° lat centered on that grid point for at least 5 days. This is accomplished in two steps: first an

index that considers all grid points within a 10° lon x 5° lat centered on an LSB grid point to be blocked is defined. Then the 5-day persistence criterion to this index is applied.

The modified Blocking Index constructed to exclude LLB from the analysis adds the following constraint to the previously ones:

$$GHGS_2(\lambda_0, \Phi_0) = \frac{Z500(\lambda_0, \Phi_S) - Z500(\lambda_0, \Phi_S - 15°)}{15°} < -5m/°lat \tag{A.4}$$

A.2 Meridional Gradient Intensity

The Meridional Gradient Intensity (MGI) Index is computed associating to each IB event its value of GHGS

$$MGI(\lambda_0, \Phi_0) = GHGS(\lambda_0, \Phi_0) \tag{A.5}$$

By definition, MGI cannot be lower than 0.

A.3 Blocking Intensity

The Blocking Intensity (BI) Index is created with a slightly modified bidimensional extension of the BI index by Wiedenmann et al. (2002). For each point where a IB event is detected, we firstly define MZ as the value of Z500(λ_0,Φ_0), and we define as Z_u and Z_d the minimum of Z500 field within 60° upstream and downstream at the same latitude (Φ_0) of the chosen point, respectively. Hence we define:

$$RC(\lambda_0, \Phi_0) = \frac{\frac{Z_u + MZ}{2} + \frac{Z_d + MZ}{2}}{2} \tag{A.6}$$

from which is possible to compute the Blocking Intensity for each LSB event:

$$BI(\lambda_0, \Phi_0) = 100[(MZ/RC) - 1.0] \tag{A.7}$$

The minimum values for BI is 0 and higher values implies stronger events.

A.4 Wave Breaking Index

In order to detect whether an IB event is associated with a cyclonic or an anticyclonic wave breaking, we define the horizontal stretching deformation S as done by Kunz et al. (2009b):

$$S = \frac{1}{a\cos\phi}\left(\frac{\partial u}{\partial \lambda} - \frac{\partial (v\cos\phi)}{\partial \phi}\right) \tag{A.8}$$

if $S < 0$ hence the wave breaking is cyclonic, if $S > 0$ the wave breaking is anticyclonic. In order to be able to apply this with just geopotential height values, we reformulate the definition applying the geostrophic approximation as defined:

$$u_g = -\frac{g}{fa}\frac{\partial Z}{\partial \phi}, \qquad v_g = \frac{g}{fa\cos\phi}\frac{\partial Z}{\partial \lambda} \tag{A.9}$$

therefore we obtain a version of S with only a dependence on Z:

$$S = -\frac{2g}{fa^2\cos\phi}\left(\frac{\partial^2 Z}{\partial \lambda \partial \phi}\right) \tag{A.10}$$

Since $-\frac{2g}{fa^2\cos\phi}$ is defined negative for any value of ϕ_0 in the Northern Hemisphere and we measure the wave breaking in that point where the reversal of the meridional gradient of geopotential height is present (i.e. $\frac{\partial Z}{\partial \phi} > 0$) the sign of S is determined simply by $\frac{\partial Z}{\partial \lambda}$

We define the WBI for each grid point as:

$$WBI(\lambda_0, \Phi_0) = \frac{Z500(\lambda_W, \Phi_S + 7.5^\circ) - Z500(\lambda_E, \Phi_S + 7.5^\circ)}{\lambda_W - \lambda_E} \tag{A.11}$$

where Φ_S is defined in the Blocking Index and $\lambda_W = \lambda_0 - 7.5^\circ$and $\lambda_E = \lambda_0 + 7.5^\circ$.

So finally to detect the sense of the wave breaking we obtain:

$$WBI < 0 \quad \rightarrow \quad Anticyclonic \quad Wave \quad Breaking \tag{A.12}$$

$$WBI > 0 \quad \rightarrow \quad Cyclonic \quad Wave \quad Breaking \tag{A.13}$$

A.5 Jet Latitude Index

In order to investigate the daily changes of the position of the eddy-driven jet streams, we introduce the Jet Latitude Index (JLI) following Woollings et al. (2010b). Different versions

of the JLI have been used in this work, for both the Pacific and the Atlantic basin. Here below the method used is reported:

- The zonally averaged zonal wind speed between 60° W and 0° longitude (for the Atlantic jet) or between 120°W and 180°W (for the Pacific jet) is selected.
- The vertical average from 925hPa to 700hPa is performed. In the case of CMIP5 models, only the 850hPa level is used.
- For climate models, an interpolation on 2.5°x 2.5 °is performed. A 5-day running mean is applied to reduce the noise caused by synoptic systems. No de-seasoning is performed.
- The maximum value of wind speed between 15° N and 75° N (for the Atlantic jet) or between 15° N and 65° N (for the Pacific jet) is identified.
- The latitude of the maximum value of wind speed defines the daily value of the JLI. The associated zonal wind speed maximum defines the jet speed.

Appendix B

List of Papers

- Davini, P. , C. Cagnazzo, S. Gualdi, and A. Navarra;
  Bidimensional diagnostics, variability and trends of Northern Hemisphere Blocking
  Journal of Climate, 2012, 25 (19), 6496-6509, doi:10.1175/JCLI-D-12-00032.1

  In this paper, Northern Hemisphere winter blocking is analyzed through the introduction of a set of new bidimensional diagnostics based on the geopotential height that provide information about the occurrence, the duration, the intensity and the wave breaking associated with the blocking. This analysis is performed with different reanalysis datasets, in order to evaluate the sensitivity of the index and the diagnostics adopted. In this way, we are able to define a new category of blocking placed at low latitudes that is similar to mid-latitude blocking in terms of the introduced diagnostics but that is unable to divert or block the flow. Furthermore, over the Euro-Atlantic sector we show that it is possible to phenomenologically distinguish between high latitude blocking occurring over Greenland, north of the jet stream and dominated by cyclonic wave breaking, and the traditional mid-latitude blocking localized over Europe and driven by anticyclonic wave breaking. These latter events are uniformly present in a band ranging from Azores up to Scandinavia. Interestingly, a similar distinction cannot be pointed out over the Pacific basin, where the blocking activity is dominated by high latitude blocking occurring over Eastern Siberia. Finally, considering the large impact that blocking may have on Northern Hemisphere, an analysis of the variability and the trend is carried out. This shows a significant increase of Atlantic low latitude blocking frequency and an eastward

displacement of the strongest blocking events over both Atlantic and Pacific Ocean.

- P. Davini, C. Cagnazzo, P.G. Fogli, E. Manzini, S. Gualdi, A. Navarra; **European Blocking and Atlantic Jet Stream Variability in the NCEP/NCAR Reanalysis and the CMCC-CMS climate model**
  Climate Dynamics, 2013, under review

  The relationship between atmospheric blocking over Europe and the Atlantic eddy-driven jet stream is investigated in the NCEP/NCAR Reanalysis and in the CMCC-CMS climate model. This is carried out using a bidimensional blocking index based on geopotential height and a diagnostic providing daily latitudinal position and strength of the jet stream. It is shown that European Blocking is not decoupled from the jet stream but it is mainly associated with its poleward displacements. Moreover, the whole blocking area placed on the equatorward side of the jet stream, broadly ranging from Azores up to Scandinavia, emerges as associated with poleward jet displacements. The diagnostics are hence applied to two different CMCC-CMS climate model simulations in order to evaluate the biases in the jet stream and in the blocking representation. This analysis highlights large underestimation of European blocking, typical feature of general circulation models. Interestingly, observed blocking and jet biases over the Euro-Atlantic area are consistent with the blocking-jet relationship observed in the NCEP/NCAR Reanalysis. Finally, the importance of SSTs is investigated showing that realistic SSTs can reduce the bias in the jet stream variability but not in the frequency of European Blocking. This suggests that blocking-related diagnostics can provide more information about the Euro-Atlantic variability than diagnostics based simply on the Atlantic jet stream.

- Davini, P. , C. Cagnazzo, R. Neale and J. Tribbia; **Coupling between Greenland Blocking and the North Atlantic Oscillation**
  Geophysical Research Letter, 2012, 39, L14701, doi:10.1029/2012GL052315

  Through the adoption of a bidimensional blocking index based on geopotential height, it is shown that the blocking frequency over Greenland is not only a key element in describing the North Atlantic Oscillation (NAO) index, but it also operates as an essential

element in modulating its pattern. When Greenland blocking is lower than average, the first Empirical Orthogonal Function (EOF) of the 500hPa geopotential height over the Euro-Atlantic region no longer resembles the NAO. Moreover, the typical trimodal variability observed in the Atlantic eddy-driven jet stream is reduced to a bimodal variability. Consistent with this result, we link the eastward displacement of the NAO pattern observed in recent years to the decreasing frequency of Greenland Blocking. Considering the large bias seen in the simulated blocking frequency in climate models, such strong coupling might have important consequences in the analysis of the NAO in climate simulations.

- J. A. Anstey, P. Davini, L. J. Gray, T. J. Woollings, N. Butchart, C. Cagnazzo, B. Christiansen, S. C. Hardiman, S. M. Osprey, S. Yang;
  Multi-model analysis of Northern Hemisphere winter blocking, Part I: Model biases and the role of resolution.
  Journal of Geosphysical Research - Atmosphere, 2013, accepted

  Blocking of the tropospheric jet stream during Northern Hemisphere winter (December-January-February) is examined in a multi-model ensemble of coupled atmosphere-ocean general circulation models (GCMs) obtained from the Coupled Model Intercomparison Project Phase 5 (CMIP5). The CMIP5 models exhibit large biases in blocking frequency and related biases in tropospheric jet latitude, similar to earlier generations of GCMs. In general, model biases decrease as model resolution increases. Increased blocking frequency at high latitudes in both the Atlantic and Pacific basins, as well as more realistic variability of Atlantic jet latitude, are associated with increased vertical resolution in the mid-troposphere to lowermost stratosphere. Finer horizontal resolution is associated with higher blocking frequency at all latitudes in the Atlantic basin, but appears to have no systematic impact on blocking near Greenland or in the Pacific basin. Results from the CMIP5 analysis are corroborated by additional controlled experiments using selected GCMs.

- J. A. Anstey, P. Davini, L. J. Gray, T. J. Woollings, N. Butchart, C. Cagnazzo, B. Christiansen, S. C. Hardiman, S. M. Osprey, S. Yang;

Multi-model analysis of Northern Hemisphere winter blocking, Part II: Future projections.

Journal of Geosphysical Research - Atmosphere, 2013, under review

Future projections of tropospheric blocking and jet latitude in Northern Hemisphere winter are examined in a multi-model ensemble of coupled atmosphere-ocean general circulation models (GCMs) obtained from the Coupled Model Intercomparison Project Phase 5 (CMIP5). These models generally predict decreased blocking activity in most regions during December-January-February (DJF) under mid-range (RCP4.5) and strong (RCP8.5) greenhouse gas forcing scenarios. Concomitant changes in the Atlantic eddy-driven jet latitude show decreased likelihood of both equatorward and poleward jet displacements and no clear systematic shift of the time-mean jet latitude. The Pacific jet, in contrast, exhibits a clear poleward shift that is larger in models with more equatorward jets. While large model biases make the validity of future projections questionable, blocking trends are found to be largely independent of model bias and changes in model spatial resolution.

Bibliography

Ambaum, M., 2008: Unimodality of wave amplitude in the northern hemisphere. *Journal of the Atmospheric Sciences*, **65 (3)**, 1077–1086.

Ambaum, M., B. Hoskins, and D. Stephenson, 2001: Arctic oscillation or north atlantic oscillation? *Journal of Climate*, **14 (16)**, 3495–3507.

Anstey, J. A., et al., 2013a: Multi-model analysis of northern hemisphere winter blocking, part i: Model biases and the role of resolution. *Journal of Geophysical Research - Atmosphere*, **accepted**.

Anstey, J. A., et al., 2013b: Multi-model analysis of northern hemisphere winter blocking, part ii: Model biases and the role of resolution. *Journal of Geophysical Research - Atmosphere*, **submitted**.

Archer, C. and K. Caldeira, 2008: Historical trends in the jet streams. *Geophysical Research Letters*, **35 (8)**, L08 803.

Athanasiadis, P. and M. Ambaum, 2009: Linear contributions of different time scales to teleconnectivity. *Journal of Climate*, **22 (13)**, 3720–3728.

Athanasiadis, P., J. Wallace, and J. Wettstein, 2010: Patterns of Wintertime Jet Stream Variability and Their Relation to the Storm Tracks. *Journal of Atmospheric Science*, **67 (5)**, 1361–1381.

Austin, J., 1980: The blocking of middle latitude westerly winds by planetary waves. *Quarterly Journal of the Royal Meteorological Society*, **106 (448)**, 327–350.

Baldwin, M. and T. Dunkerton, 2001: Stratospheric harbingers of anomalous weather regimes. *Science*, **294 (5542)**, 581–584.

Barnes, E. and D. Hartmann, 2010a: Dynamical feedbacks and the persistence of the NAO. *Journal of Atmospheric Science*, **67**, 851–864.

Barnes, E. and D. Hartmann, 2010b: Influence of eddy-driven jet latitude on North Atlantic jet persistence and blocking frequency in CMIP3 integrations. *Geophysical Research Letter*, **37**, L23 802.

Barnes, E., D. Hartmann, D. Frierson, and J. Kidston, 2010: Effect of latitude on the persistence of eddy?driven jets. *Geophysical Research Letter*, **37**, L11 804.

Barnes, E., J. Slingo, and T. Woollings, 2011: A methodology for the comparison of blocking climatologies across indices, models and climate scenarios. *Climate Dynamics*, 1–15.

Barnston, A. and R. Livezey, 1987: Classification, seasonality and persistence of low-frequency atmospheric circulation patterns. *Monthly Weather Review*, **115 (6)**, 1083–1126.

Barriopedro, D., R. García-Herrera, and R. Huth, 2008: Solar modulation of northern hemisphere winter blocking. *Journal of Geophysical Research*, **113 (D14)**, D14 118.

Barriopedro, D., R. Garcia-Herrera, A. Lupo, and E. Hernandez, 2006: A Climatology of Northern Hemisphere Blocking. *Journal of Climate*, **19**, 1042–1063.

Barriopedro, D., R. Garcia-Herrera, and R. Trigo, 2010: Application of blocking diagnosis methods to General Circulation Models. Part I: a novel detection scheme. *Climate Dyamics*, **35 (7-8)**, 1373–1391.

Benedict, J., S. Lee, and S. Feldstein, 2004: Synoptic View of the North Atlantic Oscillation. *Journal of the Atmospheric Science*, **61 (2)**, 121–144.

Benzi, R., P. Malguzzi, A. Speranza, and A. Sutera, 1986: The statistical properties of general atmospheric circulation: observational evidence and a minimal theory of bimodality. *Quarterly Journal of the Royal Meteorological Society*, **112 (473)**, 661–674.

Berggren, R., B. Bolin, and C. Rossby, 1949: An aerological study of zonal motion, its perturbations and break-down. *Tellus*, **1 (2)**, 14–37.

Berrisford, P., B. Hoskins, and E. Tyrlis, 2007: Blocking and Rossby Wave Breaking on the Dynamical Tropopause in the Southern Hemisphere. *Journal of the Atmospheric Science*, **64**, 2881–2898.

Brayshaw, D., B. Hoskins, and M. Blackburn, 2008: The storm-track response to idealized sst perturbations in an aquaplanet gcm. *Journal of the Atmospheric Sciences*, **65 (9)**, 2842–2860.

Brayshaw, D., B. Hoskins, and M. Blackburn, 2009: The Basic Ingredients of the North Atlantic Storm Track. Part I: LandSea Contrast and Orography. *Journal of the Atmospheric Science*, **66**, 2539–2558.

Buehler, T., C. Raible, and T. Stocker, 2011: The relationship of winter season north atlantic blocking frequencies to extreme cold or dry spells in the era-40. *Tellus A*, **63 (2)**, 212–222.

Cagnazzo, C., E. Manzini, M. Giorgetta, P. D. Foster, and J. Morcrette, 2007: Impact of an improved shortwave radiation scheme in the MAECHAM5 General Circulation Model. *Atmospheric Chemistry and Physics*, **7**, 2503–2515.

Cash, B. and S. Lee, 2000: Dynamical processes of block evolution. *Journal of the atmospheric sciences*, **57 (19)**, 3202–3218.

Cassou, C., 2008: Intraseasonal interaction between the madden–julian oscillation and the north atlantic oscillation. *Nature*, **455 (7212)**, 523–527.

Cassou, C., L. Terray, J. Hurrell, and C. Deser, 2007: North Atlantic Winter Climate Regimes: Spatial Asymmetry, Stationarity with Time, and Oceanic Forcing. *Journal of Climate*, **17**, 1055–1067.

Cehelsky, P. and K. Tung, 1987: Theories of multiple equilibria and weather regimesa critical reexamination. part ii: Baroclinic two-layer models. *J. Atmos. Sci*, **44 (21)**, 3282–3303.

Charney, J. and J. DeVore, 1979: Multiple Flow Equilibria in the Atmosphere and Blocking. *Journal Of Atmospheric Sciences*, **36 (7)**, 1205–1216.

Charney, J., J. Shukla, K. Mo, and C. Massachusetts Inst. of Tech., 1981: Comparison of a barotropic blocking theory with observation. *Journal of the Atmospheric Sciences*, **38 (4)**, 762–779.

Charney, J. and D. Straus, 1980: Form-drag instability, multiple equilibria and propagating planetary waves in baroclinic, orographically forced, planetary wave systems. *Journal of Atmospheric Sciences*, **37**, 1157–1176.

Cheng, X. and J. Wallace, 1993: Cluster analysis of the northern hemisphere wintertime 500-hpa height field: Spatial patterns. *Journal of Atmospheric Sciences*, **50**, 2674–2696.

Colucci, S., 1985: Explosive cyclogenesis and large-scale circulation changes: Implications for atmospheric blocking. *Journal of the atmospheric sciences*, **42 (24)**, 2701–2717.

Colucci, S., 1987: Comparative diagnosis of blocking versus nonblocking planetary-scale circulation changes during synoptic-scale cyclogenesis. *Journal of the atmospheric sciences*, **44 (1)**, 124–139.

Colucci, S. and T. Alberta, 1996: Planetary-scale climatology of explosive cyclogenesis and blocking. *Monthly weather review*, **124 (11)**, 2509–2520.

Croci-Maspoli, M., C. Schwierz, and H. Davies, 2007a: Atmospheric blocking: space-time links to the NAO and PNA. *Climate Dynamics*, **29**, 713–725.

Croci-Maspoli, M., C. Schwierz, and H. Davies, 2007b: A multifaceted climatology of atmospheric blocking and its recent linear trend. *Journal of climate*, **20 (4)**, 633–649.

D'Andrea, F., et al., 1998: Northern Hemisphere atmospheric blocking as simulated by 15 atmospheric general circulation models in the period 1979-1988. *Climate Dynamics*, **14 (6)**, 383–407.

Deser, C., A. Phillips, V. Bourdette, and H. Teng, 2012: Uncertainty in climate change projections: The role of internal variability. *Climate Dynamics*, 1–20.

Doblas-Reyes, F., M. Casado, and M. Pastor, 2002: Sensitivity of the northern hemisphere blocking frequency to the detection index. *J. Geophys. Res*, **107 (10.1029)**.

Dole, R. and N. Gordon, 1983: Persistent anomalies of the extratropical northern hemisphere wintertime circulation: Geographical distribution and regional persistence characteristics. *Monthly weather review*, **111 (8)**, 1567–1586.

Egger, J., 1978: Dynamics of blocking highs. *Journal of Atmospheric Sciences*, **35**, 1788–1801.

Eichelberger, S. and D. Hartmann, 2007: Zonal jet structure and the leading mode of variability. *Journal of Climate*, **20**, 5149–5163.

Elliott, R. and T. Smith, 1949: A study of the effects of large blocking highs on the general circulation in the northern-hemisphere westerlies. *Journal of Meteorology*, **6 (2)**, 67–85.

Feldstein, S., 2000: The timescale, power spectra, and climate noise properties of teleconnection patterns. *Journal of climate*, **13 (24)**, 4430–4440.

Ferranti, L., F. Molteni, and T. Palmer, 1994: Impact of localized tropical and extratropical sst anomalies in ensembles of seasonal gcm integrations. *Quarterly Journal of the Royal Meteorological Society*, **120 (520)**, 1613–1645.

Fichefet, T. and M. Morales-Maqueda, 1997: Sensitivity of a Global Sea Ice Model to Treatment of Ice Thermodynamics and Dynamics. *Journal of Geophysical Research*, **102 (12)**, 609–646.

Fogli, P. G., et al., 2009: INGV-CMCC Carbon (ICC): A Carbon Cycle Earth System Model. Report 0061, CMCC.

Franzke, C., S. Lee, and S. Feldstein, 2004: Is The North Atlantic Oscillation a Breaking Wave? *Journal of the Atmospheric Science*, **61**, 145–160.

Frederiksen, J., 1983: A unified three-dimensional instability theory of the onset of blocking and cyclogenesis. ii: Teleconnection patterns. *Journal of the atmospheric sciences*, **40 (11)**, 2593–2609.

Frederiksen, J., 1997: Adjoint sensitivity and finite-time normal mode disturbances during blocking. *Journal of the atmospheric sciences*, **54 (9)**, 1144–1165.

García-Herrera, R. and D. Barriopedro, 2006: Northern hemisphere snow cover and atmospheric blocking variability. *JOURNAL OF GEOPHYSICAL RESEARCH-ALL SERIES-*, **111 (D21)**, 21 104.

Garriot, E., 1904: Long range forecasts. *U.S. Weather Bureau Bullettin*, **35**.

Gillett, N., H. Graf, and T. Osborn, 2003: Climate change and the north atlantic oscillation. *GEOPHYSICAL MONOGRAPH-AMERICAN GEOPHYSICAL UNION*, **134**, 193–210.

Green, J., 1977: The weather during july 1976: some dynamical considerations of the drought. *Weather*, **32 (4)**, 120–126.

Grose, W. and B. Hoskins, 1979: On the influence of orography on large-scale atmospheric flow. *Journal of Atmospheric Sciences*, **36**, 223–234.

Haines, K., P. Malanotte-Rizzoli, and M. Morgan, 1993: Persistent jet stream intensifications: A comparison between theory and data. *Journal of the atmospheric sciences*, **50 (1)**, 145–154.

Häkkinen, S., P. Rhines, and D. Worthen, 2011: Atmospheric blocking and atlantic multidecadal ocean variability. *Science*, **334 (6056)**, 655–659.

Hansen, A. and T. Chen, 1982: A Spectral Energetics Analysis of Atmospheric Blocking. *Monthly Weather Review*, **10**, 1146–1165.

Hansen, A. and A. Sutera, 1986: On the probability density distribution of planetary-scale atmospheric wave amplitude. *Journal of Atmospheric Sciences*, **43**, 3250–3265.

Hansen, A. and A. Sutera, 1993: A comparison between planetary-wave flow regimes and blocking. *Tellus A*, **45 (4)**, 281–288.

Hartmann, D. and S. Ghan, 1980: A statistical study of the dynamics of blocking. *Monthly Weather Review*, **108**, 1144.

Held, I., 2000: The general circulation of the atmosphere. Woods Hole Program in Geophysical Fluid dynamics, 66 pp.

Held, I. and A. Hou, 1980: Nonlinear axially symmetric circulations in a nearly inviscid atmosphere. *Journal of the Atmospheric Sciences*, **37 (3)**, 515–533.

Held, I., M. Ting, and H. Wang, 2002: Northern winter stationary waves: theory and modeling. *Journal of climate*, **15 (16)**, 2125–2144.

Hilmer, M. and T. Jung, 2000: Evidence for a recent change in the link between the north atlantic oscillation and arctic sea ice export. *Geophys. Res. Lett*, **27 (7)**, 989–992.

Holton, J., 2004: *An introduction to dynamic meteorology*, Vol. 1. Academic press.

Hoskins, B., I. James, and G. White, 1983: The shape, propagation and mean-flow interaction of large-scale weather systems. *Journal of the atmospheric sciences*, **40 (7)**, 1595–1612.

Hoskins, B. and D. Karoly, 1981: The steady linear response of a spherical atmosphere to thermal and orographic forcing. *Journal of the Atmospheric Sciences*, **38 (6)**, 1179–1196.

Hoskins, B. and P. Sardeshmukh, 1987: A diagnostic study of the dynamics of the northern hemisphere winter of 1985-86. *Quarterly Journal of the Royal Meteorological Society*, **113 (477)**, 759–778.

Hoskins, B. and P. Valdes, 1990: On the existence of storm-tracks. *Journal of the atmospheric sciences*, **47**, 1854–1864.

Hurrell, J., 1995: Decadal trends in the north atlantic oscillation: regional temperatures and precipitation. *Science*, **269 (5224)**, 676–679.

Hurrell, J., Y. Kushnir, G. Ottersen, and M. Visbeck, 2003: An overview of the north atlantic oscillation. *Geophysical Monographical Series*, **134**, 1–36.

Illari, L., 1984: A diagnostic study of the potential velocity in a warm blocking anticyclone. *Journal of the atmospheric sciences*, **41 (24)**, 3518–3527.

Illari, L. and J. Marshall, 1983: On the interpretation of eddy fluxes during a blocking episode. *Journal of Atmospheric Sciences*, **40**, 2232–2242.

Jung, T., M. Hilmer, E. Ruprecht, S. Kleppek, S. Gulev, and O. Zolina, 2003: Characteristics of the recent eastward shift of interannual nao variability. *Journal of climate*, **16 (20)**, 3371–3382.

Jung, T., et al., 2011: High-resolution global climate simulations with the ECMWF model in Project Athena: Experimental design, model climate and seasonal forecast skill. Journal of Climate, in press.

Kaas, E. and G. Branstator, 1993: The relationship between a zonal index and blocking activity. *Journal of the Atmospheric Sciences*, **50 (18)**.

Kalnay, E., et al., 1996: The NCEP/NCAR 40-Year Reanalysis Project. *Bulletin of the American Meteorological Society*, **77**, 437–471.

Kidston, J. and G. Vallis, 2010: Relationship between eddy-driven jet latitude and width. *Geophysical Research Letters*, **37**, L21 809.

Kimoto, M. and M. Ghil, 1993a: Multiple flow regimes in the northern hemisphere winter. ii: Sectorial regimes and preferred transitions. *Journal of the atmospheric sciences*, **50 (16)**, 2645–2673.

Kimoto, M. and M. Ghil, 1993b: Multiple flow regimes in the northern hemisphere winter. part i: Methodology and hemispheric regimes. *Journal of the Atmospheric Sciences*, **50 (16)**, 2625–2644.

Kunz, T., K. Fraedrich, and F. Lunkeit, 2009a: Impact of Synoptic-Scale Wave Breaking on the NAO and Its Connection with the Stratosphere in ERA-40. *Journal of Climate*, **22 (20)**, 5464–5480.

Kunz, T., K. Fraedrich, and F. Lunkeit, 2009b: Synoptic scale wave breaking and its potential to drive NAO-like circulation dipoles: A simplified GCM approach. *Quarterly Journal of the Royal Meteorological Society*, **135**, 1–19.

Legras, B., T. Desponts, and B. Piguet, 1987: Cluster analysis and weather regimes. *Proceedings of the ECMWF Workshop on the Nature and prediction of extra-tropical weather systems. ECMWF. Shinfield Park, Reading*, 123–149.

Legras, B. and M. Ghil, 1985: Persistent anomalies, blocking and variations in atmospheric predictability. *Journal of the atmospheric sciences*, **42 (5)**, 433–471.

Lejenäs, H. and R. Madden, 1992: Traveling planetary-scale waves and blocking. *Monthly weather review*, **120 (12)**, 2821–2830.

Lejenäs, H. and H. Okland, 1983: Characteristics of northern hemisphere blocking as determined from a long time series of observational data. *Tellus A*, **35 (5)**, 350–362.

Li, C. and J. Wettstein, 2011: Thermally-driven and eddy-driven jet variability in reanalysis. *Journal of Climate*.

Luo, D. and T. Gong, 2006: A possible mechanism for the eastward shift of interannual nao action centers in last three decades. *Geophys. Res. Lett*, **33**, L24 815.

Luo, D., Z. Zhu, R. Ren, L. Zhong, and C. Wang, 2010: Spatial pattern and zonal shift of the north atlantic oscillation. part i: A dynamical interpretation. *Journal of the Atmospheric Sciences*, **67 (9)**, 2805–2826.

Lupo, A. and P. Smith, 1995: Climatological features of blocking anticyclones in the northern hemisphere. *Tellus A*, **47 (4)**, 439–456.

Lutgens, F. and E. Tarbuck, 2001: *The atmosphere*. 8th ed., Prentice-Hall.

Madec, G., P. Delecluse, M. Imbard, and C. Levy, 1998: OPA8.1 Ocean General Circulation Model reference manual. Ipsl technical report, IPSL.

Malguzzi, P. and P. Malanotte-Rizzoli, 1984: Nonlinear stationary rossby waves on nonuniform zonal winds and atmospheric blocking. part i: The analytical theory. *Journal of Atmospheric Sciences*, **41**, 2620–2628.

Malguzzi, P. and P. Malanotte Rizzoli, 1985: Coherent structures in a baroclinic atmosphere. ii: A truncated model approach. *Journal of the atmospheric sciences*, **42 (23)**, 2463–2477.

Malguzzi, P. and A. Speranza, 1981: Local multiple equilibria and regional atmospheric blocking. *Journal of Atmospheric Sciences*, **38**, 1939–1948.

Manzini, E., C. Cagnazzo, P. Fogli, A. Bellucci, and W. Muller, 2012: Stratosphere-troposphere coupling at inter-decadal timescales: Implications for the north atlantic ocean. *Geophysical Research Letters*, **39 (L05801)**.

Manzini, E., M. Giorgetta, M. Esch, K. Kornblueh, and E. Roeckner, 2006: The Influence of Sea Surface Temperatures on the Northern Winter Stratosphere: Ensemble Simulations with the MAECHAM5 Model. *Journal of Climate*, **19 (20)**, 38633881.

Martius, O., L. Polvani, and H. Davies, 2009: Blocking precursors to stratospheric sudden warming events. *Geophys. Res. Lett*, **36**, L14 806.

Masato, G., B. Hoskins, and T. Woollings, 2011: Wave-breaking characteristics of Mid-latitude Blocking. *Quarterly Journal of Royal Meteorological Society*.

Matsueda, M., 2009: Blocking predictability in operational medium-range ensemble forecasts. *SOLA*, **5 (0)**, 113–116.

Matsueda, M., R. Mizuta, and S. Kusunoki, 2009: Future change in wintertime atmospheric blocking simulated using a 20-km-mesh atmospheric global circulation model. *Journal of Geophysical Research*, **114**, D12 114.

McIntyre, M. E. and T. Palmer, 1983: Breaking Planetary Waves in the Stratosphere. *Nature*, **305**, 593–600.

McWilliams, J., G. Flierl, V. Larichev, and G. Reznik, 1981: Numerical studies of barotropic modons. *Dynamics of Atmospheres and Oceans*, **5 (4)**, 219–238.

McWilliams, J. C., 1980: An application of equivalent modons to atmospheric blocking. *Dynamics of Atmospheres and Oceans*, **5**, 43–66.

Michelangeli, P., R. Vautard, and B. Legras, 1995: Weather regimes: Recurrence and quasi stationarity. *Journal of the atmospheric sciences*, **52 (8)**, 1237–1256.

Moss, R., et al., 2010: The next generation of scenarios for climate change research and assessment. *Nature*, **463 (7282)**, 747–756.

Mullen, S., 1987: Transient eddy forcing of blocking flows. *Journal of Atmospheric Sciences*, **44**, 3–22.

Nakamura, H., 1994: Rotational evolution of potential vorticity associated with a strong blocking flow configuration over europe. *Geophysical research letters*, **21 (18)**, 2003–2006.

Nakamura, H., M. Nakamura, and J. Anderson, 1997: The Role of High- and Low-Frequency Dynamics in Blocking Formation. *Monthly Weather Review*, **125 (9)**, 2074–2093.

Nakamura, H. and T. Sampe, 2002: Trapping of synoptic-scale disturbances into the North Pacific subtropical jet core in midwinter. *Geophysical Research Letters*, **29 (16)**, 1761.

Nakamura, H. and J. Wallace, 1990: Observed changes in baroclinic wave activity during the life cycles of low-frequency circulation anomalies. *Journal of Atmospheric Sciences*, **47**, 1100–1116.

Nakamura, H. and J. Wallace, 1993: Synoptic behavior of baroclinic eddies during the blocking onset. *Monthly weather review*, **121 (7)**, 1892–1903.

Namias, J., 1947: Characteristics of the general circulation over the northern hemisphere during the abnormal winter 1946-47. *Monthly Weather Review*, **75 (8)**, 145–152.

Ndarana, T., D. Waugh, L. Polvani, G. Correa, and E. Gerber, 2012: Antarctic ozone depletion and trends in tropopause rossby wave breaking. *Atmospheric Science Letters*.

Nitsche, G., W. J.M., and C. Kooperberg, 1994: Is there evidence of multiple equilibria in planetary wave amplitude statistics? *Journal of the atmospheric sciences*, **51 (2)**.

North, G., T. Bell, R. Cahalan, and F. Moeng, 1982: Sampling errors in the estimation of empirical orthogonal functions. *Mon. Wea. Rev*, **110 (7)**, 699–706.

Peixoto, J. and A. Oort, 1992: *Physics of Climate*. Am. Inst. of Phys., New York, 520 pp.

Pelly, J. and B. Hoskins, 2003: A New Perspective on Blocking. *Journal of the Atmospheric Science*, **60**, 743–755.

Peters, D. and D. Waugh, 1996: Influence of barotropic shear on the poleward advection of upper-tropospheric air. *Journal of Atmospheric science*, **53**, 3013–3031.

Peterson, K., J. Lu, and R. Greatbatch, 2003: Evidence of nonlinear dynamics in the eastward shift of the nao. *Geophys. Res. Lett*, **30 (2)**, 1030.

Pierrehumbert, R. and P. Malguzzi, 1984: Forced coherent structures and local multiple equilibria in a barotropic atmosphere. *Journal of Atmospheric Sciences*, **41**, 246–257.

Postel, G. and M. Hitchman, 1998: A Climatology of Rossby Wave Breaking along the Subtropical Tropopause. *Journal of Atmospheric science*, **56 (3)**, 359–373.

Rayner, N., D. Parker, E. Horton, C. Folland, L. Alexander, D. Rowell, E. Kent, and A. Kaplan, 2003: Global analyses of sea surface temperature, sea ice, and night marine air temperature since the late nineteenth century. *J. Geophys. Res*, **108 (D14)**, 4407.

Reinhold, B. and R. Pierrehumbert, 1982: Dynamics of weather regimes- quasi-stationary waves and blocking. *Monthly Weather Review*, **110**, 1105–1145.

Rennert, K. and J. Wallace, 2009: Cross-frequency coupling, skewness, and blocking in the northern hemisphere winter circulation. *Journal of Climate*, **22 (21)**, 5650–5666.

Renwick, J. and J. Wallace, 1996: Relationships between north pacific wintertime blocking, el niño, and the pna pattern. *Monthly weather review*, **124 (9)**, 2071–2076.

Rex, D., 1950a: Blocking action in the middle troposphere and its effect upon regional climate: I. An aerological study of blocking action. *Tellus*, **2**, 196–211.

Rex, D., 1950b: Blocking action in the middle troposphere and its effect upon regional climate: Ii. the climatology of blocking action. *Tellus*, **2 (4)**, 275–301.

Richardson, L., 1922: Weather prediction by numerical methods. Cambridge University Press.

Riviere, G. and I. Orlanski, 2007: Characteristics of the Atlantic Storm-Track Eddy Activity and Its Relation with the North Atlantic Oscillation. *Journal of the Atmospheric Science*, **64 (2)**, 241–266.

Rodwell, M., D. Rowell, and C. Folland, 1999: Oceanic forcing of the wintertime north atlantic oscillation and european climate. *Nature*, **398 (6725)**, 320–323.

Roeckner, E., et al., 2006: Sensitivity of Simulated Climate to Horizontal and Vertical Resolution in the ECHAM5 Atmosphere Model. *Journal of Climate*, **19**, 3771–3790.

Rossby, C., 1950: On the dynamics of certain types of blocking waves. *Journal Chinese Geophysical Society*, **2**, 1–13.

Rossby, C. et al., 1939: Relation between variations in the intensity of the zonal circulation of the atmosphere and the displacements of the semi-permanent centers of action. *J. Mar. Res*, **2 (1)**, 38–55.

Sampe, T., H. Nakamura, A. Goto, and W. Ohfuchi, 2010: Significance of a midlatitude sst frontal zone in the formation of a storm track and an eddy-driven westerly jet*. *Journal of Climate*, **23 (7)**, 1793–1814.

Santos, J., J. Pinto, and U. Ulbrich, 2009: On the Development of Strong Ridge Episodes over the Eastern North Atlantic. *Geophysical Research Letters*, **36 (17)**, L17 804.

Scaife, A., J. Knight, G. Vallis, and C. Folland, 2005: A stratospheric influence on the winter nao and north atlantic surface climate. *Geophys. Res. Lett*, **32 (18)**, L18.

Scaife, A., T. Woollings, J. Knight, G. Martin, and T. Hinton, 2010: Atmospheric Blocking and Mean Biases in Climate Models. *Journal of Climate*, **23**, 6143–6152.

Scaife, A., et al., 2011: Improved atlantic winter blocking in a climate model. *Geophysical Research Letters*, **38 (23)**.

Scherrer, S., M. Croci-Maspoli, C. Schwierz, and C. Appenzeller, 2006: Two-dimensional indices of atmospheric blocking and their statistical relationship with winter climate patterns in the Euro-Atlantic region. *International Journal of Climatology*, **26**, 233–249.

Schneider, T., 2006: The general circulation of the atmosphere. *Annu. Rev. Earth Planet. Sci.*, **34**, 655–688.

Schwierz, C., M. Croci-Maspoli, and H. Davies, 2004: Perspicacious indicators of atmospheric blocking. *Geophys. Res. Lett*, **31**, L06 125.

Shabbar, A., J. Huang, and K. Higuchi, 2001: The relationship between the wintertime north atlantic oscillation and blocking episodes in the north atlantic. *International journal of climatology*, **21 (3)**, 355–369.

Shutts, G., 1983: The propagation of eddies in diffluent jetstreams: eddy vorticity forcing of blocking flow fields. *Quarterly Journal of the Royal Meteorological Society*, **109**, 737–761.

Sillmann, J. and M. Croci-Maspoli, 2009: Present and future atmospheric blocking and its impact on European mean and extreme climate. *Geophysical Research Letters*, **36 (10)**, L10 702.

Sillmann, J., M. Croci-Maspoli, M. Kallache, and R. W. Katz, 2011: Extreme Cold Winter Temperatures in Europe under the Influence of North Atlantic Atmospheric Blocking. *Journal of Climate*, **24 (22)**, 5899–5913.

Simmons, A., S. M. Uppala, D. Dee, and S. Kobayashi, 2007: ERA-Interim: New ECMWF reanalysis products from 1989 onwards. *ECMWF Newsletter*, **110**, 25–35.

Simmons, A., J. Wallace, and G. Branstator, 1983: Barotropic wave propagation and instability, and atmospheric teleconnection patterns. *Journal of the Atmospheric Sciences*, **40 (6)**, 1363–1392.

Stan, C. and D. Straus, 2007: Is blocking a circulation regime? *Monthly weather review*, **135 (6)**, 2406–2413.

Stephenson, D., A. Hannachi, and A. O'Neill, 2004: On the existence of multiple climate regimes. *Quarterly Journal of the Royal Meteorological Society*, **130 (597)**, 583–605.

Stephenson, D., V. Pavan, and R. Bojariu, 2000: Is the north atlantic oscillation a random walk? *International Journal of Climatology*, **20 (1)**, 1–18.

Stephenson, D., H. Wanner, S. Bronnimann, and J. Luterbacher, 2003: The history of scientific research on the north atlantic oscillation. *GEOPHYSICAL MONOGRAPH-AMERICAN GEOPHYSICAL UNION*, **134**, 37–50.

Strong, C. and R. Davis, 2008: Variability in the Position and Strength of Winter Jet Stream Cores Related to Northern Hemisphere Teleconnections. *Journal of Climate*, **21**, 584–592.

Strong, C. and G. Magnusdottir, 2008: Tropospheric Rossby Wave Breaking and the NAO/NAM. *Journal of Atmospheric Science*, **65 (9)**, 2861–2876.

Sumner, E., 1954: A study of blocking in the atlantic-european of the northern hemisphere. *Quarterly Journal of the Royal Meteorological Society*, **80 (345)**, 402–416.

Swanson, K., 2001: Blocking as a local instability to zonally varying flows. *Quarterly Journal of the Royal Meteorological Society*, **127 (574)**, 1341–1355.

Taylor, K., R. Stouffer, and G. Meehl, 2012: An overview of cmip5 and the experiment design. *Bulletin of the American Meteorological Society*, **93 (4)**, 485.

Thompson, D. and J. Wallace, 1998: The arctic oscillation signature in the wintertime geopotential height and temperature fields. *Geophysical Research Letters*, **25 (9)**, 1297–1300.

Thorncroft, C., B. Hoskins, and M. McIntyire, 1993: Two Paradigms of Baroclinic Wave Life-Cycle Behaviour. *Quarterly Journal of the Royal Meteorological Society*, **119**, 17–55.

Tibaldi, S. and F. Molteni, 1990: On the Operational Predictability of Blocking. *Tellus*, **42A**, 343–365.

Tibaldi, S., E. Tosi, A. Navarra, and L. Pedulli, 1994: Northern and Southern Hemisphere Seasonal Variability of Blocking Frequency and Predictability. *Monthly Weather Review*, **122 (9)**, 1971–2003.

Tribbia, J., 1984: Modons in spherical geometry. *Geophysical & Astrophysical Fluid Dynamics*, **30 (1-2)**, 131–168.

Trigo, R., I. Trigo, C. DaCamara, and T. Osborn, 2004: Climate impact of the European winter blocking episodes from the NCEP/NCAR Reanalyses. *Climate Dynamics*, **23**, 17–28.

Tsou, C. and P. Smith, 1990: The role of synoptic/planetary–scale interactions during the development of a blocking anticyclone. *Tellus A*, **42 (1)**, 174–193.

Tung, K. and R. Lindzen, 1979: A theory of stationary long waves. part i: A simple theory of blocking. *Mon. Wea. Rev*, **107 (6)**, 714–734.

Tung, K. and A. Rosenthal, 1985: Theories of multiple equilibriaa critical reexamination. part i: Barotropic models. *J. Atmos. Sci*, **42 (24)**, 2804–2819.

Tyrlis, E. and B. Hoskins, 2008a: Aspects of a Northern Hemisphere Atmospheric Blocking Climatology. *Journal of Atmospheric Science*, **65**, 1638–1652.

Tyrlis, E. and B. Hoskins, 2008b: The Morphology of Northern Hemisphere Blocking. *Journal of Atmospheric Science*, **65**, 1653–1665.

Uppala, S. M., et al., 2005: The ERA-40 re-analysis. *Quarterly Journal of the Royal Meteorological Society*, **131 (612)**, 2961–3012.

Valcke, S., 2006: OASIS3 User Guide. Prism Report Series 2, CERFACS.

Valdes, P. and B. Hoskins, 1989: Linear stationary wave simulations of the time-mean climatological flow. *Journal of Atmospheric Sciences*, **46**, 2509–2527.

Vallis, G., 2006: *Atmospheric and oceanic fluid dynamics: fundamentals and large-scale circulation*. Cambridge Univ Pr.

Vautard, R., 1990: Multiple weather regimes over the north atlantic analysis of precursors and successors. *Monthly weather review*, **118 (10)**, 2056–2081.

Vial, J. and T. Osborn, 2012: Assessment of atmosphere-ocean general circulation model simulations of winter northern hemisphere atmospheric blocking. *Climate dynamics*, **39 (1)**, 95–112.

Walker, G., 1924: Correlation in seasonal variations of the weather, ix: A further study of world weather. *Indian Meteor. Mem.*, **24**, 275–332.

Walker, G. and E. Bliss, 1932: World weather v. *Memorial of Royal Meteorological Society*, **134**, 193–210.

Wallace, J. and D. Gutzler, 1981: Teleconnections in the geopotential height field during the Northern Hemisphere winter. *Monthly Weather Review*, **109**, 784–812.

Wiedenmann, J., A. Lupo, I. Mokhov, and E. Tikhonova, 2002: The Climatology of Blocking Anticyclones for the Northern and Southern Hemispheres: Block Intensity as a Diagnostic. *Journal of Climate*, **15**, 3459–3473.

Woollings, T., 2008: Vertical structure of anthropogenic zonal-mean atmospheric circulation change. *Geophys. Res. Lett*, **35**, L19 702.

Woollings, T. and M. Blackburn, 2012: The north atlantic jet stream under climate change and its relation to the nao and ea patterns. *Journal of Climate*, **25 (3)**, 886–902.

Woollings, T., A. Charlton-Perez, S. Ineson, A. G. Marshall, and G. Masato, 2010a: Associations between stratospheric variability and tropospheric blocking. *Journal of Geophysical Research*, **115**, D06 108.

Woollings, T., A. Hannachi, and B. Hoskins, 2010b: Variability of the North Atlantic eddy-driven jet stream. *Quarterly Journal of the Royal Meteorological Society*, **136**, 856–868.

Woollings, T., A. Hannachi, B. Hoskins, and A. Turner, 2010c: A Regime View of the North Atlantic Oscillation and Its Response to Anthropogenic Forcing. *Journal of Climate*, **23**, 1291–1307.

Woollings, T., B. Hoskins, M. Blackburn, and P. Berrisford, 2008: A New Rossby Wave Breaking Interpretation of the North Atlantic Oscillation. *Journal of Atmospheric Science*, **65**, 609–326.

Woollings, T., J. Pinto, and J. Santos, 2011: Dynamical evolution of North Atlantic ridges and poleward jet stream displacements. *Journal of Atmospheric Science*, **68**, 954–963.

Zhang, X., L. Jin, C. Chen, D. Guan, and M. Li, 2011: Interannual and interdecadal variations in the north atlantic oscillation spatial shift. *Chinese Science Bulletin*, **56 (24)**, 2621–2627.